El 16

UDC 621.315.61
621.317.333

ACTA POLYTECHNICA SCANDINAVICA

ELECTRICAL ENGINEERING SERIES No. 16

Studies on Partial Discharges on Solid Dielectrics— a Contribution to the Discharge Resistance Testing of Insulating Materials

ANDREAS KELEN

Central Laboratories,
ASEA, Västerås

STOCKHOLM 1967

STUDIES ON PARTIAL DISCHARGES ON SOLID DIELECTRICS- A CONTRIBUTION TO THE DISCHARGE RESISTANCE TESTING OF INSULATING MATERIALS

Contents

Printed in Sweden by
Elanders Boktryckeri AB Göteborg 1967

PARTIAL DISCHARGE RESISTANCE TESTING OF INSULATING MATERIALS

Andreas Kelen

Central Laboratories, ASEA

Contents

Introduction

The development of electrical power apparatus shows a distinct trend towards greater size and increasing power density of units. At the same time, increasingly more severe demands are being made on the reliability of such equipment. However, over-dimensioning can be less and less tolerated for economic reasons. Modern insulation technology is thus being faced by important problems. Increasing attention is being paid to insulation research owing to both the progressive exploitation of the potentialities inherent in materials and the accelerating rate at which new materials become accessible. Against this background, there is no doubt that the study of insulation ageing is an important subject.

When insulation is subject to a high electrical stress, partial discharges become a phenomenon of great relevance to insulation ageing and insulation life. Cables and capacitors are examples of equipment in which partial discharges cause breakdown within a relatively short time. On the other hand, in the case of rotating machine insulation, damage due to discharges may cause slight and slowly progressing deterioration.

The problems related to partial discharges and their effects on insulation may be divided into different aspects as, for example, in the following way:

1. The occurrence of partial discharges
2. Gas discharge physical mechanisms
3. Effects on condensed matter
4. Ageing of insulating materials and insulation; discharge resistance testing
5. Detection and intensity measurement
6. Discharge protection

A great number of papers have been published in this field. Bibliography can be found in review papers and books, e.g., in Whitehead's monograph[119], in Mason's reviews of breakdown in solid insulation[77] and of discharge intensity measurement[81], and in Kreuger's monograph on discharge detection and measurement[66]. Problems related to discharge measurement and resistance testing of materials have been systematically treated in papers, reports and theses by workers in university and research laboratories, e.g., the Laboratoire de Génie Electrique of the University of Toulouse in collaboration with Electricité de France (Lacoste, Leroy), the Laboratoire Central des Industries

Electriques in Fontenay-aux-Roses (Hérou, Fabre, Fallou, Knosp), the Electrical Industries Research Association (Garton, Mason, Mole, Parkman) and the Central Electricity Research Laboratory (Stannett, Douglas), both at Leatherhead. Important contributions in this field have been made by workers of industrial laboratories in several countries.

The subjects 1, 4, 5 and 6 in the above list are the ones that have been most frequently treated in the literature. Physical studies in the domains 2 and 3 are sparse.

The present paper is concerned with the methods of partial discharge resistance testing of insulating materials. It begins with a brief description of the occurrence of partial discharges, discharge mechanisms and discharge action on matter. This chapter mainly aims at giving information required in connection with the subsequent exposure. Repetition of information which may be found in the reviews is avoided as far as possible.

The second part of the paper presents published testing methods. The discussion of the methods is preceded by a description of some cases of discharge ageing in rotating machine insulation. The greater part of this material has not hitherto been published. After this, some guiding principles for the accelerated ageing testing of insulation are proposed. Different approaches to discharge resistance testing are critically reviewed against this background.

Testing methods adopted in the author's laboratory are described in the third part of the paper. The effects of experimental parameters are discussed against the background of accumulated experience. Tests providing supplementary information on the discharge resistance of insulating material are recommended. A new simplified approach towards the assessment of the internal discharge resistance of materials is suggested on the basis of the results of separate studies[55, 56], which clarify the background for the determination of the energy dissipation from internal discharges.

Definitions and notation

Definitions

Systematic efforts to obtain a standard terminology, especially within IEC TC 42, seem to be bearing fruit. Since unified terminology is a great advantage, the author has refrained from suggesting his own terminology and has chosen to follow recommendations given by Mason[80] and Kreuger[66]. The notation and dimensions used are based on international standards[50].

Partial discharge

An electrical discharge that only partially bridges the insulating medium between conductors, i.e., internal and surface discharges and corona.

Internal discharges

Partial discharges in cavities or at the edges of conducting inclusions in solid or liquid insulation. The cavity may be entirely enclosed in insulation, or it may be covered on one side by a conductor.

Surface discharges

Partial discharges from a conductor in a gaseous or liquid medium on to or across the surface of solid insulation that is not covered by the conductor.

Corona

Partial discharges in gases or liquids around conductors that are remote from solid insulation.

Discharge-inception voltage

Lowest voltage at which discharges of a specified magnitude recur in successive cycles when an increasing alternating voltage is applied to insulation.

Discharge-extinction voltage

Lowest voltage at which discharges of a specified magnitude will recur when an alternating voltage, which exceeds the discharge-inception voltage, is reduced.

Discharge-ignition voltage

Voltage that must be applied between conducting or dielectric surfaces to cause a discharge in the gas between them.

Discharge remanent voltage

Minimum voltage between conducting or dielectric surfaces that will maintain a gas discharge between them.

Discharge magnitude

Loss of charge, as measured at the terminals of a sample, caused by a single discharge.

Discharge energy

Energy dissipated by a single discharge.

Discharge resistance of insulating materials

Resistance of a material to deterioration and dielectric breakdown when exposed to discharges under prescribed test conditions.

Notation

U volts	Voltage, actual value. Values characteristic of alternating voltage may be denoted by (R.M.S.), (peak)
U_i volts (R.M.S.)	Discharge-inception voltage
U_e volts (R.M.S.)	Discharge-extinction voltage
U_{di} volts	Discharge-ignition voltage
U_{dr} volts	Discharge remanent voltage
U_p volts	Paschen breakdown voltage of a gas
C farads	Capacitance of a specified object
c farads	Local capacitance related to an individual discharge
d_d metres	Thickness of a dielectric layer
d_g metres	Thickness of a gas layer, in particular a gap with constant width
k	Relative permittivity of dielectric
γ $\Omega^{-1}m^{-1}$	Conductivity
I_m amperes	Current reading of mean-discharge-current measuring device
I_{mc} amperes	Current correction for power-frequency component
I_{md} amperes	Mean discharge current
Q coulombs	Discharge magnitude
N	Number of discharge pulses
$\dot{N}$ hertz	Discharge pulse rate
f hertz	Frequency of alternating voltage
W joules	Discharge energy
W_{tot} joules	Energy dissipation from discharges in an object
t seconds	Time
P watts	Power dissipation from discharges in an object
G J/kg	Index characterizing the discharge resistance of insulating materials in tests giving a measure of the quantity of eroded material.

1. The occurrence of partial discharges and their action on materials

1.1 General description

Partial discharges consist of local gas discharge pulses of very short duration occurring when the breakdown strength of a gas space in, or adjacent to, insulation is exceeded. It is a characteristic feature of partial discharges that charge deposition on an insulating surface from the individual discharge pulse alters the field distribution and thus affects the conditions for the occurrence of subsequent discharges. Partial discharges at direct voltage have been studied by Salvage[104, 105] and by Rogers and Skipper[103] and will not be discussed in this paper. In the case of an applied alternating voltage, a regular succession of discharge pulses in synchronism with the time derivative of the voltage occurs.

The breakdown strength of a gas is a function of its composition, pressure, the electrode spacing and field geometry. Paschen's law states that the breakdown voltage is a function of the product of distance and gas pressure. Temperature and pressure variations of the breakdown voltage of a gap with given thickness can thus be derived. Paschen's law is valid up to about 10^5 V · torr. For the case of metal electrodes and homogeneous fields, the well-known Paschen curves apply, see Fig. 1.1. The findings of Hall and Russek[40], which are confirmed by, e.g., Fieux's measurements[33], are widely held in support of the view that the Paschen values are also valid for the case of dielectric boundaries. Other workers, e.g., Mason[75], consider that breakdown against a dielectric boundary occurs at a slightly lower voltage.

In the review by Mason[77] and in Kreuger's book[66] the applied voltage corresponding to the local discharge-ignition voltage of a gas volume is given for different geometrical configurations of the solid boundaries.

The discharge repetition rate at alternating voltage in small cavities in insulation is determined by the amplitude and frequency of the voltage as illustrated in Fig. 1.2.*a*, where the whole cavity is assumed to be uniformly affected by each discharge pulse. The pulse repetition rate can be easily derived and is found to be

$$\dot{N} = 4 \frac{U_g(\text{peak})}{U_{di} - U_{dr}} f \qquad \text{Hz}$$

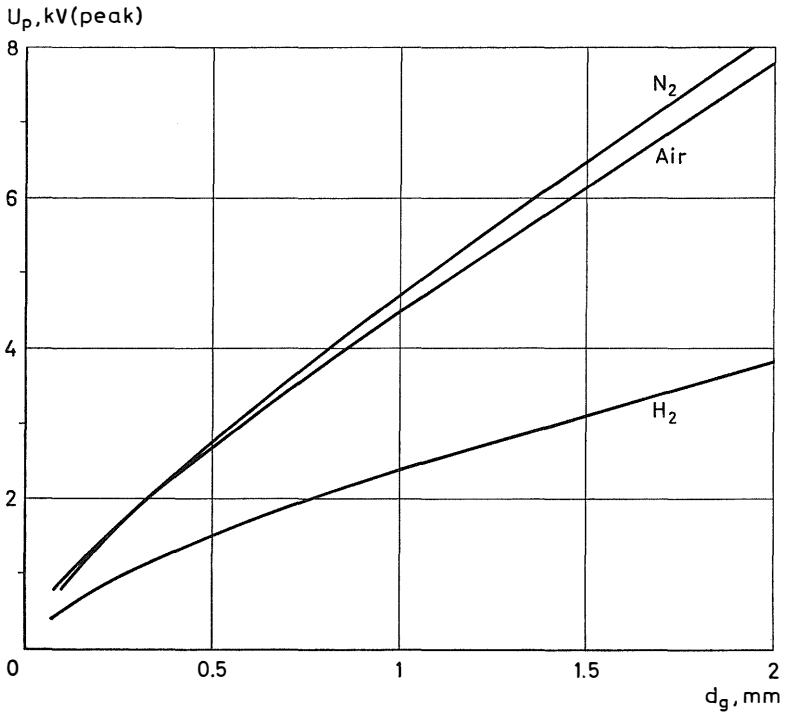

Fig. 1.1. Homogeneous field breakdown voltage U_p of air, nitrogen and hydrogen at atmospheric pressure as a function of the electrode spacing.

where

U_g = the voltage across the cavity

U_{di}, U_{dr} = the discharge-ignition and discharge remanent voltages

f = the frequency of the voltage

At the same time, the voltage across the dielectric in series with the cavity varies as shown in Fig. 1.2.*b*.

This implies that the voltage across the cavity varies between the limits U_{di} and U_{dr}, whereas the applied voltage is $U = U$ (peak) sin ωt. Once a discharge has occurred at an applied voltage U_{i0}, e.g., if induced by an overvoltage peak or by primary ionisation caused by a high-energy particle traversing the void, subsequent discharges will even strike at a lower amplitude of the applied voltage, ideally almost down to 0.5 U_{i0}. The possibility of a still lower limit is discussed by Veverka[114]. The occurrence of discharges in voids is treated in great detail in Whitehead's book[119].

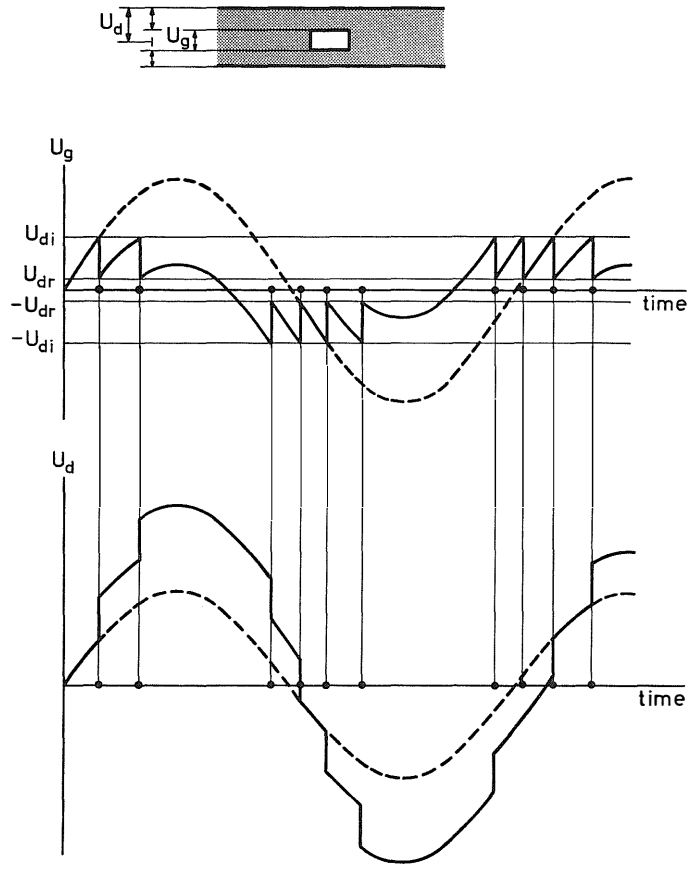

Fig. 1.2. Variation of voltage with time.

a. Across void.
b. Across dielectric in series with the void.

If the gas space is limited by extended parallel plane boundaries, individual discharges occur locally and affect a limited part of the gap. A family of discharges distributed over the gap as shown in Fig. 1.3., which reproduces an oscillographic record of a discharge group during one half-cycle of the applied voltage, now corresponds to each discharge pulse in a small cavity. The pulse sizes appear to vary in a random way. Pulse-size distributions and their dependence on various parameters have been studied by several workers, particularly by the Toulouse school[19]. An interesting feature of pulse oscillograms like the one shown in Fig. 1.3 is the low degree or even lack of correlation between the pulse size and the instantaneous value of the applied voltage. This might appear rather surprising in view of the time interval between the

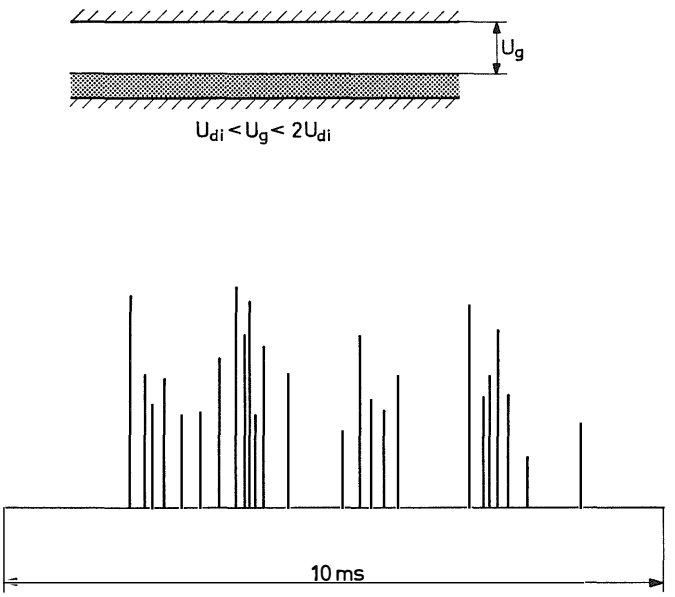

Fig. 1.3. Oscillogram of discharge pulses in a gap between a conductor and a dielectric during one half-cycle of the voltage.

first and the last pulse of a group not being at all negligible compared with the duration of the voltage half-wave. It might be expected that the domains of the gap which are discharged in about the middle of the pulse sequence would be over-stressed and that the corresponding discharge pulses would be above the average. That this is not generally the case indicates the presence of interference between statistical distributions affecting the individual discharge both in time (the time lag for the individual discharge) and in space (local modifications of the field distribution and dispersion in magnitude of the primary and secondary phases of the discharge, see 1.2.). The following qualitative picture might be envisaged. The first discharge in a series strikes at a site on the gap boundary, where surface charges from a major previous discharge of opposite polarity remain, or which has an irregularity giving rise to field distortion, or has increased electron emission properties. This results in a local field reduction having a certain protective range. The second discharge consequently strikes at some distance away, when the next site reaches the critical conditions, and so on. The site farthest away is on the edge of the discharge zone. A certain intensification of the discharge action at the edge of a zone with constant gas gap is often observed[36]. This picture implies what is generally assumed but rarely stated[43, 94], namely that the voltage across a gap of constant thickness between insulating surfaces only changes slightly at and

above the ignition voltage, while the voltage applied to the external electrodes rises or decreases sinusoidally with time. Discharges in subsequent voltage waves would have a tendency to occur at the same places, which is in accordance with much experimental evidence. The distribution and size of surface charges remaining after discharge pulses have been studied by means of a dielectric powder technique by Bertein[12]. Surface charges and local property changes of exposed polyethylene have been investigated by Thomas by means of both a powder method and a technique of "heat development" of the affected areas[112]. The size of the areas affected by discharges has been shown to vary statistically. This area is influenced by the surface resistivity. Grosskreuz[39] uses a xerographic method for evaluating the discharge size.

A formal application of the pulse rate/applied voltage considerations for small voids to the parallel gap case would lead to the expectation of a step-shaped pulse rate/voltage amplitude dependence. However, the statistical distribution of the discharge-pulse sizes tends to smooth out the steps. Bartnikas[9,10] has performed measurements which indicate that the smoothing is almost complete; the pulse rate/voltage distribution scarcely reveals any trace of steps for voltages corresponding to integral multiples of the discharge-inception voltage of the gap. Similar results have also been obtained by Böning[17].

Fig. 1.4. shows a typical example of the pulse rate/voltage dependence measured by the author in the range between once and twice the inception voltage in a gap of constant width.

Voids and gaps occurring in practice usually have geometrical configurations and surface properties which do affect the occurrence of discharges in a more complicated way than discussed above. However, what is said above applies as a qualitative description of some typical aspects of the phenomena.

In closed voids the situation is complicated by discharge effects acting back on the discharge conditions. Self-extinction of discharges[40,77,93,102] is a well-known phenomenon in this connection. Self-induced discharge intensity changes may be caused by variations in the composition and pressure of the atmosphere in the cavity, and by the formation of a conductive surface layer (see 1.2.). Depending on the nature of the mechanisms involved (formation of discharge products, secondary chemical reactions, diffusion, etc.), the level of the discharge intensity may be stable, slowly varying or fluctuating with discharge-free intervals. In polyethylene, for example, periods with discharges have been observed with discharge-free intervals of several hours[102].

The shape of the void is of importance to the discharge intensity. The field in ellipsoid-shaped voids departs from homogeneity, if the size of the void is comparable with the electrode spacing[105]. In flat voids, field distortion at the edge increases the discharge intensity as demonstrated by Heller[42].

Pulse amplitude measurements in voids in different dielectrics are reported by Dakin and Works[25].

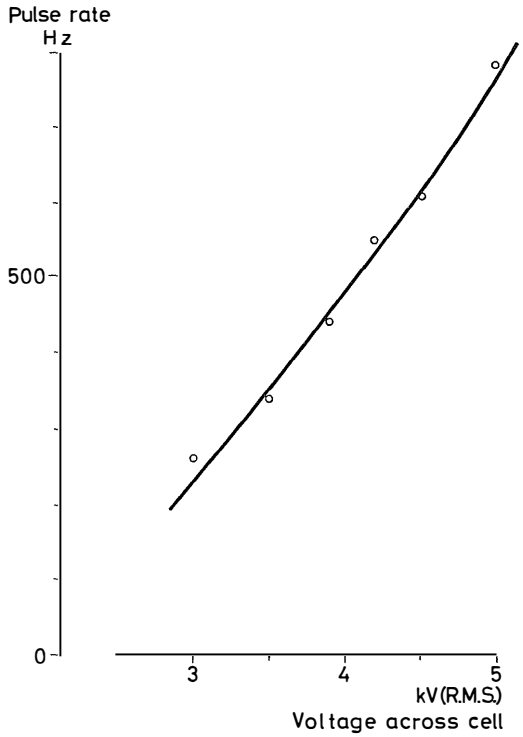

Fig. 1.4. Discharge pulse rate in an air gap of constant width as a function of the applied voltage.

For the special case of spherical voids in a dielectric, the screening action of a conducting surface layer has been theoretically derived in[54]. If the dielectric has the relative permittivity k_3 and negligible conductivity, while the surface layer with inner and outer radii r_1 and r_2 has the relative permittivity $k_2 = k_3$ and the conductivity γ_2, the relative permittivity of the gas in the void being assumed to be unity, the expression for the ratio A of the homogeneous electrical stress in the void to the stress in the undisturbed dielectric is approximately

$$A \approx 1.25 \times 10^{-8} \frac{k_3}{\gamma_2 \left(1 - \left(\frac{r_1}{r_2}\right)^3\right)}$$

if γ_2 is given in $\Omega^{-1}\mathrm{m}^{-1}$ and a frequency of 50 Hz is assumed.

Fig. 1.5 shows the dependence of A on r_1/r_2 for different values of the parameters k_3 and γ_2.

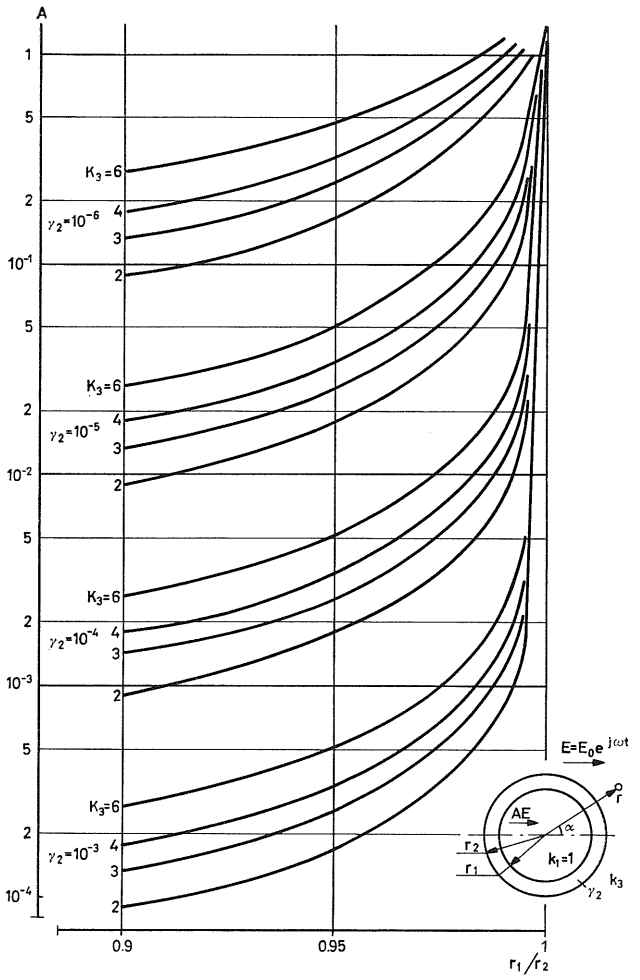

Fig. 1.5. Stress reduction in a spherical void with a conducting surface layer.

Information about γ_2 and r_1–r_2, e.g., from studies of discharge action on insulating materials, enables the screening effect on internal discharges in small voids to be estimated.

Discharges from metal or other conducting edges in contact with insulation occur along the surface of the insulation. Owing to greater feeding capacitance, their intensity exceeds that of the types of discharge discussed above. Mason[79] has described the evolution of radial discharges into ring-formed discharges in air at normal pressure, and in other atmospheres. His explanation of the phenomenon is based on the assumption that positive ions accumulate in an

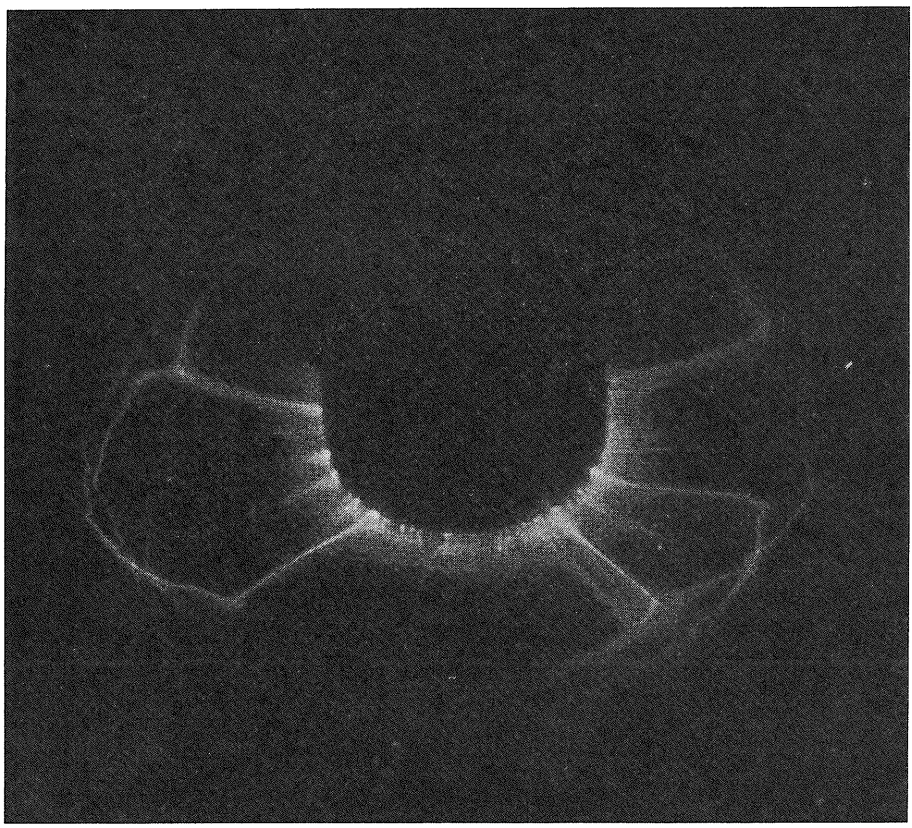

Fig. 1.6. Radial and circular discharges from a cylindrical electrode in contact with a plane insulation surface.

annular zone around the electrode. A powerful radial discharge produces a local field, which forces it to develop into a circular discharge. The author has observed similar phenomena in air at atmospheric pressure, see Fig. 1.6[52].

1.2 **The individual discharge pulse**

The physics of partial discharge pulses are not yet well understood.

Individual pulses in flat voids in polyethylene have been studied by Mason[75] with a photographic technique. In voids 0.3 mm deep circular light spots 0.2–0.5 mm in diameter were recorded at the discharge-inception voltage. Increasing of the voltage produced patterns of considerably greater size, both star-shaped and of a diffuse circular shape.

Discharge pulses are extremely fast. Most published results of pulse shape recording seem unconvincing owing to excessive response time of the

measuring circuitry. Bui-Ai[19] describes different pulse shapes, depending on polarity, for discharges between a conductor and a dielectric. The results of Bailey obtained by means of a sampling oscilloscope with discharges in polyethylene[7] represent, to the author's knowledge, the best measurements up to now. He states that the main part of discharges in a 1.25 mm gap lasts less than 1 ns, preceded by a build-up time of about 2 ns. In small voids, build-up and rise times appear to be somewhat greater. The pulse shape changes with exposure time owing to changing insulation surface conditions. Surface discharge pulses last longer, 50–500 ns according to Kreuger[66]. Measurements of the light emission caused by discharges in voids[11] yield longer time intervals than current oscillograms. Afterglow due to different mechanisms can explain this discrepancy.

A discharge pulse creates mobile charges which are transferred by the field. The actual charge transfer in the discharge is not accessible in principle to measurement. If suitable models are assumed, the charge transfer may be derived from pulse magnitude measurements yielding the change of polarisation of the dielectric, when affected by the discharge. This question, which is of great relevance to our subject, is treated, for example, in Kreuger's book[66], and in a very detailed manner by Bui-Ai[19]. It is dealt with in 1.4. and is also discussed in[56].

Discharge magnitudes, as derived from measured pulse magnitudes where simple analogue schemes are assumed, range from 1–300 pC in small voids in, e.g., polyethylene[75], over 10^3–10^5 pC in gaps of constant thickness of the order of 1 mm between conductor and a dielectric ([19], own observations), to 10^3–approx. 2×10^5 pC for surface discharges[79].

The elementary mechanisms active in discharges may comprise impact ionisation and excitation, radiation, photodissociation, electron attachment, recombination, and particle emission from surfaces. Investigations of the physics of discharges in narrow gaps at atmospheric pressure are not very numerous and they almost entirely concern discharges between conducting surfaces. As the author suggests in a separate paper[56], there might be reason to expect that discharges against insulators possess some distinctive features as compared with discharges between conductors.

As has been mentioned in 1.1, the validity of the Paschen values for the breakdown of gas in a homogeneous field between dielectric boundaries is assumed by many workers but opposed by others.

It is an open question whether the affected part of a gap is completely short-circuited by the discharge, or whether there exists a voltage that is not negligible compared with the breakdown voltage at which the discharge is extinguished. Different views are held on this question, which are mainly based on discharge pulse measurements without reference to the underlying physics.

From gas discharge physics it is known that short Townsend avalanches and streamers have active diameters of 0.1 mm or less. On the other hand, the above-mentioned investigations of the dielectric surface area affected by one discharge range from maximum 3 mm diameter (Mason, discharges in voids in polyethylene[75]) up to about 10 mm diameter (Bertein, surface discharges on insulating sheets[12]). This discrepancy is explained by the observation that discharges against insulation generally involve a sequence of events. The primary discharge directed against the surface creates conditions likely to initiate secondary discharges, of the type producing Lichtenberg figures, tangentially to the surface. This question, too, is discussed in[56]. As to the quantitative results of Bertein[12] and Thomas[112], it may be suggested that powder patterns might be affected by pressure waves—discharges are distinctly audible—and that melting patterns probably have an energy threshold, the reported discharge areas, thus representing upper and lower limits, respectively.

1.3 **Discharge action**

The primary effects of discharges are due to electrons, ions and photons. Cumulative effects may consist in heating and mechanical impact of shock waves.

1.3.1 *Molecular scale*

While photons and ions mainly supply the impact site with their potential energy, electrons also possess kinetic energy. In dense gases the probability of electrons possessing energies of, say two, three or more times the first ionisation level will be very small. Electrons with energies of 100 eV and above will scarcely occur at all in partial discharges. Most electrons will probably have energies below, perhaps, 30 eV. Chemical binding energies, however, are of the order of 1.5 to 4.5 eV, cohesion interactions between solids around 0.1 eV, while the energy necessary to remove an atom from, for example, a metal or semiconductor crystal exceeds 25 eV[63]. Hougen[47] assuming a Maxwellian distribution of electron energies derives 4.2 per cent of the free electrons in a gas having energies in excess of 11 eV.

The primary action of discharges influences both the gas volume and the solid boundaries. The production of ozone and nitrogen oxides in air is well known. It is rightly held[37] that even pure nitrogen, when subject to discharges, is not a chemically inert medium. Noble gases, although chemically inert, perhaps act on matter under the influence of discharges. The production of unstable excited and ionised species implies the possibility of energy transfer from noble gases to other matter capable of undergoing subsequent chemical reactions.

Ionisation and/or radical formation may occur on a surface exposed to discharges. These processes are not known in great detail. However, the primary interactions and associated secondary processes are held to be analogous to nuclear radiation effects, about which considerable experience has been accumulated. A difference, however, consists in the penetration power. Discharge electrons and ions have a very short range indeed in condensed matter. The effect of the primary impact depends on the coupling energy in the affected matter between the impact site and its immediate surroundings. Takacs and Freeman have demonstrated that the ionisation cross-section of electrons with energies below 20 eV depends on the chemical structure of the target[111]. In the case of a polymer molecule, for instance, the immediately affected bond may be broken. Alternatively, the weakest bond in the structural group may subside (e.g., hydrogen evolution in polyethylene). Lastly, the excitation may be carried still farther and if distributed over a sufficient number of bonds, it may be dissipated into thermal vibrations. The stabilising action of charge-conjugated rings is explained in this way (e.g., the stability of polystyrene and aromatics).

It is a general experience that charges deposed by discharges on dielectric surfaces often tend to be very resident[38, 24]. Reynolds[98, 99], for example, has found from measurements that the same charge distribution remains on a polyethylene surface after one month's storage as immediately after discharge exposure. Electrons may be trapped in their place of incidence after hitting the dielectric surface. They may also—at least in matter with suitable molecular structure—migrate through short-range conduction mechanisms until they reach an energetically advantageous position, i.e., a trap. The location of electrons is thus not necessarily limited by the penetration depth as determined by their kinetic energy. However, the suggestion of Boeck[13] that discharge electrons successively penetrate deep into a polymer sample seems exaggerated. Similar effects may also influence the location of free radicals. A radical site may migrate without actual transport of matter when electrons switch over from one interatomic bond to the next one in some analogy to the diffusion of holes in covalent crystals[34, 35].

The primary effects of discharge action on an atomic scale—ion and/or radical formation in a very narrow layer of the solid surface—are followed by one or several generations of alternative secondary effects, depending on the properties of the affected material and the nature of the ambient. Some of these effects are: *a* liberation of side groups from polymer chains accompanied by the formation of double bonds (unsaturation); *b* scission of the main chain; *c* depolymerising chain reactions; *d* formation of cross-links between macromolecules; *e* oxidation; *f* oxidative degradation through action of secondary peroxide radicals; *g* dehydration of hydratised ionic crystals.

1.3.2 *Microscopic and macroscopic scales*

In macroscopic terms, the processes enumerated above may manifest themselves in several ways as, for example: gas evolution, decrease of the elastic modulus owing to the plastifying effects of small molecules or reduction of chain length, increased stiffness and brittleness, i.e., rise of the elastic modulus and simultaneous decrease of the ultimate elongation, stickiness, colour changes, change of chemical surface activity, change of permittivity and resistivity. Such changes may continue even after termination of the primary cause if they are caused by secondary reactions, which imply, for example, diffusion from the surface or from deeper lying parts of the volume. After-effects of this sort may often show a marked temperature dependence. The temperature may also influence the dominating character of the changes in a material exposed to discharges, since many insulating materials consist of more than one molecule species. Moreover, different secondary reactions may compete in a microscopically homogeneous material. Thus, for example, a polymer may be degraded by oxidative breakdown at the surface and at the same time undergo embrittlement due to cross-linking somewhat below the surface. Local stresses may be produced and lead to the formation and propagation of surface cracks, which may expose new surfaces to the action of the discharges.

Some guidance on the behaviour of polymers under the action of discharges may be found in the literature on radiation effects, e.g., the monographs by Charlesby[21], Bolt and Carroll[14] and Kircher[63], where also chemical protection by active additives is reviewed. Various aspects of the ageing of polymers are treated in[2].

Mason[75] gives interesting estimates of the temperature rise of the portion of a polymer surface affected by a single discharge pulse, assuming that the energy is initially concentrated in a volume given by the bombarded area and the depth of heat penetration during the life of the pulse. He arrives at temperature rises of from some few to several hundred degrees, which is compared with, for example, the softening point of polyethylene of about 110°C. He estimates the volume of polyethylene eroded through thermal action by each discharge to be of the order of 0.001 μm^3. Garton[37] extends the calculation of the dissipated heat to the partial discharge itself and arrives at the conclusion that heat dissipation at the dielectric boundary is probably at least one order of magnitude less than the values derived by Mason.

The portion of the discharge energy striking an insulating surface without producing immediate chemical effects—the efficiency of primary chemical action owing to single-particle events probably being low—might be assessed qualitatively along these lines. Perhaps this reasoning might be extended with advantage from organic polymers, which manifestly are subject to con-

siderable chemical change, to materials with ionic bonding (mica, glass) and metals, which possess a greater resistance to the primary effects of discharges. The known effects of discharges on, for example, mica and metal surfaces might well justify an explanation in terms of local heating.

Oxidation is a mechanism of considerable importance to the behaviour of insulated metal surfaces exposed to discharges. The oxygen may be present in the atmosphere or, in the case of internal discharges after oxygen exhaustion, come from the insulation (dissolved oxygen, oxygen liberated during insulation deterioration). Nitrous compounds are likewise often formed.

A secondary deterioration mechanism on insulating surfaces exposed to discharges is suggested by Thomas[112]. If electrons penetrate beneath the surface, the next discharge of opposite polarity at the same site leaves a positive charge owing to deposition of positive ions or extraction of electrons. A double layer of opposed charges is thus formed. The properties of such charge distributions have been investigated by Gross, see, for example,[38]. If the resulting field intensity exceeds the local dielectric strength of the surface layer, local breakdowns may occur and produce microscopic channels in the surface layer.

Mason[75, 76, 77] describes the typical progress of macroscopic discharge attack on a plane polymer surface and states that it proceeds in three main stages: 1. Uniform degradation of the surface; 2. Formation of local pits; 3. Growth of one or a few deep channels.

A point of considerable interest in the first stage is the width of the directly affected layer. Mayoux[83] of the Toulouse school has studied this question with polyethylene exposed to discharges in air by applying a combination of infra-red spectroscopy and capacitance measurements. He concludes that a layer approximately 50 μm thick of degraded polyethylene is formed, after which it is gradually eroded away from the surface and grows with the same speed at its interface with the sound material. Thus, a 50 μm degraded layer is eating its way downwards. This layer has an irregular, spongy structure.

Ilčenko[49] reports a transition from extended to local attack at increasing intensity of internal discharges.

Mason's third stage seems to correspond to the phenomenon known as treeing from conductors or inclusions into insulation, i.e., the gradual penetration of tree-like channels. It has been described by, among others, Kitchin and Pratt[64] and by Olyphant[89, 90], and reviewed in[23]. Investigations of the associated breakdown mechanisms have been published in[28, 73, 106, 110, 116, 117, 118].

Olyphant[89, 90] has explained that treeing is due to the action of discharges, starting either from a pre-existing void, or from a void produced by a partial discharge at, for example, a sharp metal point. Discharges are detected in insulation with a growing tree. Their magnitude differs depending on whether the channel formation is accompanied by the formation of conducting deposits on the wall or not. If the tree is isolated from the external atmosphere, the

growth is accompanied by a pressure increase in the void as demonstrated by Bolton *et al.*[15]. A tree that penetrates insulation between conductors need not immediately establish a conducting path. Life measurements have demonstrated (Olyphant[89], own observations) a voltage life of samples with trees, which in some cases was considerably longer than the time to complete penetration of the insulation. Stobernack[110] has observed the existence of an induction period before the first signs of treeing become evident. The importance of spurious over-voltages for initiating the treeing process is mentioned by Olyphant[90]. The propagation of treeing channels has been studied by Baker[8] by means of a cine-film technique. Treeing in acrylate glass was shown to proceed in a stepwise fashion. Similar findings with an epoxide resin are mentioned in 3.9.

The fact that the walls of a growing tree may be insulating or conducting suggests a qualitative explanation of the varying tendency of branching of trees during growth in different materials. A channel with conducting walls may be assumed to be more or less at uniform potential. Subsequent discharges may be expected to occur at the tip of the channel and lead to linear growth. If, on the other hand, the tree walls are insulating, a single discharge may create a surface charge speck at some point of the channel surface depending on the local field structure. The next discharge of opposite polarity has a great probability of striking at the same point. Side channels may be produced in this way.

As has been mentioned in 1.1., the resistivity of an insulating surface exposed to discharges tends to change, usually downwards.

Apart from short-range electronic conduction in macromolecules, which is unimportant from a macroscopic point of view, electronic conduction occurs in carbon deposits. Electrolytic conduction appears to be the most important mechanism for discharge-induced reduction of the surface resistivity. Measurements of the changes of the surface resistivity of insulation during and after discharge exposure have been published in, for example,[13, 29].

Discharge- and radiation-induced changes of the surface activity of polymers have been studied in, for example,[30, 31].

The discharge action on materials is treated in, for example,[77, 92, 94] (various materials),[20] (epoxide resins),[32] (polyvinyl chloride) and[16] (micaceous insulation). Test results are reported in, for example,[44, 45, 48, 58, 74, 96, 120].

The related problem of high-voltage tracking on polymer surfaces and the possibility of insulation improvement is treated in, for example,[95].

1.4 **Electrical characteristics**

The magnitude, rate and energy of partial discharges are usually discussed on the basis of more or less elaborate circuit analogies of systems consisting of the voltage source, the stressed gas volume, the solid insulation, which

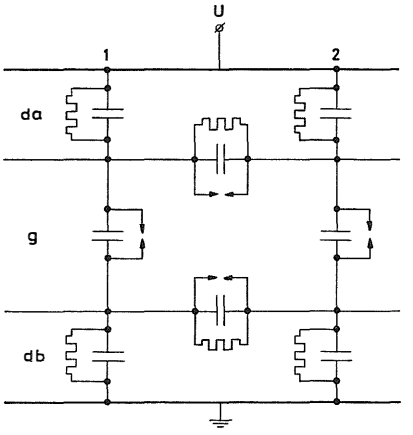

Fig. 1.7. Analogue network for the analysis of partial discharges in a gap bounded by insulation on both sides.

is characterised by its dielectric permittivity, the surface resistivity, where exposed to discharges, and of associated circuit components such as impedances in the source and the measuring circuit etc. For systematic surveys and bibliography reference should be made to the reviews of Whitehead[119], Mason[77] and Kreuger[66]. The assessment of the discharge intensity by means of dielectric loss measurements has also been studied by Böning[18]. Some points of special importance to our subject will be briefly treated in the following.

A general circuit analogy is shown in Fig. 1.7. When the applied voltage increases, at some location in the gap denoted 1, a certain area represented by C_g^1 is partly or completely discharged within a very short time. This leads to rearrangements of the charge in the dielectric in series with the discharge site, i.e., $c^1{}_{da}$ and $c^1{}_{db}$. Surface gradients are set up which also contribute to the redistribution of the charges, through coupling of, for example, the c^2's through the surface impedances $c_a^{1,2}$, $R_a^{1,2}$, $c_b^{1,2}$, $R_b^{1,2}$, etc. Secondary surface discharges may result, if the surface fields exceed a certain limit. The regions *a* and *b* may consist of the same or different dielectrics. As far as the author knows, no complete analysis of the general case, which furthermore should be treated in terms of cylindrical co-ordinates with the active discharge site in the centre, has been published. The cases treated in the literature are far-reaching simplifications.

If the gap is bounded by a conductor on one side, the region *da*, for example, vanishes as do the coupling impedances on the *a*-side, where the c_g's are connected. The remaining analogy is still complicated. Since transversal coupling of the discharge site with the surroundings is an undisputable experimental fact, attempts at an analysis have been undertaken by, for example, Heller[41],

Böning[17], Veverka[115] and Riege[100]. These authors have chosen to consider resistive lateral coupling. As a consequence of what is empirically known about the low mobility of surface charges on dielectrics exposed to discharges on the one hand[24, 99], and the conductivity level required to give any appreciable coupling effects on the discharges on the other hand[43], the author believes that capacitive lateral coupling also deserves attention.

A more far-reaching simplification is to disregard surface phenomena and to reduce the gap-dielectric analogy to a parallel arrangement of the active discharge site and the rest of the inter-electrode content lumped into one single capacitance. This circuit is illustrated in Fig. 1.8.

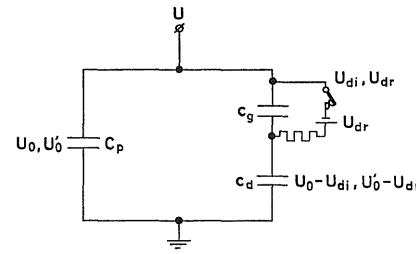

Fig. 1.8. Simplified analogue network for the analysis of the energy dissipation from partial discharges.

The energy dissipation from one discharge pulse is:

$$W = \Delta Q_p \left(1 + \frac{C_g}{C_d}\right)(U_{di} + U_{dr})$$

ΔQ_p is the charge supplied to the network when the initial voltage between the electrodes is restored. For the derivation of the equation, see[56].

A measure of the total dissipated energy or of the discharge power can be obtained through the determination of the pulse magnitude and pulse number or pulse rate. Pulse magnitude measurements with discharge detectors usually yield a value which in some way or other represents the statistical pulse amplitude distribution (the maximum pulse during a standardized time interval, the most probable pulse per cycle, etc.). Pulse rate measurements usually yield the total rate of pulses above a certain threshold or the rate of the pulses (maximum, most probable, etc.) given by the discharge detector. Variations in the pulse size distribution—either between different exposures or gradually during one exposure—may affect the ratio between the derived discharge energy or power and the true discharge energy or power.

When the mean discharge current is measured, the measuring procedure itself gives a proper averaging.

The factor $1+C_g/C_d$ in the energy equation reflects the fact that the energy dissipated by a single discharge exceeds $\frac{1}{2}c_g(U_{di}^2-U_{dr}^2)$. An additional contribution stems from the charge flow, which causes a change in the polarisation of c_d, as has been pointed out in[27] and further discussed in[54,56]. Garton[37] and others have earlier drawn attention to this effect without commenting on it in details. It is implicitly contained in Kreuger's[66] derivations of discharge characteristics.

The coupling effects between discharge sites in gas-solid dielectric arrangements of various types have been theoretically studied by some workers. Bui-Ai [19], for example, demonstrates that discharges on one side of a dielectric plate with gas gaps on both sides provoke and influence discharges on the opposite side.

The presence of a series impedance between the object containing the discharge site and the voltage source affects the discharge magnitude and pulse rate, as has been observed in this laboratory (see 3.6.) and analysed theoretically by Bui-Ai[19]. The effect of a series resistor on the pulse rate is equivalent to a rise of the discharge remanent voltage.

2. Discharge resistance testing I. Principles and survey

2.1 Deterioration of electrical insulation owing to partial discharges

Ample experience has been accumulated to prove that electrical insulations when exposed to partial discharges are liable to undergo damage leading to faults within time intervals far less than lifetimes under similar conditions, but in the absence of discharges[22, 70, 71]. The following practical examples may illustrate some points of interest.

Two water-wheel generators, each rated at 40 MVA, 9800 V (R.M.S.), 50 Hz, with shellac-micafolium stator insulation were installed in 1939 at Stadsforsen Power Station in the north of Sweden. During the war, the decision was taken to run the generators at overload and to accept a reduced lifetime of the insulation owing to the excessive thermal loading. One of the generators was rewound in 1953 after more than 110,000 service hours, of which 40 per cent at overload. The other generator was kept in service until a fault occurred in 1958. A considerable part of the stator winding of both generators underwent examination. The general findings, as reported by Nylund[86,87], were the following. All investigated coils in the first generator showed signs of thermal ageing in the coil-end insulation and in the slot insulation adjacent to the conductor strand. The binding and shellac resins in coils, which were only thermally aged, were no longer thermoplastic, and the organic wrapping (paper, textile) had become brittle. Nevertheless, the conductor strand was still rigidly anchored in the main insulation, which indicates that the coil as a whole was still able to take up the mechanical constraints occurring in service. While the thermal constraints were similar for all of the examined coils, the electrical constraints were different, depending on the location of the coil in the phase group. The investigation revealed that the state of the coil insulation was closely related to the coil voltage.

Three ageing groups could be discerned:

1. 0–3 kV to earth: thermal ageing only.
2. 3–4.3 kV to earth: more pronounced ageing, partial loss of adherence between conductor strand and insulation.
3. 4.3–5.6 kV to earth: far-reaching destruction of organic components, local calcination of mica splittings, strands movable in insulation, strand

insulation heavily degraded, presence of oxidation products in insulation and on copper strands (also nitrous compounds). Damage on outer surface of insulation.

These findings clearly demonstrate the effects of partial discharges on insulation. However, it should be borne in mind that the discharge action in the related case was combined with thermal ageing. The above-mentioned thermally induced increase in the rigidity of the binder might have aggravated the tendency of the insulation to delaminate under the action of mechanical constraints, which could have led to increased discharge activity in the insulation. Moreover, mechanical action, e.g., relative movement due to vibrations, seemed to have contributed to the insulation deterioration as witnessed by the presence of powder, together with chemical deterioration products, in fissures. The insulation of all the coils in the voltage range above 4.5 kV to earth was judged to be liable to failure owing to the bad condition of the strand insulation.

The most far-reaching examples of ageing were found in some coils from the second generator, which had suffered electrical faults. After the strand insulation had heavily deteriorated as described above, individual strands had gradually entered into relative motion with a grinding effect on each other and on the slot insulation. This phenomenon has also been observed in another machine.

Figs. 2.1–2.3 illustrate the insulation damage described above.

Another case of interest is the ageing of 6.6 kV electric motors. Insulation damage has been observed which cannot be attributed to thermal ageing alone. Roberts,[101] for example, describes damage at line voltage predominantly in interturn insulation and acid attack on the copper conductors in the slot part of stator coils. The role of partial discharges is thus evident. However, deterioration has been demonstrated in some cases in coils at voltages below the level at which intensive discharges in voids would be expected[6]. Thus, chemical deterioration sometimes occurs in a way and in sites which requires a more complex interpretation. Electrochemical corrosion mechanisms initiated by the chemical action of discharges have been proposed as an explanation as mentioned in[53].

These examples of discharge action on machine insulation demonstrate the complexity of the ageing situation. In contrast to, for example, homogeneous cable insulation, where the relevant feature of the discharge action is the gradual loss of dielectric strength of the insulation between the conductor and earth, the effects of discharge action in rotating machine insulation should be judged in relation to the combined dynamics of electrical, thermal, mechanical and chemical factors liable to influence the state of the insulation.

It is generally accepted in modern electrical power engineering that the

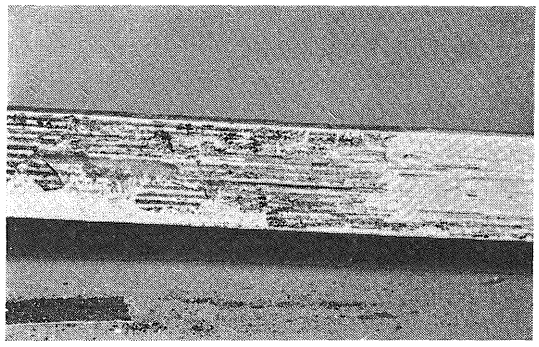

Fig. 2.1. Generator coil insulation damaged by partial discharges.

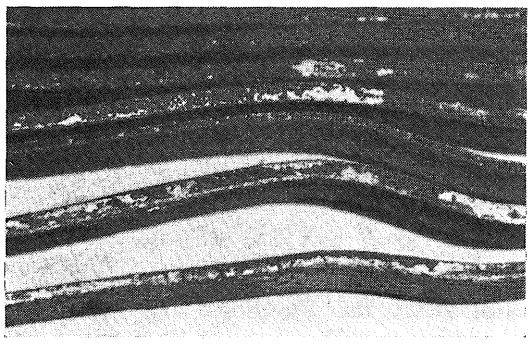

Fig. 2.2. Deformation of conductor strands caused by mechanical vibrations after deterioration of the strand insulation owing to partial discharges.

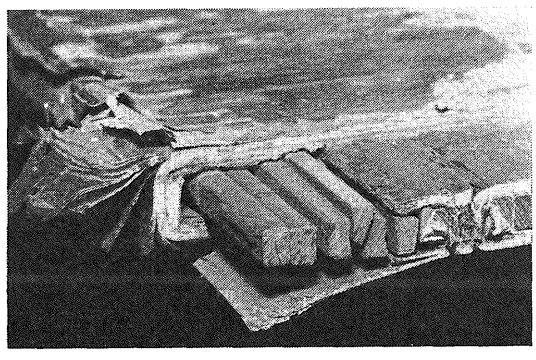

Fig. 2.3. Deformation of conductor strands caused by mechanical vibrations after deterioration of the strand insulation owing to partial discharges.

service life expectancy of apparatus is influenced to a considerable degree by the occurrence and intensity level of the discharges. The question of acceptable discharge intensity levels is of great importance in this connection. It is generally agreed that there is probably no safe threshold below which discharges would be completely innocuous. On the other hand, accumulated service experience demonstrates a satisfactory functional ability of apparatus in which discharges do occur. Different views on the discharge problem have developed in different fields of power engineering. Where insulation is subject to heavy electrical stresses, as, for example, in cables and capacitors, the tendency is to avoid discharges. The main attention is directed towards sensitive discharge detection techniques in order to assess product quality. International and national standards for such products pay much attention to the sensitivity thresholds of discharge detection equipment. Product development on the basis of acceptable levels and increased discharge endurance of insulation is attempted with great caution.

On the other hand, in rotating machine and to some degree in transformer engineering, there is a greater tendency to accept the presence of discharges during service. Consequently, the requirements on sensitive discharge detection, although still considered to be of great importance, are not so extreme. At the same time, the assessment of the discharge endurance of insulating materials and insulation is given very close attention. This is why extensive efforts are being made to develop adequate materials testing techniques.

2.2 On the principles of ageing testing[60]

The purpose of the testing of materials or devices is to obtain information, with the alternative aim of contributing to the realisation of a technical solution or of controlling the quality of a solution already obtained. The question to be answered by the testing is: what is best? or alternatively: is the solution good enough? It aims at the actual technical and economical function of the product in question and may be considered to have, in certain respects, a subjective aspect. The testing results, however, appear in terms of measured results and are therefore objective. Unawareness of this duality easily leads to misconceptions concerning testing and interpretation of test results.

Accelerated testing is needed for the assessment of the deterioration in time of materials, structural elements, and products, i.e., ageing and wear. Its aim is to obtain some kind of life prediction. Although laws of general validity can hardly be laid down, the following rules may, however, be found to be of some use as a guidance in the choice of accelerated testing procedure suitable for specific purposes.

A test ought to give answers of the type "live/dead" or "good enough/unsatisfactory" to permit the assessment of products or product parts so that either a choice can be made between alternatives or the quality of a choice can be verified. The quality criterion should be derived from technical experience gained from similar products and ought consequently to be specific to a considerable degree. The stresses on the object under test ought to reproduce the technical service conditions as closely as possible. Care must be taken that the changes in conditions which constitute the accelerating factor of the test will not create a new situation for the object.

Tests aimed at producing guiding information of value to the development of products need not possess the same high degree of specificness. More general response criteria can be chosen. They should be correlated, however, to the objective physical, chemical and other conditions of the object under test.

Intensification of the stresses to which the object is exposed may concern an intensive parameter, e.g., the temperature. The allowable intensification is then limited by the appearance of new mechanisms of change and significantly displaced equilibria. When the exposure has a periodic character, the frequency of the exposure cycle can be increased to a limit set by time constants —thermal, mechanical, etc.—characteristic of the object under test, and by time constants of material changes in the object (diffusion, chemical reactions, etc.).

Deterioration in simple cases is caused by a single process. The experimenter is concerned in many cases, however, with a chain of mechanisms. Ageing due to some dominant mechanism may bring the object to a state, where a different mechanism, owing to the same or a different factor of the constraint complex, gains importance for the subsequent change and so on. The observations of generator insulation ageing related in 2.1. are an illustration of such complex ageing.

2.3 **Basic views on discharge resistance testing of insulating materials**

Power insulation development involves several successive steps, which may comprise, for example: the choice of suitable materials and processing techniques, application into shape, the development of the insulation system, i.e., a realistic configuration of processed insulation and conductor, the design of the complete insulated structure. Suitable testing techniques are important for successful progress in all of these steps. The scope and consequently the philosophy behind the tests for the different steps in the development chain ought to be considered separately. This might be expected to lead to certain differences in the scope and techniques for tests intended to serve different steps in the development chain. They naturally form an evaluation

ladder, as the test procedure sequence has been very appropriately called by Mathes. For his views on the problem, see, for example,[82].

One and the same material may be used for different insulations in various types of equipment, where the typical stresses may differ and be of varying intensity. While the effects of discharge action on a given material in a certain specific application will signify the end of serviceability, these effects in a different application can hardly be considered as impairing the service characteristics of the insulation at all. Assessment tests for materials and simple combinations of materials should therefore give general information about their tendency to, and manner of, being affected by discharges. The results of such tests serve as guides for development work. The behaviour under the action of discharges of a structure composed of several materials formed into a certain shape by suitable technological processes is governed by the responses of the individual materials, which are assumed to be known from appropriate materials tests. However, there is always a possibility that significant deviations from the predicted behaviour of the structure may occur. These are caused by interaction between the materials, effects due to the technological procedure, and changes in exposure conditions and material reactions due to shape factors. The technical parameters chosen must therefore be checked by a different type of test, in which the stress pattern is correlated more closely to the service function under consideration. This implies the necessity of a more thorough modelling of the stress configuration met in service as compared with material assessment tests. On the other hand, the criterion applied to the test may be simpler in conception. The quality criterion adopted in many elaborate functional tests—as judged by some appropriate physical measure—is of the type "live/dead" mentioned in 2.2.

In power engineering functional tests for verifying the soundness of the chosen design must be performed, as a rule, on suitably designed models, since tests on full-scale products in many cases are excluded for economic reasons. Since the expected service life of the apparatus usually considerably exceeds 10 years, the testing procedure must also comprise some suitable means of intensification of the stresses leading to accelerated ageing. Increased voltage, frequency and temperature are adopted for discharge resistance testing. The combination of the above considerations leads to the concept of functional testing of insulating systems as a most important step prior to the final choice of the full-scale design.

Tests for evaluating materials and material combinations will mainly be discussed in the following. Work on functional testing of insulating systems exposed to discharges is in progress in different laboratories. However, sufficient experience of suitable quality criteria and the proper assessment of the integrated stresses have not yet been obtained to enable definite conclusions to be

drawn. Some aspects of system testing, however, will be mentioned in the following discussion of discharge resistance testing.

A considerable number of papers and reports describe methods for the discharge resistance testing of insulating materials. They differ in the geometrical arrangement of the discharge zone (arrangement of electrodes and dielectric, discharges between either metal and dielectric or dielectric and dielectric), in the condition of the atmosphere at the discharge site (closed or ventilated, air or other ambient), in the application of additional stresses to the dielectric (thermal, mechanical) and in the criteria applied to the assessment of the effects of the exposure.

It is a widely held opinion that the voltage-life of a sample exposed to discharges constitutes the most appropriate criterion for the discharge resistance of materials and that voltage-life tests are preferable for comparative assessments of insulating materials. This view is authoritatively advocated by Mason, see, for example,[78] and is supported by Kreuger[66], Stannett[84, 107, 108] and others. It seems to be widely held in the U.S.A., Great Britain and Germany[113], and is reflected in the drafting of the first IEC recommendation for discharge resistance testing of insulating materials, which at present is undergoing the last steps of the acceptance procedure (IEC TC 15B Endurance testing of insulating materials).

Another philosophy of discharge resistance testing of materials underlines the importance of the determination of the integral quantity of material affected by the action of discharges. This philosophy is widely, although not exclusively, held in France and constitutes the basis for investigations in several laboratories in other countries. As discussed in more detail below, the author is greatly in favour of this line of thinking.

The main argument of the voltage-life philosophy has been stated by Mason[78]: "The procedure is simple and the reproducibility of the results and the clear differentiation between materials ... indicate that they (*i.e.*, *specified testing techniques*) should be used as standard methods". Mason adds, however, the reservation: "It must be emphasized that correlation between the results of these tests and the behaviour of materials in service has still to be established, and the results should not be used for design purposes without consideration of differences between test and service conditions".

Voltage-life tests use a simple functional criterion for the assessment of the degree of deterioration of the tested material. The integral effects of the exposure are not determined. According to the discussion of the test philosophy in 2.2., voltage-life tests are functional tests, which should be performed where necessary (e.g., in cable engineering), i.e., if information about the specific feature of gradual loss in dielectric strength is sought. In such cases, care must be taken to see that there is an adequate correspondence between the stresses during service and in the test, with due allowance for acceleration.

The gradual breakdown of insulation through local channel formation caused by partial discharges is certainly of great importance in all branches of high-voltage power engineering. However, as has been demonstrated in 2.1 other material changes also influence the serviceability of insulation, especially where the stresses are of a complex nature as in rotating machinery. The author, therefore, suggests that discharge resistance tests for material evaluation should be based primarily on methods giving information about the integral material response, e.g., in terms of the quantity of degraded material suitably normalised with respect to discharge quantity. Such information should be supplemented by data from the same or additional tests of the loss of insulating ability of the materials concerned. The present difficulty of basing insulation life predictions on the absolute values of test results can be partly solved by means of comparative tests with the inclusion of materials for which sufficient service experience is available.

The suggested foundation for the choice of appropriate discharge resistance tests for materials avoids the complication of the establishment of a close correspondence between test and reality, which is an essential requirement for functional tests. This gives the experimenter increased freedom to concentrate on test conditions that can be properly controlled. The reproduction of all relevant service conditions is postponed to the subsequent stage involving the evaluation testing of insulating systems.

The use of test results based on the above considerations for insulating system engineering entails a comparative assessment of the liability of individual materials to overall deterioration and local deterioration, respectively, possibly supplemented by information about their tendency to self-extinction of internal discharges. The relative importance of the separate partial characteristics depends on the technical application in question. The evaluation of the test results will generally tend to rule out materials considered to be inferior for the actual purpose, rather then to single out some superior material. It may rightly be questioned whether the inclusion of materials with poor results according to the resistance tests necessarily need impair the life expectancy of the complete insulating system. This need not always be the case. Interaction between materials and special features of the stresses due to the specific design of the insulating system may result in its satisfactory performance as a whole. This question can only be resolved by means of functional system evaluation testing. However, since system testing is expensive in terms of both time and money as compared with materials testing, such a step is only justified if the "bad" material in question possesses some very attractive features for systems engineering, apart from its discharge resistance.

The following discharge situations are relevant to the ageing of insulation in apparatus:

Discharges in open atmosphere from conducting edges may occur on the

outer surface of cable insulation at cable terminations, and on the outer surface of machine coils where they leave the stator slot. Machine coils may also be exposed to discharges in the gap between the insulation and the slot, with edge effects by the cooling ducts. In all these cases, discharge suppression is usually achieved by means of resistive or capacitive field-grading measures. These are reviewed in[61], and the theory of field grading with the modern non-linearly conducting coatings is developed in[62].

Discharges in closed gas volumes between a conductor and insulation occur in defects, voids and gaps owing to adhesion loss at the inner surface of the insulation of, for example, machine coil insulation, transformer insulation and cable insulation. In some cases, attempts are made to suppress such discharges with methods that make the internal surface of the insulation conductive in order to reduce the field intensity on the conductor surface. Loss of adhesion between the strand insulation or strand bundle insulation and the main insulation in rotating machines may result in discharges. These may destroy the conductor insulation, after which the situation described above is established. The dielectric strength of the insulation may be reduced by pitting and treeing, which is particularly feared in cable and capacitor insulation. Loss of compactness in rotating machine insulation may develop locally or over extended regions. The mechanical rigidity may be impaired, and the heat flow resistance increased. The measuring techniques for determining the discharge intensity in apparatus are reviewed in, for example, [66,81]. A method for assessing the compactness of generator coil insulations through measurement of the heat-transfer coefficient is proposed in[59].

Discharges on the surface of a high-voltage conductor may also appear in the absence of macroscopic gas inclusions owing to local stress concentrations (edges of capacitor foils, mechanical irregularities on cable conductors).

Discharges between insulation surfaces occur in voids and fissures in the interior of the insulation. The effects may be similar to those mentioned above.

In addition to the effects of discharge action on the state and the properties of the insulation, discharge action also tends to alter the conditions for subsequent discharges. Two main trends are of importance. The first is a self-accelerating tendency resulting in a successive increase of the discharge intensity owing to changes in geometry of the voids in which discharges occur and in the field distribution. The other is a tendency for the attack to slow down owing to partial or total self-extinction of the discharges as a consequence of stress reduction as discussed in 1.1.

2.4 **Review of discharge resistance testing methods**

The discharge resistance testing methods reviewed below are divided into three groups: 1. total attack tests, 2. voltage-life tests and local attack tests,

and 3. internal discharge tests including treeing tests. The discussion of the tests in each group is preceded by tables summarising the main features of each individual testing method.

2.4.1 *Methods for determining the total discharge attack*

TOTAL ATTACK TEST METHODS

No. Developed by	Schematic arrangement	Material deterioration related to:	Exposure dose determined by measuring:	Material deterioration determined by measuring:
1 LCIE I (Hérou, Fallou, Bertein)		P	U, t (I)	Δm Dielectric strength
2 LCIE II		P	U, t (I)	Δm Dielectric strength
3 Caflisch, Woboditsch		P	U, t	Δm, ε, tg δ, Dielectric strength Tensile strength, elongation
4 Lab. Génie El. Toulouse (Lacoste)	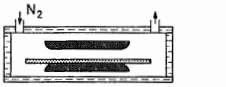	P	U, t Q, $\hat{N}$ (max Q in amplitude spectrum)	H_2-evolution
5 CERL (Stannett)	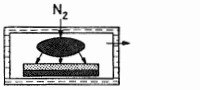	W_{tot}	U, t, Q	H_2-evolution
6 Present work		P	I_{md}, t, (U)	Δm CO_2-evolution
7 Lang		W_{tot}	U, $\int Q\,dt$	Erosion depth

Sample Electrode Insulation

Table 1.

In the L.C.I.E. method[44, 45] the exposure cell consists of a plane arrangement of highly discharge-resistant plates (Mycalex, Pyrex) held at a certain distance by an insulating frame. Voltage is applied to electrodes on the outer surfaces of the cell. The sample is inserted in the gap, see Fig. 2.4.*a*.

Discharges occur between two dielectric surfaces. The weight loss of the sample is usually taken as a measure of the deterioration.

The relation between the dissipated discharge power and the voltage applied to the cell has been theoretically shown to exhibit a flat maximum at a voltage, which is a function of the thicknesses of the sample and the gap. The sample thickness and cell voltage are chosen to yield discharge exposure at this maximum region in order to minimise the influence of variations of the sample thickness on the exposure conditions. Apart from the initial adjustment of the cell voltage, no discharge intensity determinations are usually made.

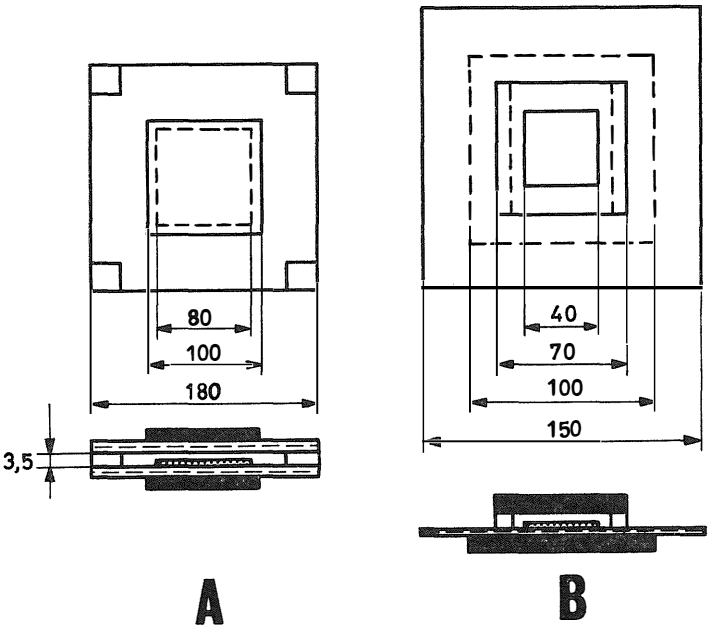

Fig. 2.4. Cell for total attack tests on insulating materials (L.C.I.E. cell).

In a variant of the cell, only part of the external surfaces is covered by electrodes in order to obtain separate information about direct discharge attack and the chemical action of the cell atmosphere, respectively.

In a recent modification of the cell the discharges occur between a metallic surface and the dielectric sample, see Fig. 2.4.*b*.

It is important when L.C.I.E. cells are being used that the sample should be plane and remain so during the test, since otherwise discharges may occur on both sides in an uncontrolled manner. This has been shown to affect the exposure conditions (see 3.5).

Similar cells with the sample exposed to discharges on both sides have been devised by, for example, Caflisch, Winkelkempner. In such arrangements there is an interdependence of the discharges on both sides as shown in[19].

Several variants of a cell[19,68,72] developed in the course of thesis work at the Electrical Engineering Laboratory of the University of Toulouse under the guidance of Professor R. Lacoste consist of a demountable Pyrex container with pressure seals. The cell contains two plane circular electrodes. The discharge zone extends between the high-voltage electrode and the plane sample, which is glued on to the low-voltage electrode by means of silicone grease and/or adhesive, see Fig. 2.5. Gas, usually nitrogen, is flushed through the cell from a cylinder. An arrangement of valves enables gas samples to be injected into

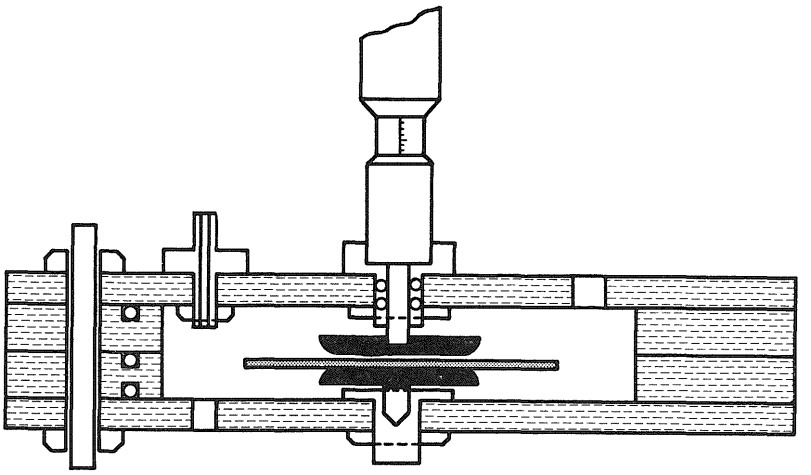

Fig. 2.5. Cell for total attack test on insulating materials (Toulouse cell).

a gas chromatograph. The concentration of a chosen gaseous degradation product is taken as a measure of the material deterioration. The choice of the gas component is made after a preliminary mass-spectroscopic analysis of the composition of the degradation products. In the case of polyethylene and similar unsubstituted aliphatic polymers, the hydrogen concentration is measured. The intensity of the discharge exposure is determined by pulse amplitude distribution measurements. The maximum of the distribution (i.e., the most frequently occurring discharge magnitude) is usually considered to be a measure of the entire distribution. The gap and sample thicknesses in this cell are also usually chosen to correspond to an experimentally determined maximum of the power/gap-width function. The integral degradation of the sample is obtained through integration of the envelope of the individual hydrogen (or other) evolution values as a function of time. The total discharge energy (i.e., the power-time integral) may serve as an alternative argument for the empirical degradation function.

At the C.E.R.L., Meats and Stannett[84] have developed a cell similar in function to the Toulouse cell, but with a different geometry, where in particular the gas volume is greatly reduced (25 ml). The high-voltage electrode with a spherical surface faces the plane sample. Gas (usually nitrogen) is supplied through small holes in the high-voltage electrode. The concentration of a suitable gaseous deterioration product is determined by gas chromatography.

Lang[69] has described a testing method with a spherical high-voltage electrode surface in open air facing the plane sample. The erosion depth under the electrode is correlated to the measured total charge associated with the discharges.

This relation is stated to be characteristic of the material under test and to be essentially insensitive to variations of the test parameters. However, not many details have been published about the method. Provided that geometrical similarity is preserved during the whole course of the attack, the eroded volume is proportional to a power of the erosion depth, and the method can be said to produce some measure of the quantity of deteriorated material as a function of the dissipated energy. The shape of the eroded portion might be subject, however, to change if the surface of the sample becomes conducting owing to moisture or other deposits.

The author and his collaborators have developed a testing method similar to the recent variant of the L.C.I.E. method. Details are given in Chapter 3. The discharge energy is determined from mean-discharge-current measurements, and the quantity of the deteriorated material is found by weighing as a routine procedure supplemented by carbon evolution determination for checking purposes.

The following general remarks can be made about tests based on the assessment of the quantity of degraded material:

1. The methods of determining the quantity of degraded material may be either direct or indirect. The direct methods may involve the determination of the concentration of some degradation product (gas chromatography, mass spectroscopy, chemical analysis, etc.) and yield instantaneous values, which must be integrated in order to yield the total degradation. They may also be directly integrating (accumulation of degradation products, e.g., in a suitable absorber, geometrical determination of the eroded volume, etc.). The main indirect method is the determination of the weight loss of the sample. Care must be taken to avoid systematic errors owing to, for example, oxidation or hygroscopicity of the sample.

Infra-red spectrophotometry is suitable for detecting chemical changes in a surface layer, but is not usually sensitive enough to make the method attractive for routine degradation measurements. This technique, which is direct and integrating if applied to the analysis of the exposed sample, is mainly of interest in special research. Electron spin resonance spectroscopy, which is a very sensitive method for the detection and identification of free radicals and the determination of their concentration, is to a still higher degree an exclusive research tool (necessity of complete absence of oxygen, special temperature requirements, etc.).

2. A large discharge zone is required, if gravimetric degradation measurements are performed, in order to obtain sufficient sensitivity. This is not required with gas chromatographic or mass spectroscopic techniques. Moreover, with these techniques, it is advantageous if the gas volume of the cell is as low as possible. The gas flow may be either straight or recirculating.

3. The discharge zone should be designed to produce as uniform an attack as possible. The size of the discharge zone should not change during exposure owing to sample erosion, surface deposits, etc.
4. The group of testing methods reviewed here satisfy the rules stated in 2.2 for the assessment of ageing properties of individual materials and simple combinations of materials.

2.4.2 *Methods for determining the voltage-life*

VOLTAGE-LIFE AND LOCAL ATTACK TESTS

No.	Developed by	Schematic arrangement	Material deterioration related to	Exposure dose determined by measuring	Material deterioration determined by measuring
1.	E.R.A. I (Mason)		U, t	U, f, t	Time to breakdown
2.	E.R.A. II (Mason)		U, t	U, f, t	Time to breakdown
3.	Dakin Perkins		U, t	U, f, t	Time to breakdown
4.	Starr, Endicott	see No. 3	U, t	Voltage linearly increasing	Time to breakdown
5.	Artbauer, Griač		U, t	U, t	Time to breakdown Dielectric strength
6.	C.E.R.L.	see Table 1:5	U, t	U, f, t	Time to breakdown
7.	Lang	see Table 1:7	U, t	U, f, t	Time to breakdown
8.	Damstra		U, t	U, f, t	Time to breakdown
9.	Stobernack I	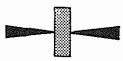	U, t	U, t	Dielectric strength
10.	Stobernack II				

Sample Electrode Insulation

Table 2.

In voltage-life tests with surface discharges, the deterioration criterion is the time to failure of the sample as a result of electrical breakdown. Differences between the various methods concern the arrangement of the electrodes and the sample.

The basic configuration consists of a cylindrical high-voltage electrode resting on a flat sample in contact with a plane low-voltage electrode. Results of tests with such a cell are given in great detail by Mason[78], who also describes a number of modifications, both of his own and of others. The formation of an electrolytically conducting surface layer round the H.V. electrode disturbs

the test[78,88]. Mason states that blowing of air into the discharge region is a sufficient counter-measure. Mechanically weak materials can be deformed by the weight of the electrode; a minute gap is recommended in such cases. Several workers make a point of rounding off the electrode edge. Several electrodes are combined in a common mounting and connected in parallel. This enables the dielectric sample to be utilised in a most effective manner. The test may be accelerated by raising of the frequency of the high voltage. A frequency of 1000 Hz is stated to be an acceptable limit where disturbing effects due to dielectric heating are still insignificant. The frequency is assumed to influence the voltage-life linearly, and the life is often given in terms of the number of voltage cycles.

Cylindrical electrodes with greater radius (25 and 55 mm) have been used by some authors, e.g., Perkins *et al.*[74].

Cylindrical low-voltage electrodes have been suggested by Mason for the exposure of mechanically stressed samples[78]. The high-voltage electrodes are orientated perpendicular to the samples.

A high-voltage electrode with a spherical surface, mounted some distance away from the sample and with gas blown into the discharge zone through holes in the electrode, used by Meats and Stannett for total attack determinations[84], has also been applied for voltage-life tests[107].

Damstra[26] recommends a needle-shaped high-voltage electrode some distance away from the sample surface. It is stated that the results are not markedly influenced by the radius of the needle tip. The test is accelerated through increasing the frequency of the voltage.

Starr and Endicott[109] have presented theoretical foundations for life tests with a linearly increasing voltage amplitude. They suggest criteria for revealing changes of the breakdown mechanism caused by the test.

Hewitt and Dakin[46] have investigated the influence of a number of parameters (temperature, sample thickness, humidity, electrode and sample geometry, etc.) on the test results.

The applied high voltage in the type of test discussed here serves a double purpose. It produces the surface discharges—tangential, perpendicular or oblique—which strike the sample surface, and it causes an electrical stress in the sample which eventually provokes breakdown. It is generally assumed that the voltage-life of a material must be determined at several voltage levels, usually three or four. This implies that the breakdown, which indicates the termination of a test, occurs at different stress levels. This well-known complication is usually disregarded. Some attempts have been made, however, to avoid it. One example is the exposure of test samples during certain time intervals, after which the dielectric breakdown strength of the exposed spots is determined separately[13,110].

When discharges occur from the edge of a cylindrical electrode, changes in

the state of the surface of the sample will often tend to influence gradually the size of the discharge zone[52], and, consequently, the discharge intensity in a given place (see Fig, 3.21). The exposure may then tend to change with time both in intensity and location. This must be regarded as a shortcoming in the method. An alternative solution is to arrange a plane discharge zone in a gap under a high-voltage electrode, see, for instance, Artbauer[4,5].

Voltage-life tests are reported by many authors to yield a relation between the voltage and the sample life measured in cycles, which is assumed to follow an exponential law, and a power-law dependence of the voltage-life on the stress. The decrease of the time to breakdown with increasing voltage is considerable. Owing to the large dispersion in the results, the information obtained from voltage-life tests is generally considered to be rather qualitative and mainly useful for comparative purposes.

In the light of the rules for ageing tests stated in 2.2, the voltage-life techniques are suitably characterised as being functional tests, as has been discussed in 2.2. The exposure conditions generally differ markedly from those encountered in service. The changes of the exposure during the test, which are often associated with these methods, do not either represent typical service conditions. The author agrees, however, with Mason[78] that the increased severity of the test as compared with reality may be an advantage for quick relative classification of insulating materials.

2.4.3 *Methods for determining the internal discharge resistance*

INTERNAL DISCHARGE TESTS

No.	Developed by	Schematic arrangement	Material deterioration related to	Exposure dose determined by measuring	Material deterioration determined by measuring
1.	Aleksandrov Kreuger Jokiniemi	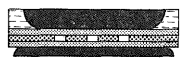	W,U	U,f,t	Time to breakdown
2.	E.R.A. (Parkman)	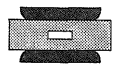	U,t	U,f,t	Time to breakdown
3.	Leu	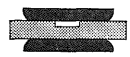	U,t	H.F.-noise voltage t	Dielectric strength
4.	Kitchin Milton Olyphant Present work	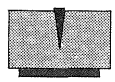	U,t	U,f,t	Time to breakdown Dielectric strength Number of pulses to breakdown

Table 3.

Several investigators have reported work on tests of the resistance of materials exposed to internal discharges. The interest shown in such tests, which are intended to simulate a situation commonly encountered in practice, is obviously the desire to derive quantitative information for direct application to equipment design work. The phenomenon of self-extinction of internal discharges, which is present to a varying degree in different materials, and the difficulty of gaining access to the exposed surfaces add, however, to the complications of such a test. This is probably the main reason why internal discharge testing techniques are still in a more preliminary stage than surface discharge testing. Some published results will be briefly reviewed here.

Artificial cavities for work with internal discharges are generally either spherical or cylindrical in shape with the axis in the direction of the field. Reynolds (private communication) has noticed the influence of the void shape on the discharge intensity. Spherical voids are produced in resin castings. Cylindrical cavities are produced either by milling or by punching; in the latter case a number of thin sheets are usually stacked together. Sealing of cavities in stacks of sheets is obtained through the application of pressure to the stack or through sealing of its rim with an adhesive. The low-voltage electrode usually consists of a plane metal plate or of a painted metal layer on the stack. The high-voltage electrode must be designed to avoid external discharges on the edge. It usually has a plane central region bounded by a rounded or sloping periphery and is potted in resin or surrounded by oil[67, 102].

Basic phenomena in cylindrical voids have been studied by Mason[75], Rogers[102] and others. Their findings explain the results summarised by Kreuger[67] concerning the influence of different parameters on insulation deterioration under the action of internal discharges. Kreuger's work is aimed at an assessment of voltage-life. He finds that the voltage-life is influenced by parameter changes, which affect the discharge power (e.g., the depth of the void). An increase of the diameter of a cylindrical void reduces the life. This may be understood against the background of the self-extinction mechanism discussed by Rogers[102]. The initial tendency for discharges in a wide cavity to concentrate on the periphery is explained by the field intensification on the periphery of a void in a dielectric medium as discussed by Heller[42].

Stannett and Meats[107] have observed a correlation between the voltage life of polyethylene exposed in the cell described in previous sections and the product of the field intensity, the maximum discharge amplitude and the pulse rate. Leu[73] has studied the formation in epoxies of channels from void surfaces.

Work with arrangements similar to the L.C.I.E. cell with static atmosphere is concerned with this topic[3, 4, 44].

Olyphant[91] quotes results which demonstrate that tests with surface and internal discharges, respectively, may lead to different classifications of materials,

and that raising the frequency of the high voltage scarcely, if at all, accelerates internal discharge tests. Both these findings are not surprising in view of the self-extinction effect.

The specific insulation deterioration pattern termed treeing has been demonstrated, as mentioned previously, to be caused by internal discharges. Treeing tests with a pointed high-voltage electrode surrounded by the material to be tested are described, for example, by Kitchin, Pratt[65], Olyphant[89,90] and in[110]. The time to breakdown under the action of a voltage of power frequency is observed. Visual observation of the degradation in transparent materials has revealed that this time may considerably exceed the time to complete penetration through the sample[89]. Leu[73] reports an induction period before appearance of the first trace of a "tree". Tests with impulse voltages are described by Milton[85].

3. Discharge resistance testing II. Experiments

3.1 Introduction

Experimental work by the author directed towards the development of suitable discharge resistance testing techniques for insulating materials and material combinations has been carried out along to the following lines:

1. Development of a testing technique aimed at an evaluation of the integral action of external discharges on materials, as the main source of information.
2. Assessment of the tendency to local penetration of insulation samples, subjected either to total attack tests or to separate exposure, as a source of supplementary information.
3. Supplementing of the external discharge techniques with methods permitting the assessment of the behaviour of materials subjected to internal discharges.
4. Work on voltage-life techniques as a contribution to IEC committee activities.

Some work, which has entailed considerable effort, is only briefly mentioned, whereas certain other questions are discussed in great detail in the light of the experience that has been obtained during the work of the types of experimental problem causing the greatest delays and errors. It should also be stressed that the accepted solutions are not always the absolutely best ones in the opinion of the author, but rather the best obtainable ones within the framework of an industrial research programme aimed at producing practical results as quickly as possible.

The experimental work described below covers the following subjects:

1. A standard test technique with external discharges in flowing air, which removes the products of oxidative degradation. Criterion: the loss of weight.
2. A modification of the standard test technique with the aim of detecting a possible deviation in standard test results owing to high oxidation sensitivity of the material under test.
3. A modification of the standard test technique entailing the direct determination of the carbon evolution from the sample. This modification serves as a check on the standard weighing method.

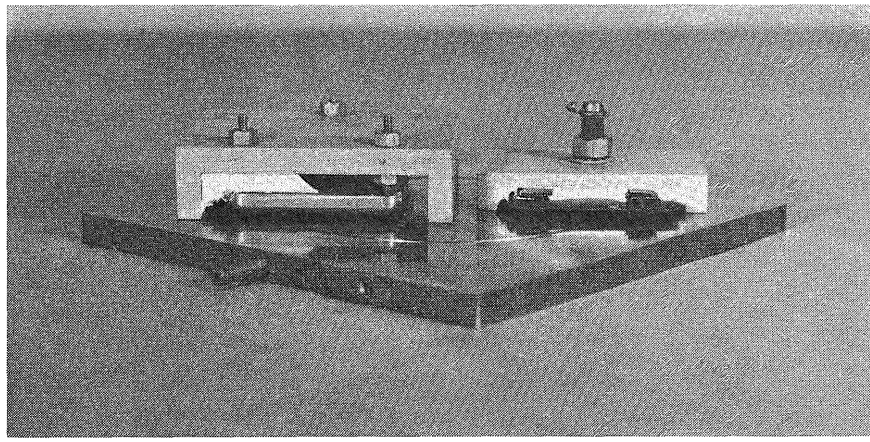

Fig. 3.1. High-voltage electrode assemblies and low-voltage electrode for standard test cell.

4. Attempts to gain information about the tendency of materials exposed in standard cells to develop local damage.
5. Development of a treeing test technique.
6. Experiments with voltage-life tests.

3.2 **Test cells**

3.2.1 *Standard cell for total attack tests*

The standard cell comprises a plane low-voltage electrode and a high-voltage electrode assembly.

The electrode assembly consists of a plane rectangular stainless steel electrode with well rounded edges, having the dimensions $70 \times 50 \times 8$ mm, mounted in an electrode support, see Fig. 3.1. The support is made of a ceramic semi-finished product called "Stumatit", which is easily worked by milling, drilling, etc., and which undergoes only slight deformation during the following oven firing at 1380°C. The basal plane of the support defines the lower boundary of the discharge gap. The gap is permanently set through adjusting the position of the electrode in relation to the support. The gap setting can be adjusted to within 0.01 mm with the aid of a gauge as shown in Fig. 3.2, which consists of a dial indicator protruding through a hole in a steel plate ground to a high degree of flatness on its upper side.

The space between the electrode and the support, both over the electrode and on the sides, is filled with plaster of paris in earlier types and with silicone rubber in recent types. This forces the injected air to flow into the gap and at the same time tends to suppress unwanted discharges elsewhere. This filling needs replacement from time to time, partly because of contamination and

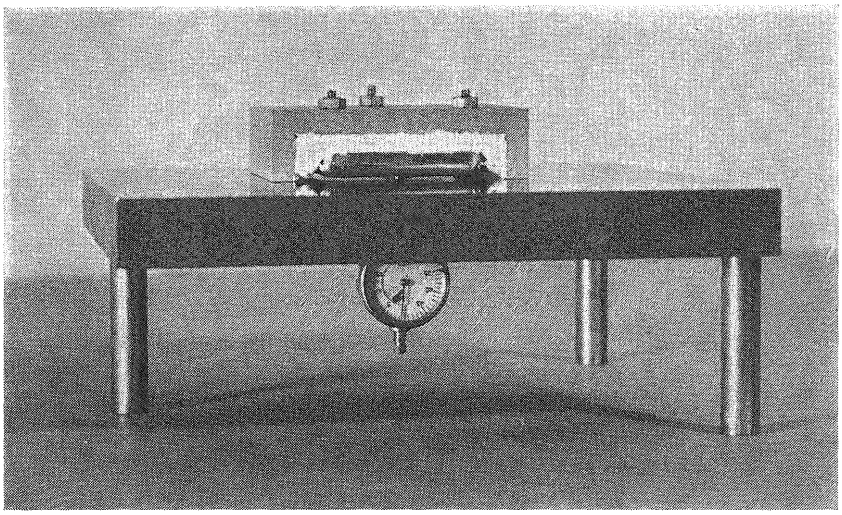

Fig. 3.2. Gauge for measuring the gap width of standard test cells.

deterioration of its external surface and partly in conjunction with the dismounting of the electrode assembly for mechanical treatment of the electrode surface. Silicone rubber was introduced because of its greater ease of handling and removal.

High-voltage electrodes are regularly inspected and cleaned with ethyl alcohol to remove organic deposits, which tend to appear during exposure. When the surface becomes permanently stained, it is repolished with fine-grade emery cloth. After long service an increasing number of small pits appear on the electrode, which necessitates grinding in the workshop.

The low-voltage electrode is also made of stainless steel. It is square in shape with the dimensions $160 \times 160 \times 10$ mm, see Fig. 3.1. The upper face is ground flat and provided with a circular groove, with a diameter of 100 mm, connected to a tube through which suction is applied in order to hold the sample in close contact with the electrode surface.

Fig. 3.3 shows how the air flow through the cell is arranged. Air is injected into a chamber of Stumatit having the same cross-section as the electrode support. On the side facing the electrode the chamber edge restricts the air flow to a passage of 1 mm in height before it reaches the electrode. The air emerges from the cell into the open at the opposite side of the electrode.

3.2.2 *Modification of standard cell for work with other gases*

The standard test cell is provided with air injection chambers on both sides. The joints and the lower rim of the cell parts are sealed with silicone rubber to permit exposure in a flowing or stationary gas.

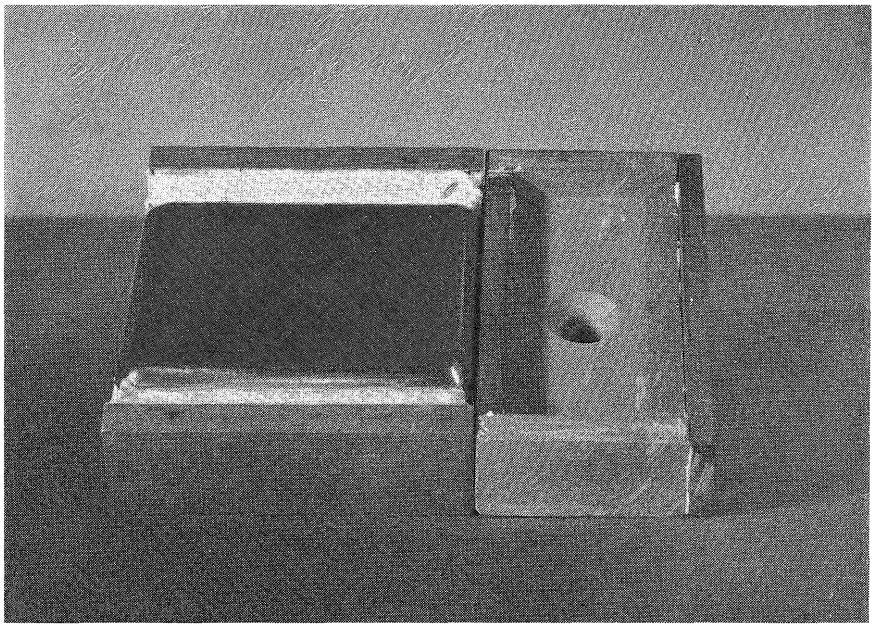

Fig. 3.3. High-voltage electrode assembly and air injection chamber.

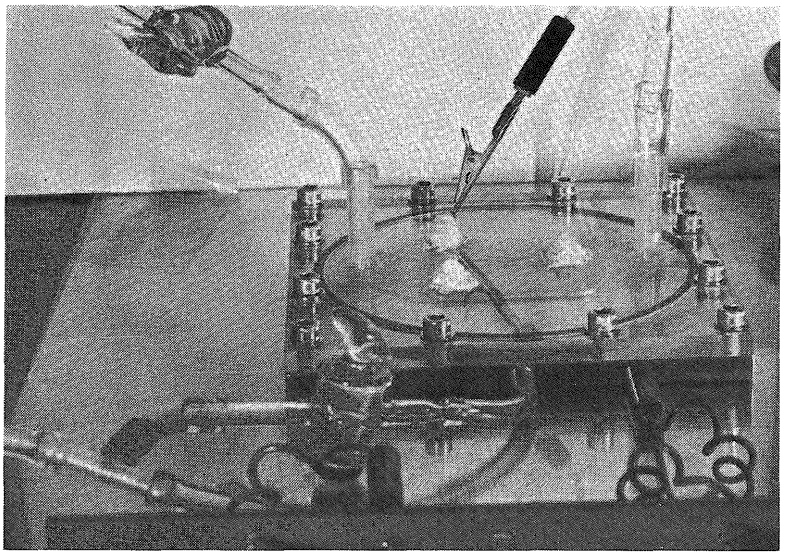

Fig. 3.4. Plexiglas cell for the determination of the carbon evolution from organic insulating materials exposed to discharges.

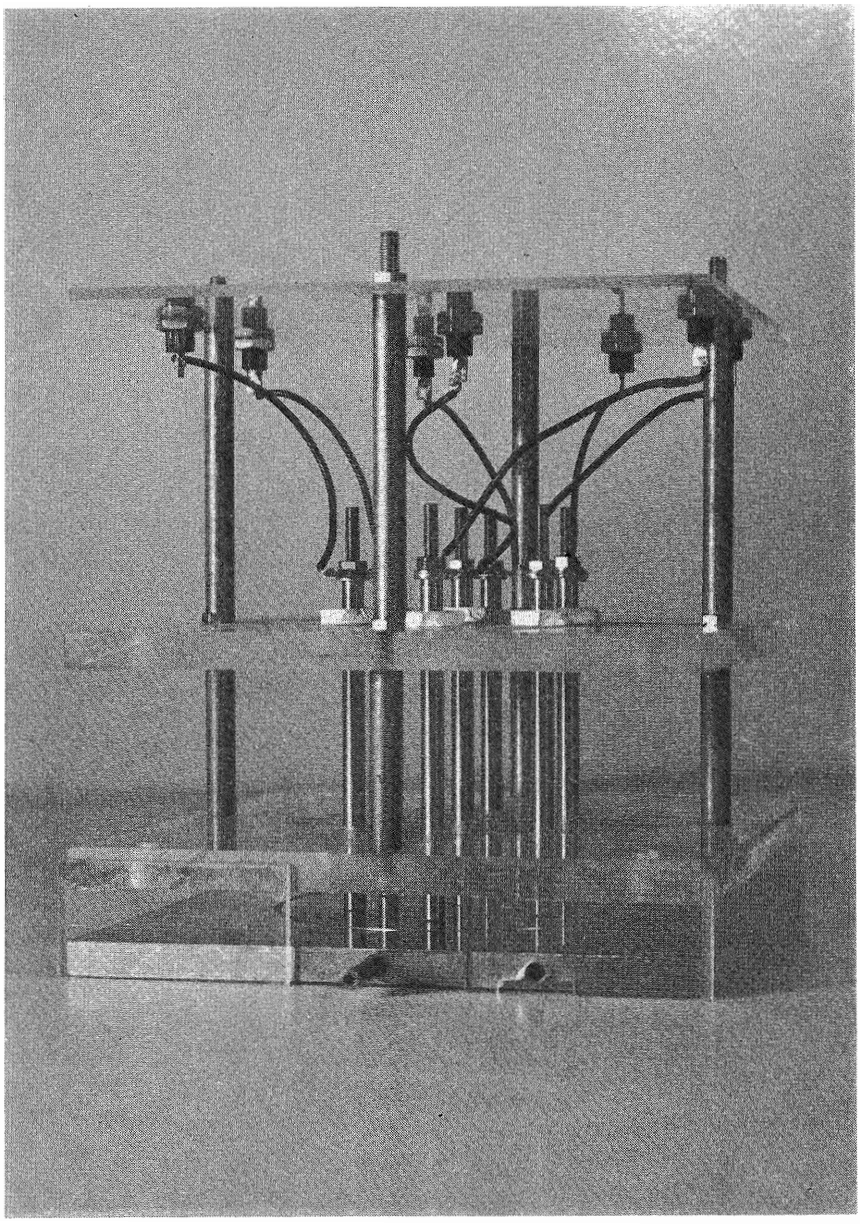

Fig. 3.5. Test cell with rod electrodes for voltage-life tests.

3.2.3 *Cell for carbon determination*

A cell with plane square electrodes, 40 × 40 mm, consists of two Plexiglas halves, which are bolted together, see Fig. 3.4. Sealing is obtained by an 0-ring. The sample is held tightly to the low-voltage electrode by a suction groove and, if necessary, silicone grease.

3.2.4 *Treeing electrodes*

A point-to-plane electrode arrangement has been adopted. The high voltage is supplied to the point electrode. Screening measurements showed that the tip radius of a certain make of sewing needle of nickel-plated brass was fairly uniform (10 μm). The needles are used without any preliminary treatment apart from cleaning. The low-voltage electrode consists of brass strip (8 × 1 mm) bent in the shape of a U. The assembly of the electrodes and the sample material into cylindrical test samples is described in 3.5. Voltage exposure of treeing samples is performed in transformer oil or silicone oil.

3.2.5 *Cell for voltage-life tests for IEC Committee work*

Seven polished stainless steel rods with a diameter of 6 mm and a length of 100 mm are arranged in a common Plexiglas support as shown in Fig. 3.6, with six electrodes placed along the periphery of a circle with a radius of 30 mm and the seventh at its centre. The electrode edges are slightly rounded. The high-voltage electrodes are free to move in the axial direction. The common plane low-voltage electrode is of the same design as that of the standard cell. The lower part of the support forms an air chamber with an inlet on one side.

3.3 Supplies

3.3.1 *High voltage*

High voltage is supplied from resin-potted transformers rated at 13 or 20 kV (R.M.S.), 125 VA, which are energised via individual Variacs. Each transformer feeds a rack with ten test sites. A capacitor of about 20,000 pF is connected permanently across the terminals of each transformer in order to reduce the effects of source impedance and inter-cell coupling on the discharge pattern (see 1.4).

The low-voltage electrodes are arranged on a rack and are separated from a common earthed aluminium plate by a Plexiglas plate. The individual low-voltage electrodes are connected to earth via resistors of about 3 kΩ with terminals on the front panel for connection of the current-measuring device. The resistors are externally short-circuited except when current measurements are being made, since they otherwise tend to deteriorate. In spite of this

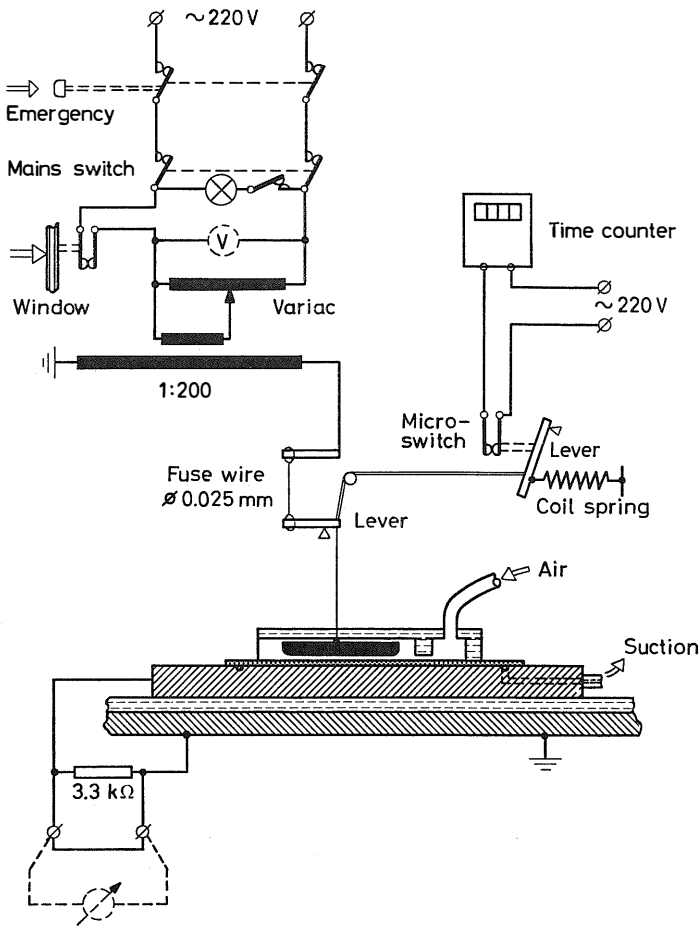

Fig. 3.6. Standard test cell with associated electrical circuits and air supply.

precaution they should be checked from time to time, because cases of deterioration have been observed, possibly due to ozone corrosion.

Each high-voltage electrode is connected to the common supply via a melting fuse, Fig. 3.6, which consists of a very thin spring-loaded metal wire (copper, 0.03 mm gauge, or Kanthal 0.025 mm gauge). The spring load is mechanically transferred to a microswitch, which on release interrupts the voltage supply to an electrical time counter. The time to breakdown will therefore be recorded.

Each supply rack is provided with suspended Plexiglas windows for safety and each window actuates a microswitch, which interrupts the power supply when the window is not in position.

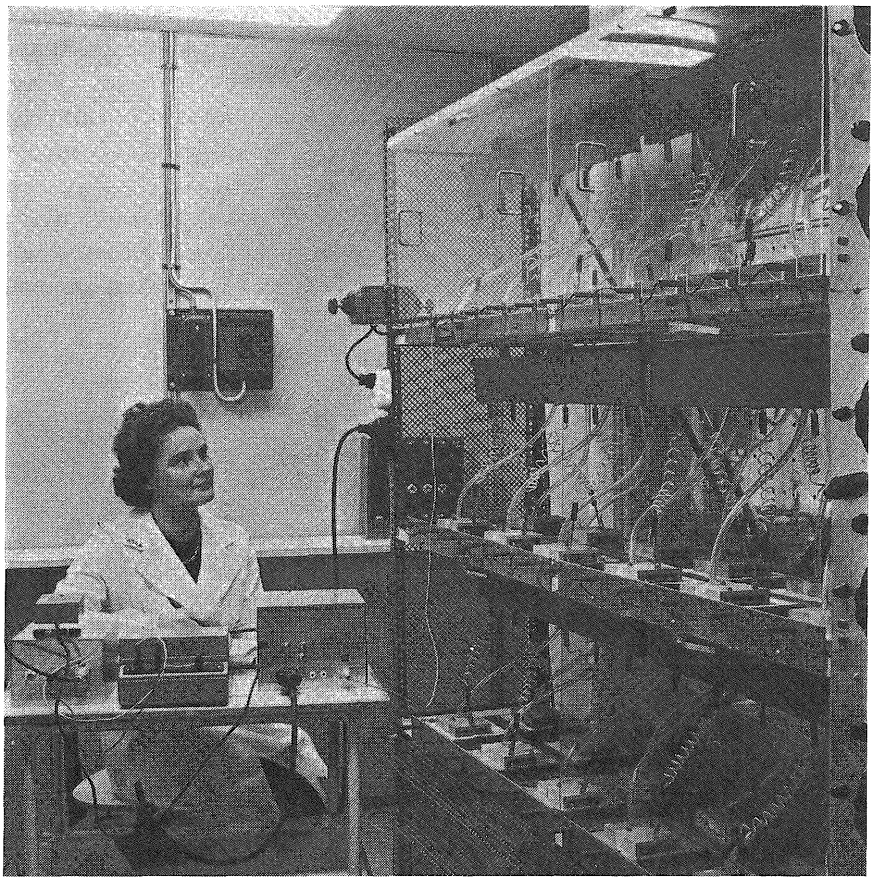

Fig. 3.7. Racks with standard test cells.

A panel on the side of the test rack is provided with the Variac dial, a switch for the line voltage and terminals for primary voltage measurement. The voltage signal lamp is provided with a switch to enable it to be switched off during observation of discharges. A large pushbutton switch enables all power to be switched off in an emergency.

The test racks, see Fig. 3.7, are designed in the first place for total attack tests, but are also used for the other tests and experiments being performed in the programme.

3.3.2 *Atmosphere*

The standard test cells require an ample supply of air, because the flow rate adopted is 2 l/min. The air should be of constant quality, dust-free and preferably with a low water content. Early attempts with drying in silica-gel beds

were found to be excessively troublesome, because of the frequent need of regeneration of the drying agent. A satisfactory solution was the installation of a self-regenerating Munters air dryer, model M 100, which supplies 150 m^3/h of air dried to 10 per cent RH or better against a pressure head of 15 mm H_2O.

For runs in standard cells with other gases, e.g., nitrogen, gas is supplied from a storage cylinder.

The air leaving working discharge cells carries a considerable concentration of ozone. Forced evacuation of the laboratory is therefore required to avoid inconvenience to the personnel. The equipment may also suffer from prolonged ozone exposure.

3.3.3 *Tests at elevated temperature*

For exposure at elevated temperature, standard test cells are installed in a heating cupboard, which can be set to temperatures up to about 200°C. Improved temperature equalisation is obtained through forced ventilation. The air supply to the cells is led through a few turns of copper tubing inside the cupboard (total length about 5 m) in order to adjust the temperature of the injected air to within 3 deg of the temperature of the heating cupboard.

3.4 **Measuring methods**

3.4.1 *Discharge current*

The mean value of the current represented by the integral charge transfer caused by discharge pulses in unit time is measured with a galvanometer. This is connected in series with a cell during the time interval when discharges of one polarity take place and disconnected during the discharge sequence of opposite polarity. Reversing the switching phase enables the discharge current components of both polarities to be determined separately. The polarity of discharges coincides with the sign of the time derivative of the voltage. If the switching instants are adjusted symmetrically in relation to the zero passages of the voltage cycle, the mean value of the power-frequency current in the time interval during which the galvanometer is connected to the cell disappears.

The switching device must be very robust and have as low a series resistance as possible. An electromechanical chopper with gold-plated or mercury-wetted contacts has therefore been chosen. The connection of the chopper and galvanometer is shown in Fig. 3.8. A phase-shift network permits adjustment of the connection interval of the galvanometer in order to minimise the power-frequency current component. Fig. 3.9 shows a typical current-voltage characteristic of a test cell. A slight power-frequency current component, however, remains after the phase-balancing. Discharge-mean-current readings are corrected through subtraction of the power-frequency current determined

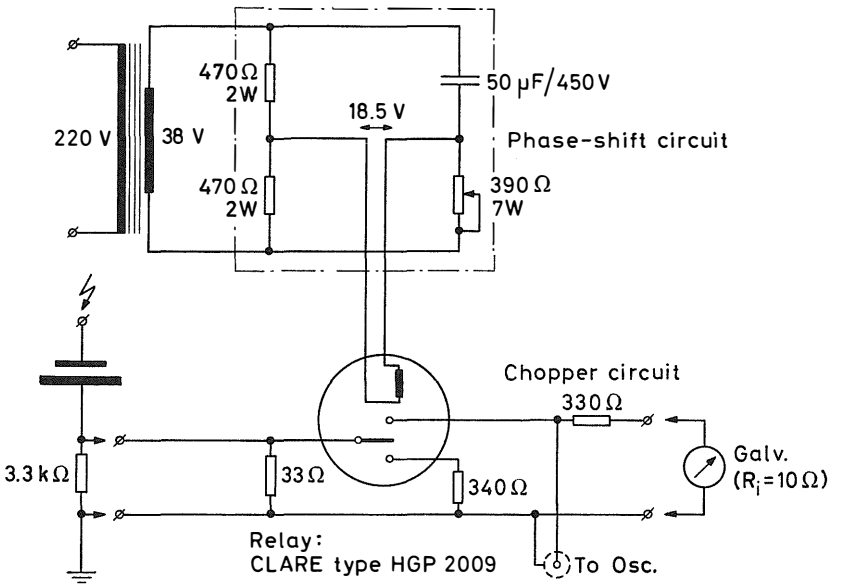

Fig. 3.8. Circuit diagram of mean discharge current measuring device.

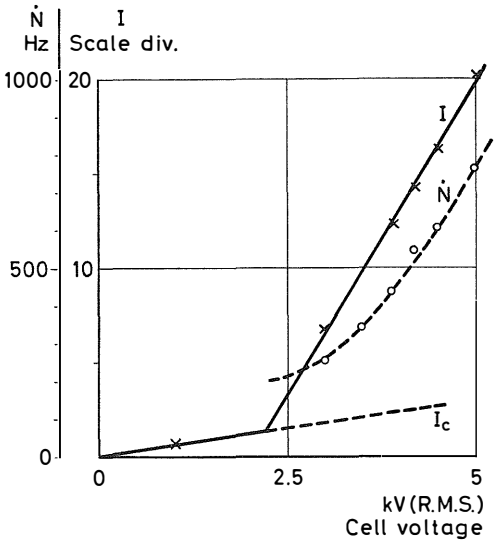

Fig. 3.9. Mean-discharge-current readings I and pulse rate $\dot{N}$ from a standard test cell as a function of the applied voltage.

by linear extrapolation, because the power-frequency signals only appear in linear impedances.

The discharge-mean-current measuring device has been calibrated with direct current, audio-frequency square waves up to 20 kHz, and sequences of rectangular pulses of variable duration and constant repetition rate, respectively. The results were identical. Variation of the pulse shape at constant pulse charge did not affect the galvanometer deflection. The positive and negative discharge-mean-current components have been repeatedly demonstrated to be identical, despite the difference in pulse shape and pulse rate when discharges occur in gaps bounded by metal and dielectric surfaces, respectively. Gradual change in the operational characteristics of the chopper were found to have a slight influence on the calibration constant of the device. Occasional recalibration of the measuring device is therefore recommended.

The equipment used in the current measuring device consists of a chopper (Stevens Arnold 6.3 V, D.C.-A.C., Clare HGP 2009) and a Norma light-spot galvanometer model 251 U with an internal resistance of 10 Ω and current ranges of from 5×10^{-8} A/scale division upwards in powers of 10. A 10 Ω resistor is connected to the contact pair working in opposite phase to the galvanometer in order to assure constant conditions in the cell circuit except during the switching time intervals. These time intervals at the tops of the voltage wave, however, are always free from discharges.

3.4.2 *Discharge pulse rate*

An oscilloscope and a pulse-rate meter are used for determining the discharge-inception and discharge-extinction voltages and for pulse-rate measurements. The signal is taken from the terminals of the 3 kΩ resistor in series with the test cell. An amplifier and discriminator stage is inserted before the pulse-rate counter. In this way, also small pulses are counted, and overloading of the counter resulting in blocking is prevented. The instruments used are a Tektronix Type 531 A oscilloscope with a plug-in CA preamplifier, and a General Radio frequency-meter type 1142 A. For high resolution work, the frequency-meter should be set to a high frequency range despite the resulting low readings.

3.4.3 *Weight determinations*

Sample weights are determined with an analytical balance of the constant load type. When samples are handled, clean nylon gloves reserved for the purpose are worn. Prior to weighing, samples are dried in a heated cupboard at as high a temperature as possible, preferably 120°C, for 0.5 or 1 hour. Materials which deform at this temperature are dried at 80°C. From the cupboard the sample is transferred direct to a desiccator containing silica gel and is allowed to cool. A period of 0.5 hours in the desiccator before weighing has been standardised.

3.4.4 *Determination of carbon evolution*

A direct-flow method is used. Air from a gas cylinder is passed through a quartz tube containing palladium-asbestos catalyst heated to 800°C in an oven to convert all carbonaceous matter into CO_2. This is absorbed in Ascarite, a reagent containing NaOH. After this, the carbon-free air is passed through the discharge cell. From the cell the air is led through another heated tube with catalyst and from there through a parallel combination of two 2 l gas pipettes, which can be connected up alternately. The air leaving the pipette passes a gas volume counter and is then released. The CO_2 concentration in a pipette is periodically analysed by a coulometric method according to Oelsen and Abresch[1] in a Ströhlein apparatus. The total CO_2 production is estimated through integration based on linear interpolation of the measured values, and is transformed into terms of sample material.

The relation between the weight loss and the CO_2 evolution from a material is calculated from the chemical formula. Thus, 1 g of polyethylene terephthalate contains 0.625 g of C, which yields 2.3 g of CO_2. For epoxy resins the ratio of weight loss to CO_2 evolution varies, depending on the resin-hardener formula. A typical value is 2.6 g of CO_2 per gramme cured resin. The sensitivity of the CO_2 determination is about 5 μg. When a 2 l gas pipette and an air flow of 0.35 l/min are used, the erosion of PET at a rate of 1 mg/h corresponds to 0.22 mg of CO_2 in the pipette. With 1 l/min this figure is reduced to 0.063 mg of CO_2.

3.4.5 *Dielectric strength*

A linearly rising alternating voltage source (1 kV/s) is used for determination of the remaining dielectric strength of treeing samples. It consists of a motor-driven Variac and a high-voltage transformer. The melting of a fuse (see 3.2.1) interrupts the high-voltage supply to the sample. The primary voltage supply to the high-voltage transformer and the supply to the Variac motor are simultaneously interrupted by a relay. The voltmeter connected across the Variac output continues to indicate the voltage.

3.4.6 *Sample capacitance measurement*

The capacitance of the sample under an electrode having an area equal to that of the high-voltage electrode is measured for determination of the discharge-mean-current correction (see 3.6). A small universal bridge, e.g., Marconi type TF 2700 with a measuring frequency of 1000 Hz, is used for this purpose. The measurement is performed between an ordinary low-voltage test cell electrode and a 6 μm thick Mylar film with a painted silver electrode of the same size as the high-voltage electrode on its upper side. Initially, the film is placed on the steel plate and the capacitance C_s of the foil is measured. The

sample is then inserted and the combined capacitance C_c is determined. The sample capacitance C_d is given by

$$C_d = \frac{C_c}{1 - \frac{C_c}{C_s}}$$

In this way, possible changes in the state of the foil are eliminated. C_s is approximately 3000 pF and C_d usually lies in the range between 100 and 300 pF. The advantage of this method lies in the ease with which a close contact is obtained between the measuring electrode and the sample surface without the latter being contaminated. The lower surface of the foil is frequently cleaned with ethyl alcohol.

3.5 **Sample preparation**

Material in the form of sheet or film is cut into square or rectangular samples with the smallest side exceeding 110 mm. The observation that discharges sometime occur between the sample and the low-voltage electrode leading to premature breakdown has led to the adoption, as a standard measure, of metallisation of the lower side of the sample. This is done through the spraying on of a colloidal silver suspension. The silvered samples are dried in order to remove any remaining solvent (this may be combined with the first drying of the sample before weighing). During prolonged exposures the metallisation is inspected together with intermediate weighing. A yellow or brown discoloration indicates oxidation. The silver layer should than be removed by washing with ethyl alcohol and the metallisation renewed.

Soft materials, for example, plastics at temperatures above the glass-transition point, may be lifted from the low-voltage electrode through the action of electrostatic forces between the high-voltage electrode and the charged sample surface. In such cases, the exposure conditions (gap width, geometry) are radically changed, and the calculated energy dissipation will be erroneous. This phenomenon can be detected visually and appears as a marked change in the discharge-mean-current and in the discharge pattern on the oscilloscope screen. A remedy, which should always be used in work at elevated temperatures, is to reinforce the sample by glueing it on to a metal plate. The use of hard aluminium plates for reinforcing prefabricated sheets and foils was discarded; the difficulties in removing the adhesive solvent were excessive. The use of rigid grid plates was found to be a satisfactory solution. The plates must be protected against corrosion, since this will otherwise affect the weight of the reinforced sample. The adhesive must be stable during exposure.

Samples for treeing tests are prepared in a form shown in Fig. 3.10 by means of a casting technique. A silicone resin mould with cylindrical depres-

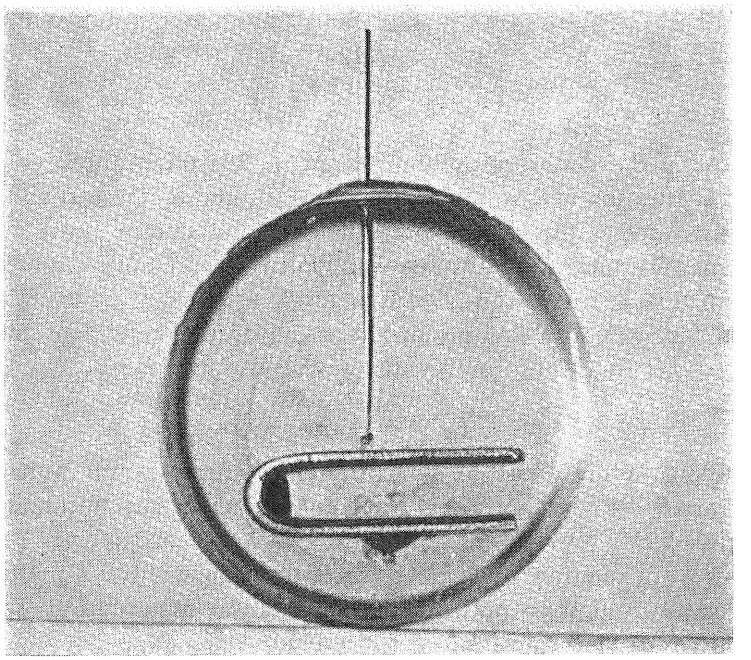

Fig. 3.10. Epoxide resin sample for treeing experiments.

sions is initially made by casting of a plate in which glass beakers are inserted. A U-shaped electrode is placed on its edge in each depression and a needle is inserted through the wall. The proper electrode spacing is manually adjusted through the insertion of a gauge strip. Resin is then charged into the mould and cured. For treeing tests on sheet material, a piece of sheet is inserted between the electrodes, and a cylindrical test sample is prepared as described above.

3.6 **Development of a standard method**

It may be assumed as a starting hypothesis that the quantity of degraded matter is proportional as a first-order approximation to the energy dissipated from the discharges. This hypothesis is supported by results of Meats and Stannett[84] and Hougen (quoted in[100]).

The expression for the discharge energy in terms of measurable magnitudes given in 1.4 can be transformed to the following expression for the dissipated discharge power:

$$P = \frac{1}{2} U_{di} I_m \left(1 + \frac{C_g}{C_d}\right)$$

or

$$P=\frac{1}{2}U_{di}I_m\left(1+\frac{d_d}{kd_g}\right)$$

where U_{di} is the discharge-ignition voltage, I_m the mean discharge current, C_g and C_d the gap and sample capacitances, d_g and d_d the gap and sample thicknesses, and k the relative permittivity of the sample, see[27, 56] for the derivation. The measured discharge-inception voltage U_i may be used as an approximation instead of U_{di}, which might be assumed to be approximately constant for work with flowing air under standardized conditions. Since ideally $U_{di}=U_i(1+C_g/C_d)^{-1}$ applies, the discharge power is given by

$$P=\tfrac{1}{2}U_iI_m$$

According to the above expressions, the discharge power is determined by the mean discharge current I_m and influenced by the thickness of the dielectric, which governs C_d, and of the gap spacing, which governs C_a and U_{di}, respectively. In addition, the permittivity of the sample affects C_d. The nature of the gas as well as its pressure and temperature influence U_{di}. The effect of the electrode area enters into the measured value of I_m.

The direct determination of the mean discharge current has the advantage that the averaging of the individual discharge pulses is carried out during the measurement, which therefore automatically takes care of possible changes in the pulse amplitude distribution.

The externally measured pulse charges, the time average of which is measured through I_m, are caused by polarisation changes in the dielectric affected by partial discharges. This mean current is denoted I_{md}. As stated in 3.4.1, a correction I_{mc} must generally be applied to I_m to account for a remaining line frequency component. Thus, $I_{md}=I_m-I_{mc}$ is the current value to be inserted in the power expression.

The dependence of I_{md} on the voltage applied to the cell is normally linear in the working range of voltages. Fig. 3.9 is a typical example. An upward bend of the $I_{md}-U$ line is sometimes observed at high voltages. In such cases, either a lifting of the sample, which alters the cell parameters, or the occurrence of edge discharges is observed.

The variation of I_{md} with the gap setting is shown in Fig. 3.11 with the cell voltage as parameter.

The pulse rate $\dot{N}$ follows the current.

An investigation of the influence of the gas flow on the discharge conditions has revealed that I_{md} and $\dot{N}$ vary markedly with the flow rate at low gas velocities, but that stable conditions are established at higher velocities, see Fig. 3.12. For routine work it is an advantage to use gas flow rates on the level part of the curve. Closer inspection of Fig. 3.12 shows that, while I_{md} is stationary

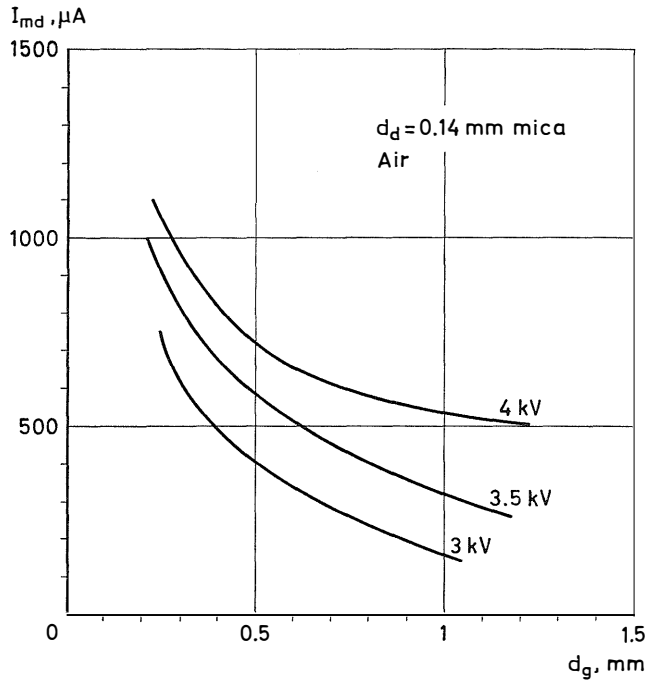

Fig. 3.11. The mean discharge current I_{md} in a standard test cell as a function of the gap width d_g.

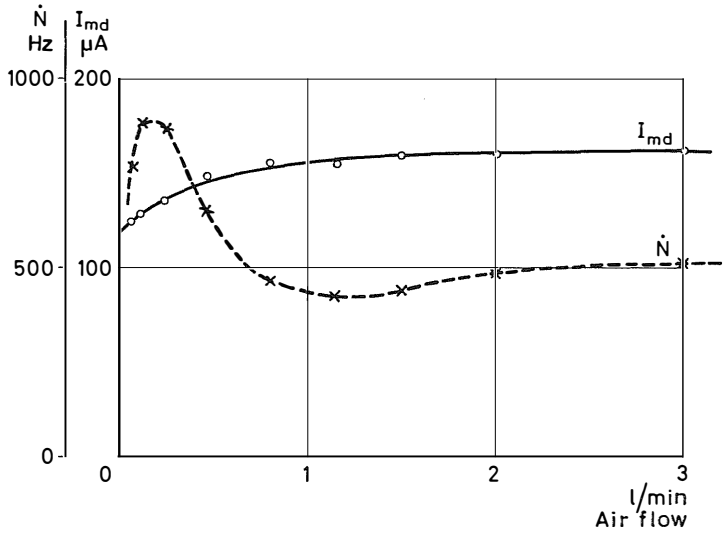

Fig. 3.12. The mean discharge current I_{md} and the pulse rate $\dot{N}$ in a standard test cell as functions of the gas flow rate through the cell.

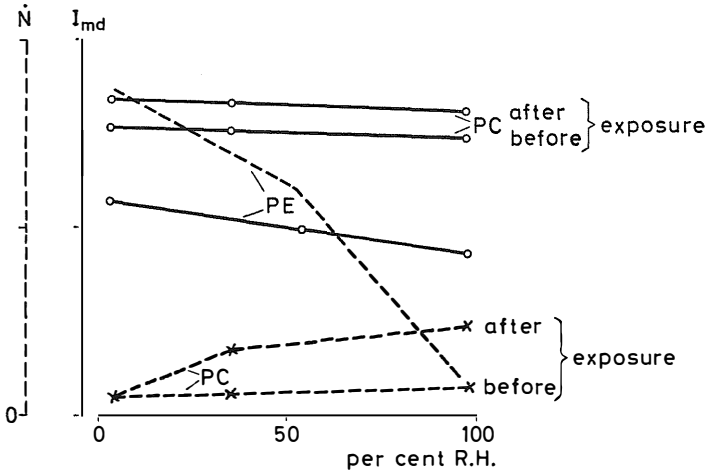

Fig. 3.13. The mean discharge current I_{md} and the pulse rate $\dot{N}$ in a standard test cell with polyethylene (PE) and polycarbonate (PC) as dielectric versus the relative humidity of the air blown through the cell.

for flow rates above about 0.5 l/min, $\dot{N}$ continues to change slightly. This is probably the result of the gas flow on the surface properties, e.g., the surface resistivity, of the sample to which $\dot{N}$ reacts in a sensitive way.

The discharge characteristics are also affected by the humidity of the gas flowing through the gap. Fig. 3.13 shows the influence of the air humidity on I_{md} and $\dot{N}$ in cells with different dielectrics. This demonstrates the importance of humidity normalisation, preferably at low levels, for a standard procedure.

During the development of the high-voltage fuse, the first variant of which was based on a published design[74] and comprised a series resistor of some megohms, it was discovered that the discharge conditions are affected by the impedance of the circuit outside the cell. A systematic study of cells arranged in series with resistors of different R_s-values revealed a dependence of I_{md} and $\dot{N}$ on R_s for a constant applied voltage as shown in Fig. 3.14. This phenomenon is considered in terms of circuit parameters as mentioned in 1.4. It implies a marked decrease of the mean pulse magnitude up to the pulse rate maximum. This may be described in qualitative terms as a consequence of the voltage drop across the series resistor caused by an individual pulse with an effect equivalent to an increase in the discharge remanent voltage as indicated by Bui-Ai[19]. The discharge sequence above the pulse rate maximum is governed by the time constant determined by the series resistance and the cell capacitance. Both the shape and the recurrence of the discharges are regular in this region, which demonstrates a collective working regime in contrast to the individual pulse regime for low series resistance values

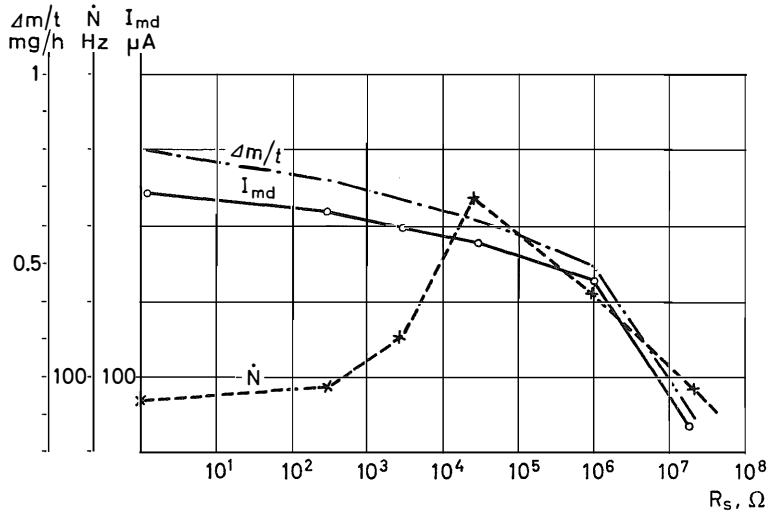

Fig. 3.14. The mean discharge current I_{md}, the pulse rate $\dot{N}$ and the weight loss per unit time $\Delta m/t$, as functions of the resistance R_s in series with the cell.

with slight coupling only between the discharge sites. An interesting feature of the phenomenon is the possibility in the constant current region of adjusting the mean pulse size at essentially constant discharge power through the insertion of resistors in series with the cell.

The shape of the $\dot{N}-R_s$ curve should be affected by factors influencing the coupling between discharge sites, e.g., through the surface resistivity of the sample. Dick in this laboratory has carried out a series of experiments with the object of using the shape of the $\dot{N}-R_s$ curve for obtaining information about the state of materials exposed in test cells.

The relation between the weight loss Δm of samples exposed in test cells and the dissipated energy may be considered as somewhat analogous to the g-factor used in studies of the influence of radiation effects on matter, i.e., the number of ruptured bonds per 100 eV of energy loss of the incident particle. However, the discharge resistance of materials should be characterised by an index, which has a higher value for better material. This is the case, for example, when the voltage-life is adopted as a criterion. Consequently, a total attack index G may be defined as follows:

$$G=\frac{Pt}{\Delta m}=\frac{U_{di}I_{md}\left(1+\frac{C_g}{C_d}\right)t}{2\Delta m}$$

The time t and the weight loss Δm are measured quantities. The discharge power P is derived from measured values of I_{md} (usually I_{mdp}, i.e., the positive

discharge mean current after correction for the power-frequency component), and C_g/C_d or d_d/kd_g. The discharge-ignition voltage U_{di} is either derived from the discharge-inception voltage of the cell, in which case the term $(1+C_g/C_d)$ disappears in the power equation, or is related to the Paschen value. In the latter case, the results of the investigation in[56] are taken into account through the assumption of $U_{di} \approx 0.8\, U_p$, which in a general way reflects the limited validity of the adopted analogue model and the possible occurrence of a discharge remanent voltage. In comparative work with a constant air-gap width, the value of U_{di} is constant and therefore without great importance.

Thus,

$$G = \frac{0.8 U_p I_{mdp} \left(1 + \frac{C_g}{C_d}\right) t}{\Delta m} = \frac{0.8 U_p I_{mdp} \left(1 + \frac{d_d}{k d_g}\right) t}{\Delta m}$$

or alternatively

$$G = \frac{U_i I_{mdp} t}{\Delta m}$$

With the usual dimensions,

$$G[\mathrm{J/kg}] = 2.9 \times 10^9 \; \frac{U_p[\mathrm{kV(peak)}]\, I_{mdp}[\mathrm{mA}]\, t[\mathrm{h}]}{\Delta m[\mathrm{mg}]} \left(1 + \frac{C_g}{C_d}\right)$$

or alternatively

$$G[\mathrm{J/kg}] = 4.1 \times 10^9 \frac{U_i[\mathrm{kV(R.M.S.)}]\, I_{mdp}[\mathrm{mA}]\, t[\mathrm{h}]}{m[\mathrm{mg}]}$$

In the present work the G-values are based on U_p rather than on U_i. Working with a gap-width of 1 mm gives $U_p = 4.5$ kV (peak). Thus,

$$G_{1\ \mathrm{mm}}[\mathrm{J/kg}] = 1.3 \times 10^{10} \; \frac{I_{mdp}[\mathrm{mA}]\, t[\mathrm{h}]}{m[\mathrm{mg}]} \left(1 + \frac{C_g}{C_d}\right)$$

A series of tests have been undertaken to investigate the influence of different factors on G.

The effect of the sample capacitance C_d has been studied by means of the following technique. Identical thin polymer foils were exposed in cells with Plexiglas plates of different thicknesses inserted between the sample and the low-voltage electrode. In this way C_d was varied from 100 to 710 pF for polycarbonate. Fig. 3.15 shows that G is not affected by changes in C_d. The testing procedure need not therefore comprise normalisation of the sample thickness or capacitance.

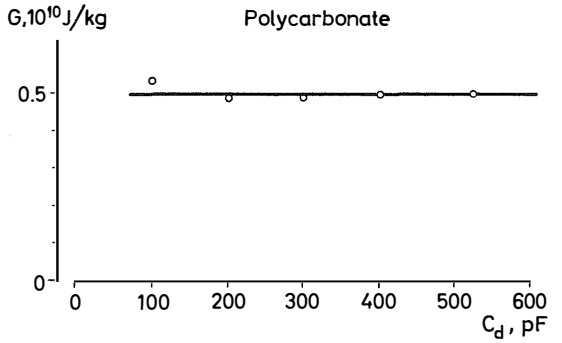

Fig. 3.15. Dependence of the discharge resistance index G on the capacitance C_d of the dielectric sample in the cell. Constant gap and cell voltage.

Changes in the cell voltage affect the current I_{md}. Fig. 3.16 shows that G remains essentially unaffected by changes in the cell voltage. Changes which are observed in some cases should be considered in the light of the apparent change in the discharge regime as a function of the current, which is discussed in[56]. However, the dispersion of the G-value due to this effect is not so great that special precautions need be taken in routine tests. The test voltage is suitably chosen to yield a mean-discharge-current value within a reasonable range. A current of 0.1 to 0.25 mA has been adopted in this laboratory. The voltage supply ought to be stabilised within about 1 per cent in order to keep the variations of the mean discharge current below approx. 3 per cent. The wave form of the voltage is important for the discharge regime in the cell. The necessary precautions should be taken to prevent possible load changes from affecting the wave form of the voltage.

Fig. 3.17 illustrates the effect of a variation of the gap width d_g on G. Here, d_g influences both C_g and U_{di}. G is calculated with the aid of U_{di}-values

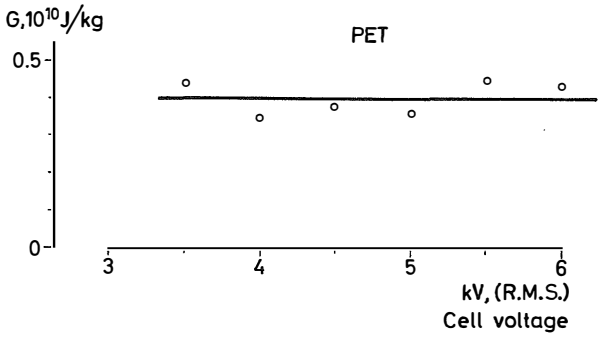

Fig. 3.16. Dependence of the discharge resistance index G on the cell voltage. Constant gap width and sample thickness.

and possible observations are recorded. After this, it is dried and weighed. If the test is continued, the high-voltage electrode is placed as close as possible to the previous site.

3.7 **Modifications of the standard method**

The purpose of the sealed standard test cell for work with other atmospheres than air is to check whether the discharge resistance value of a material as determined by the standard method is significantly affected by oxidative degradation. A low N_2-flow rate is usually applied in work with these cells. In preliminary tests with polyethylene terephthalate film, which has been adopted as a standard test material because of the considerable experience accumulated during all the development work, a good correspondence with the *G*-value of the standard method has been found. Good correspondence between *G*-values in air and N_2 has also been obtained with an epoxy resin. Runs with a slow flow rate of air, on the other hand, gave erroneous results, obviously as a result of oxidation of the sample with incomplete removal of the degradation products. A loose white deposit is often observed on the sample surface in work with the sealed cell. This is carefully removed after the weighing procedure with a suitable organic liquid, which is known not to dissolve the sample. Drying and weighing are then repeated. The results obtained with this technique help the experimenter to judge the applicability of *G*-values to the prediction of the behaviour of materials subjected to internal discharges.

The purpose of the carbon determination technique (see 3.4.4) was also to check the standard method. It was intended in the first place as a means of judging the correctness of the weight-loss determinations. An attempt was first made to determine the integrated carbon evolution from the sample by means of a closed air circuit with forced circulation. Carbon was oxidized to CO_2 as described in 3.4.4. This method was abandoned, however, because of considerable experimental difficulties, the main cause of which was that the effects of all disturbances (carbonaceous matter and water from pump, rubber or plastic tube joints, and leaks) were also integrated during the measurement. The direct-flow method described was successfully adopted. Zero runs (1 *h*) with mica inserted in the cell yielded equivalent CO_2-values of less than 5 μg for the normal mean discharge current value of 0.2 mA and of 0.04 mg for 0.4 mA, when discharges were observed to strike the Plexiglas support outside the electrode area. The sensitivity of the method (see 3.4.4.) enables determinations to be made of values corresponding to weight loss rates down to about 0.1 mg/hour. The total measuring error in *G*, assuming a constant discharge gap and normal exposure conditions is estimated to be less than 10 per cent.

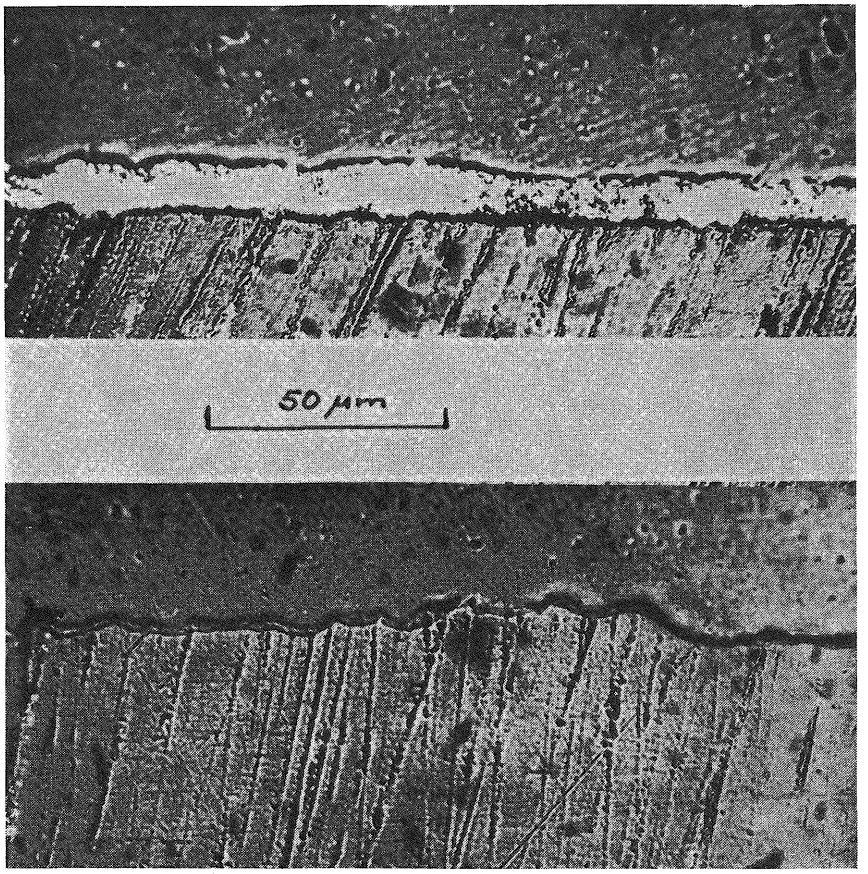

Fig. 3.18. Micrographs of transversal sections (with oblique grinding marks) of terephthalate foils.

a. Before exposure to discharges.
b. After exposure to discharges.

3.8 **Assessment of local erosion in samples after standard test**

Various attempts were made to develop techniques for revealing any tendency of the discharge attack in the standard test to produce local erosion of the sample surface.

Surface profiles were investigated through the cutting of pieces of exposed material and the preparation, by metallographic techniques, of polished specimens for microscopic examination of the transversal section. A number of photographs enabled, for example, the irregularities on an exposed PET surface to be estimated to be on the average 10 μm in width and 5 μm in depth. Details were investigated by electron micrography with oblique metal shading. Figs. 3.18*a* and *b*, show sections and Figs. 3.19*a* and *b* the surface structure

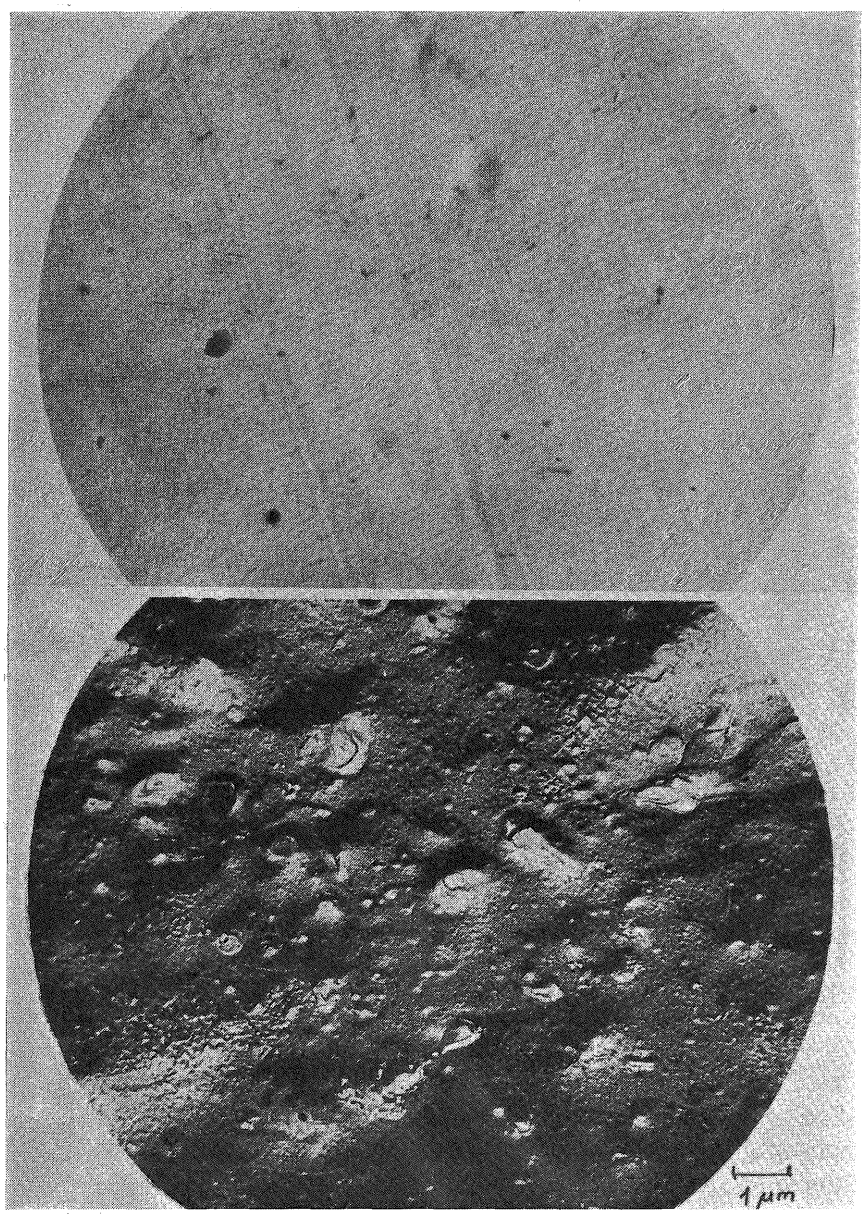

Fig. 3.19. Electron micrographs of the surface of a terephthalate foil.

a. Before discharge exposure.
b. After discharge exposure.

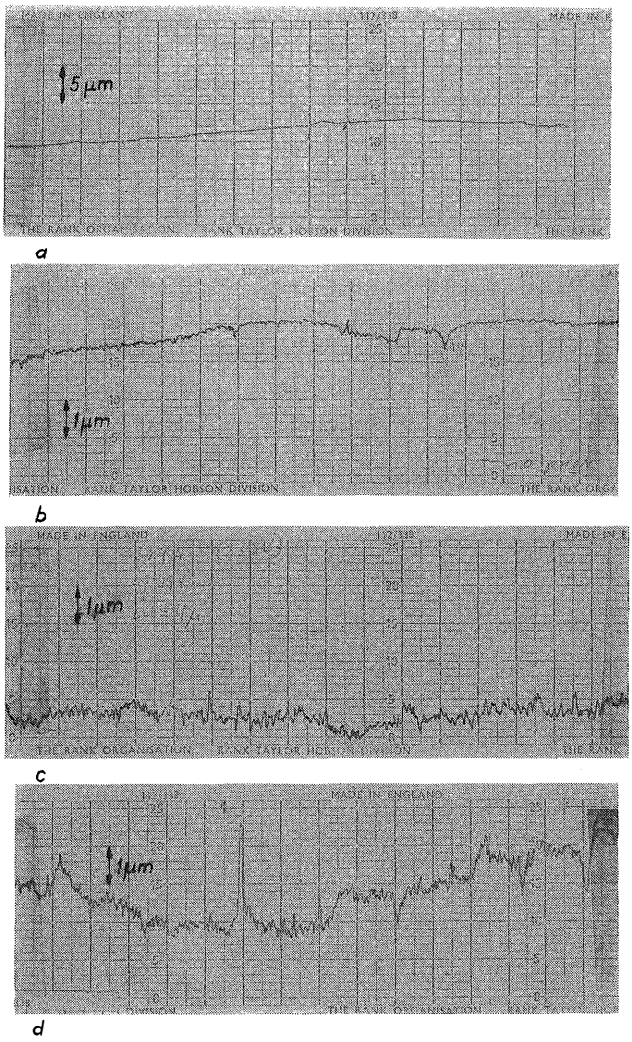

Fig. 3.20. Profilograms of polyimide foils exposed to increasing discharge doses.

a. Discharge exposure 0 hours.
b. Discharge exposure 24 hours.
c. Discharge exposure 40 hours.
d. Discharge exposure 70 hours.

of PET surfaces exposed to discharges. The conclusion was drawn from the optical investigations that erosion in the form of very thin, deep channels is not common under the exposure conditions in the standard test cell.

Trials were made to trace sample surface profiles by means of a Taylor-

Hobson apparatus, in which a sensing point 5 μm in diameter is slid across a surface with a load of 100 mg. This method is of limited value to the detection of narrow, deep pits, but it reveals protrusions. Figs. 3.20*a*, *b*, *c* and *d* show profilograms of 127 μm polyimide film exposed to increasing doses. An increasing degree of surface roughness due to the action of discharges is apparent.

Electrical measuring methods might be appropriate for indicating and assessing a tendency for narrow pits to develop from the exposed surface. Preliminary considerations of the measuring accuracy required made it clear that a successful technique would require much development work. A technique for determining the local dielectric strength of thin samples was developed by Kvandal in this laboratory to an accuracy of 1.5 per cent using coaxial needle electrodes. Repeated measurements on different sites of the same sample were made possible through the sealing of the punctures with pads of adhesive insulating tape. The breakdown tests were carried out in air; the use of transformer oil was thought to mask the effect of pits on the local dielectric strength. A great number of breakdown measurements on unexposed and exposed insulating films were statistically treated and yielded a thickness/strength relation in support of a square-root law given in, for example,[77]. After due consideration, however, the method was rejected as a standard technique for the assessment of local erosion. It was thought that this discharge attack characteristic should not be assessed in the first place on samples exposed in the standard test cell, but that the exposure conditions ought to be modified. Work on the development of a treeing test was therefore initiated.

Capacitance measurements yield integral information about the whole electrically stressed area under the electrodes and are not therefore expected to react sensitively on the occurrence of local defects. The most promising approach in this field seems to be that of Mayoux[83], i.e., measurement of C and tan δ at different frequencies. The formation of a slightly conducting surface deposit caused by, for example, electrolytic conduction in an adsorbed water film, yields a considerable contribution to C and tan δ with a decreasing trend at increasing frequency, whereas the true dielectric C and tan δ are usually far less dependent on the frequency. Changes in the state of the sample surface may be detected in many cases with great sensitivity with differential measuring techniques. This method is being applied with a General Radio impedance comparator type 1605 A.

3.9 **Treeing tests**

Moulded homogeneous epoxy-resin samples, which are transparent, were used in a series of preliminary experiments.

Voltage was applied to samples placed under a stereo microscope at 40–200 x magnification. It was observed that the growth of the main and side channels

from the point electrode appeared to proceed in jumps rather than uniformly, which confirms observations reported by Baker[8].

A number of test samples were exposed repeatedly during increasing time intervals in order to obtain information about the channel growth velocity at different applied voltages. The results are presented in[57], see p. 133 of this issue. The duration of the exposure interruption appears to affect the propagation velocity of treeing channels.

Samples were exposed so as to produce different penetration depths, which were determined visually in the stereo microscope using an ocular micrometer. The dielectric breakdown strength was then determined with a linear voltage rise. No dependence of the breakdown voltage on the thickness of the remaining material under the channel tip could be found.

Treeing tests with opaque materials are suitably performed as time-to-breakdown tests.

Treeing tests should be performed at different voltage levels. The temperature effect on the treeing resistance of materials is also an important characteristic.

3.10 **Voltage-life tests**

In the course of IEC Committee work, when tests performed in different laboratories were compared, voltage-life tests were carried out with the cell described in 3.2.5[51, 52]. Fig. 3.21 shows the appearance of an exposed PET film after breakdown. The degradation pattern was observed to change gradually during the exposure. The radial and tangential discharges described in Chapter 1 (Fig. 1.6) were observed with the present electrode configuration. The average time to breakdown was found to be influenced by the introduction of a 0.3 mm gap under the electrode with constant cell voltage. When the voltage was adjusted to give a current equal to the gapless configuration, however, the lifetimes differed less than the standard deviation of the measurements. It is perhaps worth considering whether the current rather than the cell voltage, or both these together, should be adopted as the guiding exposure measure in voltage-life tests.

3.11 **Results**

Tests with the standard and other techniques described here have been performed on a variety of pure and composite materials. Some general information about the accumulated experience will now be given.

When homogeneous materials are exposed to discharges in standard test cells, a stationary regime is established after a short time, usually not exceeding 0.5 hours. It is supposed that the modified surface layer is formed during this time, and that it subsequently grows downwards and is eroded from the top at

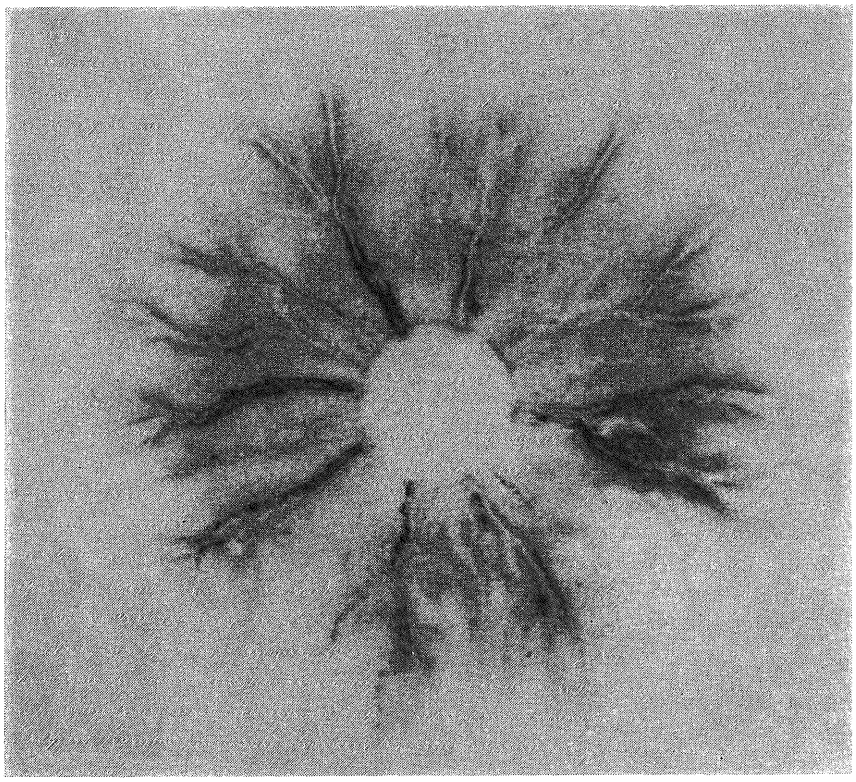

Fig. 3.21. View of a sample exposed to surface discharges in a voltage-life test.

about the same rate. Even when homogeneous materials are tested, it has been found suitable to divide the exposure into two or three periods. The first period is usually 18 to 24 hours, which gives information about possible formative effects caused by an original surface layer having properties differing from those of the body of the material.

A formative period is nearly always present in tests with filled or reinforced materials. The surface layer is likely to have a higher concentration of the base material—resin or other material—than the average. If the incorporated component is discharge-resistant, as is the case with inorganic materials, a gradual increase in the *G*-value with time is found. A stationary *G*-value should be obtained. If this is not the case, a closer investigation of the deterioration is called for. Visual and, possibly, microscopic inspection of the exposed surface is always to be recommended. Many peculiarities of discharge attack would otherwise escape attention.

As an example, samples of a certain glass-fibre-reinforced epoxy resin showed a tendency for the glass-resin bond to be destroyed in the exposed surface

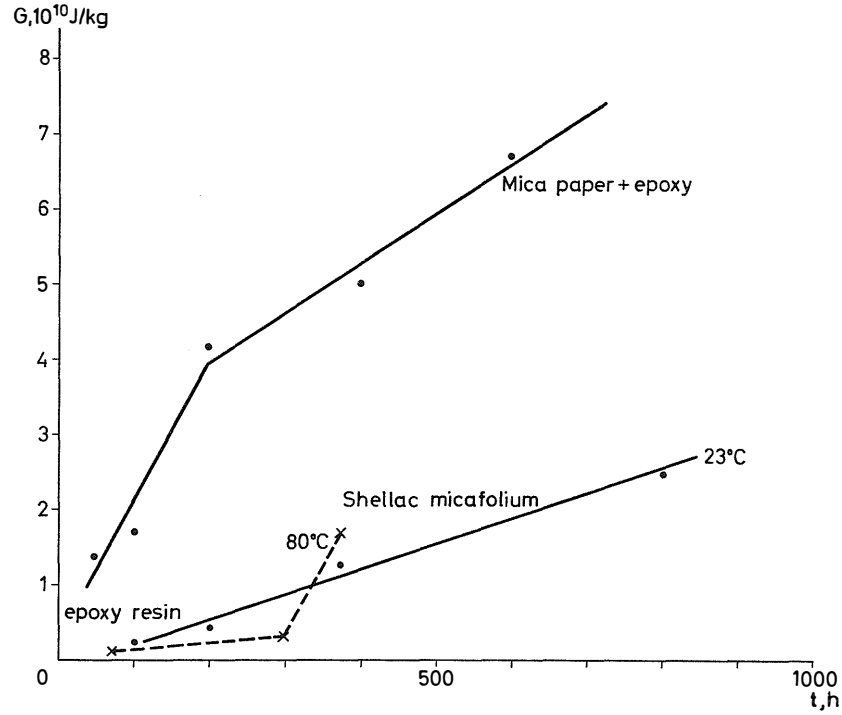

Fig. 3.22. The discharge resistance index G versus time at constant exposure intensity.

region. Individual glass fibres were then seen to have become detached along a considerable length. Optical examination, which is often impaired by similarity of the refractive indices of components of a compound material, is often assisted by manual mechanical probing of the examined site.

The discharge resistance of some, but not all, materials is temperature-dependent. The influence of the known property transition temperatures (e.g., the glass transition point) of polymers deserves attention in this connection.

A good correspondence with standard-test G-values has been obtained with, for example, polyethylene terephthalate and an epoxy composition in work with sealed cells, both with nitrogen flushing and weighing and with direct carbon determination. The carbon-determination technique, which was primarily developed for checking the weighing method, appears to be well suited for quick G-value determinations of the homogeneous materials.

When similar G-values are obtained in the standard cell and the sealed nitrogen cell, an interesting possibility of judging the behaviour of materials subjected to internal discharges arises, as discussed in 4.

Table 4 lists G-values for some materials tested in standard cells. Fig. 3.22 shows examples of the change of G with testing time for composite materials.

Table 4. Discharge resistance of polymers.

	G-index J/kg $\times 10^{10}$
Foils	
Polystyrene	1.1
Polyimide	1.0
Polyethylene	0.9
Polycarbonate	0.50.75
Polyethylene terephthalate	0.43
Cellulose acetate	0.14–0.20
Varnishes and resins	
Buton varnish	0.60
Polyimide varnish	0.35
Epoxide resin	0.55
Epoxide resin, glass-fibre-reinforced	0.70

The methods developed in the course of this work enable discharge resistance testing of insulating materials to be performed according to the guiding rules stated in 2.2. The tests are essentially non-functional. The degree of functionality increases from the standard test with flowing air to the treeing test. The pattern formed by the tests can be characterised as follows.

1. The standard test forms the basis for a relative assessment of the discharge resistance of materials. It is applied to all investigated materials.
2. The validity of the results obtained by the standard test is checked with the carbon-determination test, which is performed with selected materials.
3. The modified standard test with an inert atmosphere yields information about the applicability of standard test results to an assessment of the internal-discharge resistance of insulating materials.
4. The treeing test yields additional information about the tendency to gradual insulation loss of materials.

The evaluation scheme adopted can also be achieved with alternative testing techniques, as discussed in 4.

4. Discussion

Against the background of the theoretical and experimental information presented above, the author considers it possible to draw certain conclusions regarding the choice and successful application of discharge resistance tests to insulating materials and combinations of materials.

In those insulation applications where insulation deterioration caused by partial discharges other than gradual loss of local dielectric strength is relevant, information about the total discharge action on materials should be sought in the first stage and be supplemented with information about the tendency to gradual penetration of the materials. This applies particularly to rotating machine insulation and, to some degree, to transformer insulation.

The choice of testing methods depends to some extent on the resources of the laboratory. For total attack tests the methods with direct determination of the amount of deterioration are recommended in the first place. Of these, the chromatograph method is perhaps the most versatile one, because it enables the experimenter to choose selectively the volatile component on which measurement of the quantity of eroded material is based. On the other hand, this technique requires advanced equipment and highly skilled staff. The total cost of each determination is relatively high, if estimated in the way used in industrial research.

Simpler direct methods as, for example, the carbon-determination technique, require a far less advanced instrumentation and set-up and can be applied by staff of medium qualification. The duplication of testing facilities can be achieved more easily under conditions of economic restriction.

Both methods mentioned above have the advantage that the testing time required for taking a single reading is rather short (about 1 hour). However, the total time required for performing a complete test is determined by the exposure necessary to obtain all the information required, which, inter alia, means a stable level of the deterioration or resistivity index. The amount of sample material required for a test is rather modest.

For routine tests the indirect method of loss-of-weight determination is recommended. When proper precautions are taken to reduce the most important experimental errors, such tests can provide much information at a relatively low cost in terms of required equipment and labour. The need for a rigid experimental routine, however, can hardly be overemphasised. It is

not recommended that unskilled personnel should be employed for such work, since the skill of a trained laboratory worker (usually at technician level) is required for initiating appropriate action to be taken when anomalies occur.

The quantity of test material required with this method is greater than with the direct methods. Since the deterioration measure is an integral value, it is more important than with the methods based on quick determination of the degradation intensity either to secure constant exposure conditions and/or to obtain as complete a record as possible of the exposure intensity during the test. When many parallel tests are being run, it is a matter of convenience whether frequent observation and record-keeping, continuous graphic recording, or data logging is to be preferred. If our mean-discharge-current measuring method is adopted, it might be worth while to substitute the light-spot galvanometer by an adequate *RC* network yielding a voltage proportional to the mean discharge current. This voltage is measured by a digital voltmeter, provided, if desired, with a digital print-out. The periodic connection of such equipment to all cells can be arranged and it can also easily be accomplished automatically.

The information obtained with optical examination of the exposed samples with the naked eye and with the aid of a microscope equipped with as versatile illumination sources as possible is often very useful for both the assessment of the degradation and for the disclosure of peculiarities which might have occurred in the test.

Direct determination of material deterioration in internal-discharge test arrangements is relatively difficult. Lifetime determinations are comparatively simple, but the pronounced functional character of such tests hinders their interpretation for conditions differing from those prevailing in the model. Instead, an approach in two steps is suggested when the results of the standard test with air correspond to results of the modified test with an inert gas, e.g., nitrogen: the determination of the external-discharge resistance, which is advantageous from the point of view of exposure normalisation, and a determination of the variation with time of the discharge intensity in a test arrangement devised for appropriate internal discharge conditions. The internal-discharge resistance is then estimated through the combination of the results of the two tests. The second of these tests has some features in common with functional testing, but not to the same degree as a functional system test or the usual internal-discharge tests for materials. It is simpler in that it does not involve an explicit evaluation of the material response. When the primary discharge-resistance test has already been performed in an inert atmosphere (e.g., in gas chromatography work), no intermediate checking before the application of the results to the estimating of the internal-discharge resistance is required.

The recommendation of judging the internal-discharge behaviour of materials on the basis of results of external-discharge resistance tests presupposes that the basic mechanisms are similar. Our investigation of the power dissipation from discharges[56] has shown that variations in the discharge conditions, which tend to affect the discharge power as determined from the measured electrical characteristics, actually do take place, but that the variations are not of such a size as to invalidate discharge energy determinations based on the usual electrical measuring methods. This point is further discussed in the paper quoted above.

A separate test is recommended for supplementary local attack studies. The Damstra technique (see 2.4.2.) or a treeing test is thought to be most appropriate.

If the tests for both total and local attack are normally performed at room temperature, they should be supplemented by trial tests at the service temperature or class temperature for which the material is intended. If there are any significant deviations, the testing programme should be enlarged.

Insulation systems developed on the basis of decisions incorporating the results of discharge-resistance assessment tests on materials should be subjected before final approval to appropriate accelerated functional system tests. Parts of the information given in this paper might possibly be of some use to the planning of such tests.

In the field of extremely stressed insulations, e.g., for cables and capacitors, the aspect of gradual loss of dielectric strength dominates to such a degree that an assessment of the total degradation of materials under the action of partial discharges may be considered as being of secondary importance only. The widely held voltage-life-test philosophy has most to be said in its favour in this field of application. It should be remembered, however, that the voltage-life criterion is characteristic of functional tests, which implies that the test must be representative of service conditions. This limits the degree to which the experimental parameters can be varied. In the author's opinion, the above considerations favour in the first place the treeing test techniques or, possibly, the Damstra test. Tests based on the penetration of insulation under the action of discharges in previously arranged voids may also be envisaged. A number of method problems encountered in such tests, however, have still to be clarified. The present work indicates that it is essential that sufficient information about the discharge intensity occurring during such tests should be obtained.

Acknowledgements

The author expresses his thanks to ASEA for permission to publish this work, and for being allowed to make use of unpublished investigations of insulation ageing.

The author is greatly indebted to his collaborators for the dedication and initiative shown during the course of the investigation. Some of them appear as co-authors of papers. In addition, it is a pleasure to name Mr Lars Carlsson, Mr Nils Kvandal, Mrs Evy Långberg and Mr Narve Skaar Pedersen. The author has profited much from stimulating discussions with a number of collegues at ASEA, and also from active help from their side. He is deeply obliged to Mr Anders R. Andersson, his department head during several years, for constant encouragement and many discussions of basic principles.

Thanks are due to Mr Martin Blake, B.A., for having taken upon himself the laborious task of checking the English of the manuscript, and to Dr Sigvard Thulin for valuable comments.

The work reported here forms part of a research project for which a grant has been obtained from the Swedish Technical Research Council in 1966.

Abstract

A review is given of the occurrence of partial discharges in insulation and of the factors and mechanisms influencing them. The effects of partial discharges on insulation are described. Published testing methods for the assessment of the discharge resistance of insulating materials are systematically compared. Method development work in the authors laboratory is described, and a sequence of materials tests is proposed. A new approach to the assessment of the internal-discharge resistance of insulating materials is suggested.

References

1. Abresch, K.: Die coulometrische Analyse. Weinheim 1961. pp. 130–131.
2. Alterung von Kunststoffen (Internationales Symposium IUPAC, Düsseldorf, 19 Okt. 1959). Kunststoffe **49** (1959): 11, 57 pp.
3. Александров, Н. В., Калинина, Е. А., Трубачев, С. Г.: Определение коростойкости электроизоляционных материалов различными методами. Электричество 1961:4., pp. 61–68.
   (Aleksandrov, N. V., Kalinina E. A., Trubačev, S. G.: Determination of the discharge resistance of electrical insulating materials by various methods. Električestvo.)
4. Artbauer, J.: On the methods for determining the resistance of insulating material to discharges. Report, Vyskumny Ustav Kabelov a Izolantov, Bratislava, 1961. (Distributed in IEC TC 15 WG 4.)
5. Artbauer, J., Griač, J.: Der Durchschlag von Kunststoffen unter Einwirkung von Glimmentladungen. Elektrie 1963: 4, pp. 120–124.
6. Asea: Intern. Investigation Report V 435–41 reg. 4350, 1963.
7. Bailey, C. A.: A study of internal discharges in cable insulation. IEEE Paper No. 31, PP. 66–363 (1966) 9 pp.
8. Baker, W. P.: Electrical breakdown tracks in Perspex. Nature, London **177** (1956), pp. 887–888.
9. Bartnikas, R., d'Ombrain, G. L.: A study of corona discharge rate and energy loss in spark gaps. IEEE Trans. Power App. and Syst. **84** (1965): 9, pp. 770–779.
10. Bartnikas, R.: Pulsed corona loss measurements in artificial voids and cables. CIGRÉ 1966, Report No. 202, 37 pp.
11. Bashara, N. M.: The study of discharges in dielectric voids by photomultiplier methods. AIEE Transactions (Jan. 15, 1960) Paper 60–277.
12. Bertein, H.: Application de la méthode des figures de poudre à l'étude de la décharge par effluves dans les isolants. Revue Générale de l'Electricité **69** (1960): 2, pp. 461–474.
13. Boeck, W.: Ein neuer Durchschlagsmechanismus infolge Koroaentladungen an Isolierstoffen. ETZ-A **85** (1964): 22, pp. 730–731.
14. Bolt, R. O., Carroll, J. G. (Editors): Radiation effects on organic materials. New York 1963.
15. Bolton, B., Cooper, R., Gupta, K. G.: Impulse breakdown of Perspex by treeing. Proc. I.E.E. **112** (1965): 6, pp. 1215–1220.
16. Bouška, A.: Die Beständigkeit von trockenen und feuchten Glimmerisolierstoffen in einem stark ionisierten Raum. Elektrie 1966: 8, pp. 326–328.
17. Böning, W.: Luftgehalt und Luftspaltverteilung geschichteter Dielektrika I. Archiv für Elektrotechnik **48** (1963): 1, pp. 7–22.
18. Böning, W.: Der Zusammenhang zwischen Luftgehalt und Verlustfaktor bei Leiterumpressungen elektrischer Maschinen. ETZ-A **84** (1963): 14, pp. 467–471.

19. Bui-ai: Contribution à l'étude de la dégradation des isolants en feuilles sous l'action des décharges partielles. Thesis (Dr ès Sciences) Faculté des Sciences, Univ. of Toulouse, April 1966.
20. Cameron, A. B., Kao, K. C.: Effects of electrical discharges on some properties of an epoxide resin. Gas discharges and the Electricity Supply Industry. (Proc. intern. conf. CERL, Leatherhead, May 1962). London 1962. pp. 481–488.
21. Charlesby, A.: Atomic radiation and polymers. London 1960.
22. Church, H. F., Garton, C. G.: Some mechanisms of insulation failure. Proc. I.E.E. **100A** (1953) pp. 111–120.
23. Cooper, R.: The electric strength of solid dielectrics. British J. of Applied Physics **17** (1966): 2, pp. 149–166.
24. Croitoru, Z.: Mesure de l'état d'électrisation des feuilles isolantes. Revue Générale de l'Electricité **68** (1959) pp. 489–496.
25. Dakin, T. W., Works, C. N.: The relation of corona pulse measurement to the size of internal voids or other origin. Conference on Electrical Insulation 1964, pp. 109–113.
26. Damstra, G. C.: Accelerated voltage endurance tests at higher frequencies. Research report HR 1, N. V. Hazemeyer, Hengelo, March 1961 (Distributed in IEC TC 15 WG 4).
27. Dick, W., Kelen, A., Larsson, L., Sletbak, J.: On the significance of some test parameters for discharge endurance testing of insulating materials. Elteknik **7** (1964): 6, pp. 147–150.
28. Dittmer, B.: Der räumliche und zeitliche Entladungsaufbau in festen Isolierstoffen im ungleichförmigen Feld. Archiv für Elektrotechnik **48** (1963) pp. 150–166, 287–296, 387–402.
29. Дмитриев, А. В., Цзян Цзе-Цзянь: Изменение свойств поверхности диэлектрика под воздействием газового разряда. Ж. Т. Ф. **36** (1966):4, pp. 739–745. (Dmitriev, A. V., Chian Chieh-chiang: Property changes of dielectric surfaces exposed to gas discharges. J. Tech. Phys. USSR.)
30. Edelmann, H.: Ein Beitrag zur Messung der Alterung von Polyäthylen-Folien unter dem Einfluß einer 50-Hz-Gasentladung. ETZ-A **85** (1964): 14, pp. 434–439.
31. Ehrenberg, L., Zimmer, K. G.: Action of ionizing radiation on insulating plastics. Acta chem. Scand. **10** (1956): 5, pp. 874–875.
32. Falk, G., Rager, H.: Weich-Polyvinylchlorid im Hochspannungsfeld. ETZ-B **17** (1965): 5, pp. 103–108.
33. Fieux, R.: Étude des variations de la tension de seuil et de la tension disruptive dans une cellule à décharges partielles. Thesis (Dr de spéc.), Faculté des Sciences, Univ. of Toulouse, May 1965.
34. Fischer, H. *et al.*: ESR-Untersuchungen zum oxidativen Strahlungsabbau: Reaktionen der Peroxidradikale in bestrahlten Vinylpolymeren. Kolloid-Z **195** (1964): 2, pp. 129–134.
35. Fischer, H.: Radikalische Vorgänge bei der Alterung von Kunststoffen. Kunststoffe **55** (1965): 5, pp. 344–345.
36. Friedlander, E., Reed, J. R.: Electrical discharges in air-gaps facing solid insulation in high-voltage equipment. Proc. I.E.E. **100A** (1953) pp. 121–131.
37. Garton, C. G.: The energy of discharges and their interaction with solid dielectrics. Gas discharges and the Electricity Supply Industry. (Proc. intern. conf. CERL, Leatherhead, May 1962) London 1962, pp. 412–419.
38. Gross, B.: Compton current and polarization in gamma-irradiated dielectrics. J. Appl. Phys. **36** (1965): 5, pp. 1635–1641.

39. GROSSKREUZ, R.: Nachweis von Elektronenlawinen mittels elektrostatischer Ladungsbilder auf isolierenden Folien. Z. für angewandte Physik **21** (1966): 3, pp. 200–202.
40. HALL, H. C., RUSSEK, R. M.: Discharge inception and extinction in dielectric voids. Proc. I.E.E. pt II **101** (1954): pp. 47–55.
41. HELLER, B., CHLÁDEK, J.: Zur Physik der Koronavorgänge im festen Dielektrikum. Acta Techn. ČSAV **9** (1964): 1, pp. 1–16.
42. HELLER, B., CHLÁDEK, J.: Zur Problematik der Koronaverluste im festen Dielektrikum. Acta Techn. ČSAV **9** (1964): 4, pp. 315–322.
43. HELLER, B., CHLÁDEK, J.: Das kapazitive Ersatzschema für die Koronavorgänge im festen Dielektrikum. Acta Techn. ČSAV **10** (1965): 6, pp. 613–622.
44. HÉROU, R., FALLOU, B., BERTEIN, H.: Essais d'endurance des matériaux isolants à l'action des décharges électriques ionisantes. Bull. d'Inform. Lab. Cent. des Industries Electriques No. 27, June 1960, pp. 201 L–208 L.
45. HÉROU, R., FALLOU, B., BERTEIN, H.: Contribution à l'étude des processus de dégradation des matériaux isolants en feuilles soumis en cellule conventionelle à l'action de l'ionisation gazeuse. Bull. Soc. française des Électriciens, 8e sér. **3** (1962): 26, pp. 102–117.
46. HEWITT, G. W., DAKIN, T. W.: Voltage endurance tests on insulating materials under corona conditions. IEEE Power Apparatus and Systems (1963): 12, pp. 1033–1039.
47. HOUGEN, L. R.: Effect of corona discharges on polyethylene. Nature (London) **188** (1960): pp. 577–578.
48. HOUGEN, L. R., HAUAN, P.: Utladninger-et isolasjonsproblem. Elektroteknisk Tidskrift (Oslo) **76** (1963): 23, pp. 397–404. (Discharges—an insulation problem).
49. Ильченко, Н. С., Ковалев, А. В., Гаврилюк, Г. И.: К вопросу пробоя диэлектриков под воздействием ионизации во внутренних газовых включениях. Известия Высших Учебных Заведений, Физика, 1966:5, pp. 109–114.
(Ilčenko, N, S., Kovaljev, A. V., Gavriljuk, G. I.: On the question of the breakdown of dielectrics subject to ionisation in gas inclusions. Izvestia vyssih učebnyh zavedenij, fizika).
50. IEC Publication No. 27: Electrical symbols to be used in electrical technology. Geneva 1966.
51. KELEN, A., DICK, W.: On discharge endurance testing of insulating materials. IEC TC 15 WG 4 (Sweden), April 1963.
52. KELEN, A.: Observations on testing discharge resistance of film or sheet material with rod electrodes in contact with the sample. IEC TC 15 WG 4 (Sweden) 5, 1963.
53. KELEN, A.: Investigations dans les pays nordiques des actions des décharges électriques sur les matériaux et structures isolantes. Bull. Soc. française des Électriciens, 8e sér. **5** (1964): 57, pp. 563–566.
54. KELEN, A.: Überlegungen über den Energieumsatz in Teilentladungen und die Pulsfolge im Hinblick auf die Einwirkungen auf Dielektrika. Intern. Kolloquium Ilmenau, Oct. 1966.
55. KELEN, A., AASE, J.: Application of isothermal calorimetry for measuring power dissipation by partial discharges. Acta Polytechnica Scandinavica El **16** (1967), pp. 87–102.
56. KELEN, A.: A study of the mechanisms of partial discharges at insulating surfaces. Acta Polytechnica Scandinavica El **16** (1967), pp. 103–131.
57. KELEN, A., LARSSON, L.-E.: Some observations on the treeing breakdown of epoxide resins. Acta Polytechnica Scandinavica El **16** (1967), pp. 133–138.
58. KELEN, A.: The effect of partial discharges on insulating materials. ASEAJournal **40** (1967): 6–7, pp. 97–98.

59. KELEN, A., ÖSTERGREN, L.: Simple methods for determining the heat transfer data of solid materials and possible applications to the quality testing of electrical insulations. Appl. Sci. Res. (in press).
60. KELEN, A.: Om isolermaterialprovning för kraftteknika ändamål. Symposium "Accelereret Prövning", Risö, Nov. 1966. Ingeniören (Copenhagen), 15 April 1967. (On the testing of insulating materials for power engineering applications).
61. KELEN, A., VIRSBERG, L.-G.: Discharge suppression on the free surface of high-voltage insulation, in particular on generator coil ends. Elteknik **10** (1967) (in press).
62. KELEN, A.: On the theory of non-linear resistive field-grading coatings on insulating surfaces. Elteknik **10** (1967) (in press).
63. KIRCHER, J. F. (Ed.): Effects of radiation on materials and components. New York 1964.
64. KITCHIN, D. W., PRATT, O. S.: Treeing in polyethylene as a prelude to breakdown. AIEE-Transactions Paper 58–121, 1958.
65. KITCHIN, D. W., PRATT, O. S.: Conference on Electr. Insulation 1961, Paper No. 20.
66. KREUGER, F. H.: Discharge detection in high voltage equipment. London 1964.
67. KREUGER, F. H.: Discharge resistance of dielectric materials. NV Nederlandsche Kabelfabrieken. Report No. 63–67, 1963, (distr. in IEC TC 15 WG 4).
68. LACOSTE, R.: Méthodes nouvelles d'étude du phénomène d'ionisation. Bull. Soc. française des Électriciens 8e sér. **3** (1962): 26, pp. 118–132.
69. LANG, G. F.: Ionisation problems in large rotating machines. Insulation. 1960: 12, pp. 21–26.
70. LEROY, G.: Les problèmes d'ionisation dans les isolants solides en relation notamment avec les techniques de construction et vieillissement du nouveau matériel électrique. Bull. Soc. française des Électriciens 8e sér. **3** (1962): 26, pp. 69–87.
71. LEROY, G.: Problèmes posés par le choix des isolations des grandes machines synchrones et par leur contrôle au stade de la réception et au cours du service. AIM Bull. Montefiore 1963: 2, pp. 138–193.
72. LEROY, G., LACOSTE, R., BUI-AI: Analytical study of degradation of solid insulating materials through ionisation discharges. Gas discharges and the Electricity Supply Industry (Intern. Conf. CERL, Leatherhead. May 1962). London 1962, pp. 393–403.
73. LEU, J.: Teilentladungen in Epoxydharz-Formstoff mit künstlichen Fehlstellen. ETZ-A **87** (1966): 18, pp. 659–665.
74. MCMAHON, E., MALONEY, D. E., PERKINS, J. R.: A study of the effects of corona on polyethylene. Transactions AIEE I **78** (1959) pp. 654–662.
75. MASON, J. H.: The deterioration and breakdown of dielectrics resulting from internal discharges. Proc. I.E.E. **98 I** (1951): 109, pp. 44–59.
76. MASON, J. H.: Electrical insulation: Dielectric breakdown. High voltage tests for materials and equipment. Electrical Energy **1** (1956 Nov., Dec.) pp. 68–75, 120–126.
77. MASON, J. H.: Dielectric breakdown in solid insulation. Progress in dielectrics. **1**, London 1959, pp. 1–58.
78. MASON, J. H.: The resistance of sheet insulation to surface discharges. Proc. I.E.E. **107A** (1960): 36, pp. 551–568.
79. MASON, J. H.: The behaviour of electrical discharges over the surface of sheet insulation. Gas discharges and the Electricity Supply Industry. (Proc. intern. conf. CERL, Leatherhead, May 1962) pp. 428–438.
80. MASON, J. H.: Discharge detection and measurement: terminology. Letter to the Editor. Electronics and Power **10**, Sept. 1964.

81. MASON, J. H.: Discharge detection and measurements. Proc. I.E.E. **112** (1965): 7, pp. 1407–1423.

82. MATHES, K. N.: Discharge dependent voltage breakdown, definition and significance. Conference on Electrical Insulation (Materials and Applications) Chicago 1963, pp. 85–87.

83. MAYOUX, C.: Sur la modification de structure du polyéthylène soumis à l'action des décharges partielles dans l'air. Thesis (Dr de spéc.) Faculté des Sciences, Univ. of Toulouse, April 1966.

84. MEATS, R. J., STANNETT, A. W.: Degradation of insulating materials by electrical discharges. AIEE Paper T-153-37. (1963).

85. MILTON, O.: Application of the pointed electrode in evaluating pulse life of casting resins. Conference on Electrical Insulation 1964, pp. 89–92.

86. NYLUND, K.: Internal ASEA Techn. Mem. No. 8338 reg. 435, Oct. 1957.

87. NYLUND, K.: Internal ASEA Lab. Rep. No. 2465 reg. 435, Dec. 1958.

88. OLYPHANT, M. JR.: Effects of corona on vinyl electrical tape. Electro-Technology **67** (1961): 6, pp. 123–128.

89. OLYPHANT, M. JR.: Breakdown by treeing in epoxy resins. Gas discharges and the Electricity Supply Industry (Intern. conf. CERL, Leatherhead, May 1962). London 1962, pp. 447–460.

90. OLYPHANT, M. JR.: Corona and treeing breakdown of insulation. Progress and problems. Part 3. Insulation, 1963:4, pp. 42–46.

91. OLYPHANT, M. JR.: Internal corona testing of casting resins. IEEE Paper 31 PP. 66–510, 1966. 34 pp.

92. PARKMAN, N.: The effects of small discharges on some insulating materials. E.R.A. Rep. L/T 321, April 1955.

93. PARKMAN, N., PRINS, G. A.: Discharge magnitude and the life of insulation. Gas discharges and the Electricity Supply Industry. (Intern. conf. CERL, Leatherhead, May 1962) pp. 420–427.

94. PARKMAN, N.: The electrical properties of high polymers, in: Ritchie, P.D. (Ed.): Physics of plastics. London 1965, pp. 303–314.

95. PARR, D. J., SCARISBRICK, R. M.: The performance of synthetic insulating materials under polluted conditions. Proc. I.E.E. **112** (1965): 8, pp. 1625–1632.

96. REED, J. C., MCMAHON, E. U., PERKINS, J. R.: Effects of high voltage stresses on TFE and FEP fluorocarbon plastics. Insulation, 1964: 5, pp. 35–38.

98. REYNOLDS, S. I.: Measurement and influences of surface charges in high-voltage phenomena. Electrical Engineering **78** (1959): 11, pp. 1080–1084.

99. REYNOLDS, S. I.: Surface charges produced on insulators by short- and long-time ionisation. Nature (London) **183** (1959) pp. 671–672.

100. RIEGE, H.: Indre utladninger og deres virkning på den elektriske holdfasthet for polyetenisolasjon. Thesis (lic. techn.), Inst. for vekselströmteknikk, NTH, Trondheim, 1965. (Internal discharges and their effect on the dielectric strength of polyethylene insulation, Norw. Inst. of Technology).

101. ROBERTS, S. C.: Review of motor insulations with special reference to breakdowns by discharges encountered in the mining industry. Transactions of the South African Inst. of Electrical Engineers **52** (1961): 7, pp. 166–189.

102. ROGERS, E. C.: The self-extinction of gaseous discharges in cavities in dielectrics. Proc. I.E.E. **105A** (1958): 24, pp. 621–630.

103. ROGERS, E. C., SKIPPER, D. S.: Gaseous discharge phenomena in high-voltage d.c. cable dielectrics. Proc. I.E.E. **107A** (1960): 6, pp. 241–254.
104. SALVAGE, B.: Electrical discharges in gaseous cavities in solid dielectrics under direct voltage conditions. Gas discharges and the Electricity Supply Industry. (Intern. conf. CERL, Leatherhead, May 1962). London 1962, pp. 439–446.
105. SALVAGE, B.: Electric stresses in gaseous cavities in solid dielectrics. Proc. I.E.E. **111** (1964): 6, pp. 1162–1172.
106. SCHNUPP, P.: Das Auftreten von Durchschlagskanälen beim thermischen Durchschlag. Z. für angew. Phys. **19** (1965): 1, pp. 46–54.
107. STANNETT, A. W., MEATS, R. J.: Some factors affecting the breakdown of polythene subjected to discharges. Gas discharges and the Electricity Supply Industry (Intern. conf. CERL, Leatherhead, May 1962). London 1962, pp. 404–411.
108. STANNETT, A. W., MACKENZIE, R. A.: Changes in loss tangent of polythene subjected to partial discharge. Nature (London) **211**. (1966), pp. 626–627.
109. STARR, W. T., ENDICOTT, H. S.: Progressive stress: a new accelerated approach to voltage endurance. Transactions AIEE III, **80** (1961) pp. 463–471.
110. STOBERNACK, H.-U.: Über das elektrische Verhalten einiger Isolierstoffe unter dem Einfluß von Vorentladungen. Elektrie 1966:1, pp. 6–10.
111. TAKACS, J. A., FREEMAN, G. R.: Relative ionisation efficiencies of hydrocarbon molecules as a function of bombarding electron energy. Nature (London) **208** (1965), pp. 996–997.
112. THOMAS, A. M.: Heat developed and "powder" figures and the ionisation of dielectric surfaces produced by electrical impulses. British J. of Applied Physics **2** (1951): 4, pp. 98–109.
113. VDE: Bestimmungen für elektrische Prüfungen von Isolierstoffen. VDE 0303, Teil 7/63.
114. VEVERKA, A., HON, A.: Das Ersatzschema für die inneren Entladungen im festen Dielektrikum. Acta Technica ČSAV **8** (1963): 6, pp. 509–523.
115. VEVERKA, A., HON, A.: Zur Problematik der Anzahl der Entladungen in der Aushöhlung eines Dielektrikums. Acta Technica ČSAV **9** (1964): 3, pp. 208–216.
116. Воробьев, Г. А., Лисецкая, М. Н.: Исследование развития разряда в каменной соли в однородном поле. Физика Тверлого Тела **6** (1964):12, pp. 3493–3499.
(Vorobjev, G. A., Liseckaja, M. N.: Investigation of discharge channel development in NaCl in homogeneous fields. Sol. State Phys. USSR.)
117. Воробьев, А. А., Воробьев, Г. А., Мельников, М. А.: Распространение разряда в монокристаллах NaCl и KCl. Физика Твердого Тела **2** (1960):9, pp. 2019–2024.
(Vorobjev, A. A., *et al.*: Discharge propagation in monocrystals of NaCl and KCl. Sol. State Phys. USSR.)
118. Воробьев, А. А., Воробьев, Г. А., Горбин, Н. М.: О процессах формирования разряда в твердых диэлектриках. Физика Твердого Тела **3** (1961):11, pp. 3272–3277.
(Vorobjev, A. A., *et al.*: On discharge channel formation processes in solid dielectrics. Sol. State Phys. USSR.)
119. WHITEHEAD, S.: Dielectric breakdown of solids. Oxford 1951. 268 pp.
120. WOBODITSCH, W.: Glimmbeständigkeit von Kunststoffolien für Hochspannungskabel. Elektrie 1962: 2, pp. 187–191.

APPLICATION OF ISOTHERMAL CALORIMETRY FOR MEASURING POWER DISSIPATION CAUSED BY PARTIAL DISCHARGES

Andreas Kelen and John Aase
Central Laboratories, ASEA, Västerås

Introduction

The occurrence of partial discharges in, or adjacent to, high-voltage insulations is a problem of great concern in electrical power engineering.

Partial discharges in a gas space inside, or adjacent to, a dielectric appear when the field intensity in the gas exceeds a certain limit. If alternating voltage is applied, the discharges occur as groups of pulses of very short duration (<50 ns). The polarity of the pulses coincides with the sign of the time derivative of the applied voltage. The magnitudes of the discharges are distributed in a random way. Their distribution depends on a number of factors such as, for example, the atmosphere in the cavity, its geometry, the nature of the dielectric, the surface conductivity of the dielectric surface.

Knowledge of the discharge intensity is of importance to the testing of the endurance of insulating materials and systems exposed to partial discharges. In life tests, the time to breakdown of a sample exposed to an alternating voltage with constant amplitude is taken as a measure of the resistance of the material, and the stress is assumed to be a measure of the discharge intensity. Modern discharge detectors determine the intensity of individual discharge pulses in terms of charge. The quantity measured is the charge supplied from the high-voltage circuit to the dielectric in series with the gas volume immediately affected by an individual discharge, when the voltage across the gas volume breaks down partially or wholly. Detailed investigations of the relationship between the magnitudes characterising the discharge and the output from the measuring circuitry as a function of the test object and instrument parameters have been published in, for example,[1].

There is still some controversy about the proper way in which the discharge intensity should be measured. Modern discharge detectors usually determine the maximum discharge magnitude, i.e., the highest discharges produced in the volume under investigation. However, owing to the above-mentioned statistical character of this quantity the maximum discharge magnitude depends

to some degree on the integration time constant of the measuring device. A typical value chosen for this is about 0.1 s[1]. Discharge detectors can be combined with electronic counters for determining the discharge pulse rate.

Determination of material deterioration under the action of partial discharges requires the use of methods for assessing the quantity of degraded material and of the total dissipated discharge energy[2]. The discharge energy need not be known for comparative studies, as long as the relevant experimental conditions can be held constant. This applies to, for example, tests where insulation films or plates are exposed to discharges in a ventilated gas gap of constant thickness. The desired versatility of the test, e.g., the possibility of comparing materials of different thickness and permittivity, and the elaborateness of the discharge intensity measurements, are related in a way that gives some possibility of choice.

The situation is different in the technically very important case of internal discharges, i.e., partial discharges in a confined gas volume surrounded by the dielectric. Changes in the pressure and composition of the gas and in the properties of the dielectric surface caused by the action of partial discharges affect the discharge conditions. The discharge intensity tends to change with time and cannot be controlled. For systematic studies the discharge intensity must be assessed. This is suitably achieved by means of electrical measuring methods, e.g., discharge magnitude detectors with pulse-rate counters[1], measurement of the mean discharge current[2], (p. 54 of this issue) or determination of the distribution of discharge amplitudes[3]. The derivation of the dissipated discharge energy from such measurements depends on the assumption of an appropriate model of the system consisting of the discharge site, the rest of the test object, the energy source and the measuring circuit.

The present work aims at obtaining direct information about the dissipated partial discharge energy under specific discharge conditions.

This is achieved through the application of the isothermal calorimetric technique in this field. The results are compared with measurements of the mean discharge current and of the discharge pulse magnitude and rate. The results of the calorimetric measurements permit a new approach towards the understanding of the mechanism of partial discharges in, or adjacent to, dielectrics. This investigation is published separately[4] (p. 103 of this issue).

1. Method

The original intention was to apply the calorimetric technique to an exposure cell consisting of a plane parallel arrangement of the electrodes, one or two dielectric samples and a discharge gap.

An attempt was undertaken to determine the power dissipated by partial discharges in a cell consisting of a relatively heavy cylindrical ceramic body containing the electrode assembly. The temperature drop over a thermal resistor (a stainless steel cylinder) connecting the otherwise well insulated cell with a surrounding thermostatised container was intended to give a measure of the dissipated power. This method was abandoned because of insufficient thermal coupling between the region surrounding the high-voltage electrode and the thermal resistor, which made it difficult to avoid thermal stray losses. Moreover, this cell had a very considerable thermal time constant.

A revised concept of the principle of power measurement led to the adoption of an arrangement with separate, controlled thermal leakage paths for the high- and the low-voltage electrode regions, respectively. In this way, thermal coupling between the parts of the cell ceased to be of importance. The electrodes and supports could now be given a low thermal capacity and the time constants of the cell consequently made low. Moreover, a possible asymmetry in power dissipation between the electrodes can be detected. Provisions were also made for measuring the power carried away by gas flowing through the cell.

2. Apparatus

The measuring cell consists of two electrode assemblies held apart at a certain constant distance by means of an insulating frame and in thermal contact with heat sinks. The arrangement of the cell is shown in Fig. 1. The heat sinks are copper blocks with ducts permitting the circulation of a liquid maintained at a constant temperature. The spacer frame is made of Plexiglas. It is provided with small holes (d = 3 mm) at opposite sides for the admission or circulation of the gas, which is to constitute the atmosphere of the cell. The parallel faces of the frame are milled slightly on their outer edge in order to take up a layer of silicone grease for sealing the cell without the grease coming into direct contact with the discharge region.

The design of an electrode assembly is shown in Fig. 2. The stainless steel electrode ($50 \times 40 \times 2$ mm) is arranged in intimate contact with a glass plate ($120 \times 120 \times 2$ mm), which constitutes the thermal resistor. The temperature drop across the glass plate is measured with a centrally placed thermocouple consisting of a 2 mm × 0.01 mm constantan strip and 0.15 mm gauge silver wire. The joints are pressed together without soldering. The thermocouple is insulated electrically from the electrode by a 0.2 mm mica flake. A thin (0.005 mm) terephthalate foil, covering the whole glass plate, is mounted between the "cold" junction of the thermocouple and the copper block. A small strain gauge is glued into a shallow recess at the back of the electrode to permit a direct calibration of the thermocouple readings in terms of power. The whole electrode assembly is glued together under pressure with a thermosetting adhesive. Dielectric samples to be incorporated in a cell are glued to the electrode by means of colloidal silver varnish or epoxy resin.

The flashover voltage of the electrode assembly amounts to about 8.5 kV (R.M.S.).

During the application of high voltage to the cell, the terminals of the calibration resistance of the high-voltage electrode lie at a dangerous potential and must be suitably protected. The thermocouple leads of the high-voltage electrode, though galvanically insulated from the electrode, are nevertheless to be treated as high-voltage conductors. The thermocouple e.m.f'.s are consequently measured with a battery-powered transistorised microvoltmeter insulated from earth and line potentials.

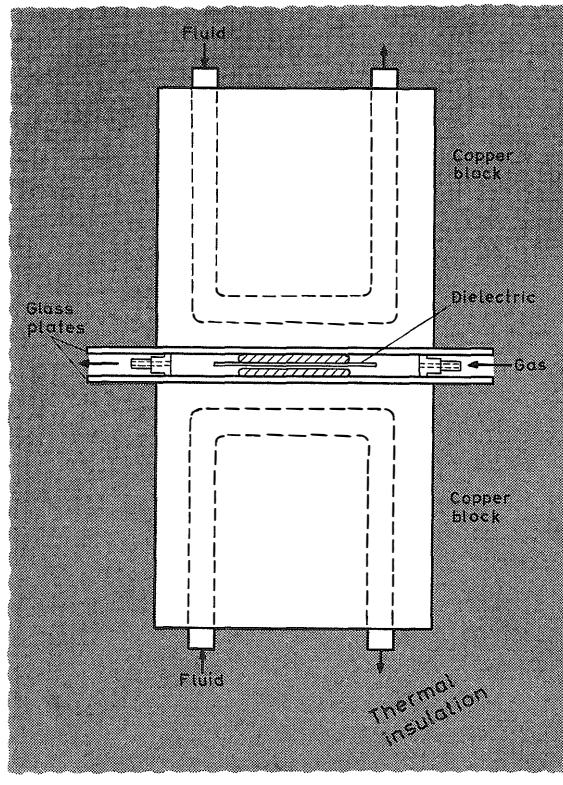

Fig. 1. Schematic arrangement of calorimetric cell.

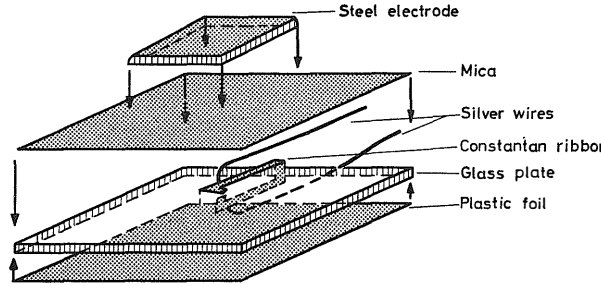

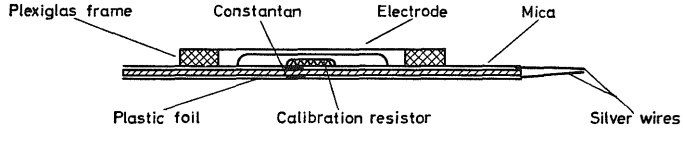

Fig. 2. Electrode assembly.

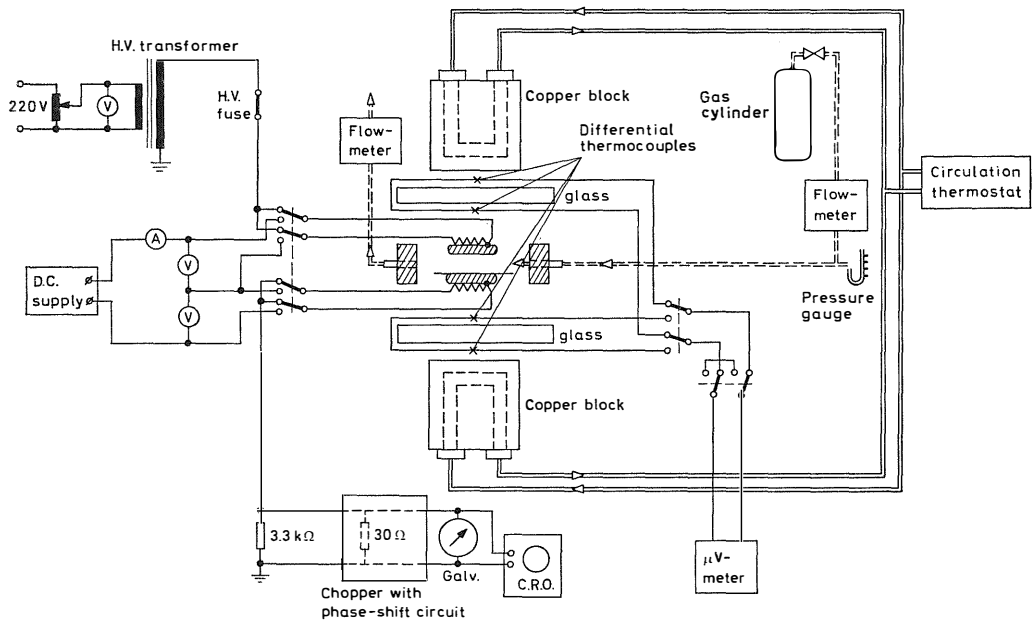

Fig. 3. Schematic diagram of circuits for measurement, calibration and feeding of calorimetric cell.

A careful insulation of all parts of the cell and the associated circuitry that might produce unintended partial discharges is an important precaution.

The set-up of the measuring circuits appears from Fig. 3.

The high-voltage electrode is fed from a 1:100 resin-potted high-voltage transformer energised over a Variac. A high-voltage fuse, consisting of a thin, spring-loaded metal wire (Kanthal, d = 0.025 mm), is provided as protection. The cell voltage is determined from the reading of a voltmeter in the primary circuit of the transformer.

A resistor (3.3 kΩ) is connected between the low-voltage electrode and earth to allow the mean discharge current to be measured. The low-voltage electrode is connected to an oscilloscope and to a current measuring device. The latter consists of an electrodynamically driven chopper energised from one of the two phases of the power supply of the high-voltage circuit and the third phase. The switching instants of the chopper contacts are made to coincide as closely as possible with the peaks of the voltage wave by means of a phase-shifting network. In this way, only positive or negative discharge pulses, respectively, are admitted to the galvanometer connected via the chopper, whereas the 50 Hz component is nearly balanced out. Connecting a ballast resistor of a value equal to the galvanometer resistance (10 Ω) to the other

chopper contact enables a constant load to be obtained on the cell (except for the switching intervals). The galvanometer is a Norma Model 251 U light-spot instrument. The current measuring unit is calibrated with both direct current and rectangular wave signals of 10 to 20,000 Hz.

The thermocouples measuring the temperature drops over the glass plates backing the electrodes are connected, as has already been mentioned, to an electronic microvoltmeter. This instrument (Medistor mod. 75 A) also comprises a d.c. compensator unit, which permits measurements with a high degree of accuracy.

The power calibration of the thermocouples is carried out through the measuring of the voltage across and the current through the calibrating resistors when fed from an electronically stabilised d.c. source.

The heat sinks are provided with thermocouples for temperature control.

The velocity of the gas flow through the cell is measured with flow-meters both in the inlet and outlet leads.

For measurement of the power carried away by the gas stream in ventilated cells, the gas flow was led through a small thermally insulated flask filled with metal wool for temperature equalisation and provided with a thermocouple. Trial runs with power supplied electrically to the test cell showed unexpected periodic variations of the temperature of the flowing gas (about 1 deg). The effect was traced back to the air conditioning system of the laboratory. Addition of a gas temperature measuring unit in the inlet lead to the measuring cell and differential temperature measurement between the gas inlet and outlet led to the complete elimination of the disturbances caused by fluctuations in the room temperature.

3. Calibrations and controls

One electrode assembly was provided with an additional thermocouple near the edge of the electrode in order to check whether the uniformity of the heat flow, which may be assumed to be good during experiments with partial discharges, is also sufficient during the calibration procedure. The result of the experiment turned out to be satisfactory; the temperature difference between the central and the peripheral thermocouples was less than the uncertainty in the temperature measurement.

A check of the temperature of the heat sinks showed a very slow drift when the temperature of the copper blocks was not controlled. Although this temperature drift is without significance to the ordinary calorimetric measurements, which usually require less than 10 min, all measurements were performed with the temperature of the copper blocks controlled in such a way that transformer oil was circulated by means of a Lauda thermostat with a temperature stability of 0.01 deg or better.

The thermal coupling between the gas flow through the measuring cell and the electrodes was investigated in two ways. First, the electrode power was calibrated with varying rates of air flow through the cell. No change in the calibration curve could be detected for gas flows from zero up to 3l/min, which demonstrates the insignificance of gas cooling of the electrodes in our measurements. The cell was then run with no electric power supplied to the electrodes, but with a flow of gas previously heated by passage through the thermostat to about 10 deg above the cell temperature. The rate of temperature rise of the copper blocks was found to be 1.6 deg during 435 min. From this the heat-transfer coefficient between one electrode and air flowing through the cell at the particular gap setting and a flow rate of 1 l/min was estimated to be of the order of 7 mW/deg.

Measurements of the mean discharge current yield values of either the positive or the negative current. Repeated checks under different discharge conditions have demonstrated that the two components are equal. Only the mean value of the positive discharge current is therefore measured. In order to compensate for the remaining phase asymmetry of the chopper action after phase adjustment, the current measurements for each discharge exposure are preceded by current readings at voltages safely below the discharge-inception voltage in order to determine the remaining 50 Hz displacement current

component. The current readings during exposure are corrected for the 50 Hz component by linear extrapolation. This correction is usually less than 3–5 per cent for higher readings.

Oscilloscope observations of the discharge pattern during the application of high voltage to the cell have demonstrated the absence of parasitic discharges from conductors outside the discharge gap of the cell.

The measuring error consists of the calibration and measuring errors of the differential thermocouples [$2 \times (2+2)$ per cent] and the current- and voltage-measurement error of the power calibration (0.3 and 0.5 per cent). The overall error in the power determinations is thus estimated to be of the order of 10 per cent.

4. Measurements

Measurements were planned in order to yield information about the correlation of the true power dissipated in test cells and the values given by some electrical measuring devices. In the first place, cells were to be run with a dielectric having the smallest possible susceptibility to changes owing to the action of discharges. Mica was chosen for this purpose. Secondly, the behaviour of organic insulation materials was to be studied.

In the following some results will be presented of the power and discharge-intensity measurements in static nitrogen and air. A number of test electrode assemblies (bare, mica-clad and clad with polyethylene terephthalate foil) and spacer frames were prepared.

The following experimental routine was applied:

1. Choice of electrode assemblies and spacer frame of known thicknesses. Assembly of the cell using silicone grease for sealing.
2. Determination of the thickness of the mounted cell (repeated at the end of the experiment).
3. Mounting of the cell between copper blocks. Insertion into the thermal shield. Connection and insulation of electrical leads. Connection of gas leads. Flushing with gas for 2 min.
4. Power calibration of each electrode (usually up to 1.5 W. Reproducibility better than 2 per cent for electrode assemblies even if used in different cells.)
5. Determination of the 50 Hz component of the mean current.
6. Increase of voltage. Determination of the discharge-inception and discharge-extinction voltages (repeated after exposure). Checking of the absence of parasitic discharges.
7. Application of the test voltage. Measurement of mean current and other possible discharge characteristics. Power measurement after 8 to 10 min (steady state attained after 4 to 5 min). Repeated current measurement.
8. Flushing with gas.

The next measurement is performed after a minimum delay of 5 to 10 min.

5. Results

The dissipation of power in several cells was determined at different voltages. The atmospheres were supplied from gas cylinders in order to avoid complications owing to humidity and possible variations of composition. A differential discharge detector (system Kreuger) with an associated pulse-rate counter was used in a series of measurements.

Fig. 4 shows the dissipation from the individual electrodes and the total dissipated power in a symmetrical and an asymmetrical cell with similar thicknesses of the dielectric (mica) and gap. There is a marked difference between the heat supplied to a covered and an uncovered electrode.

Fig. 5 demonstrates the difference in power dissipation in cells depending on the atmosphere. The dissipation in N_2 was found to be greater than in

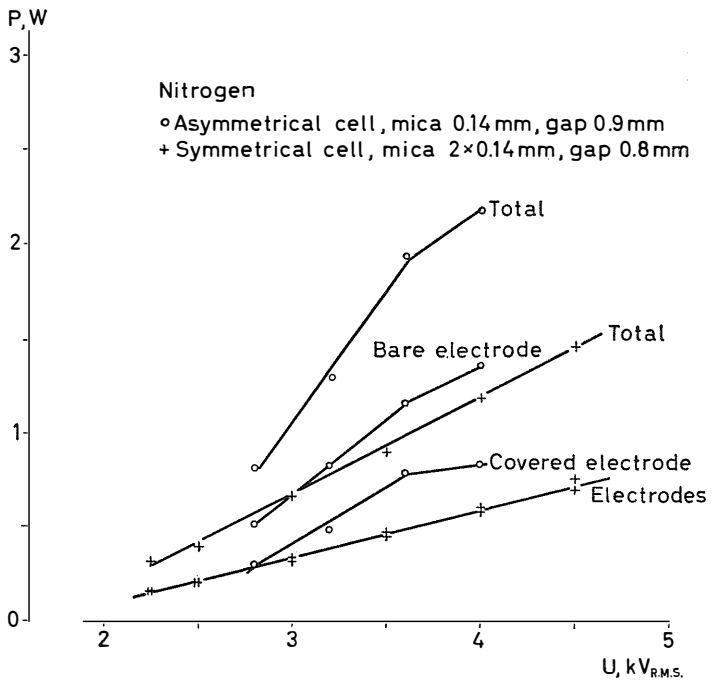

Fig. 4. Power dissipation from individual electrode assemblies and the complete cell (asymmetrical and symmetrical cells).

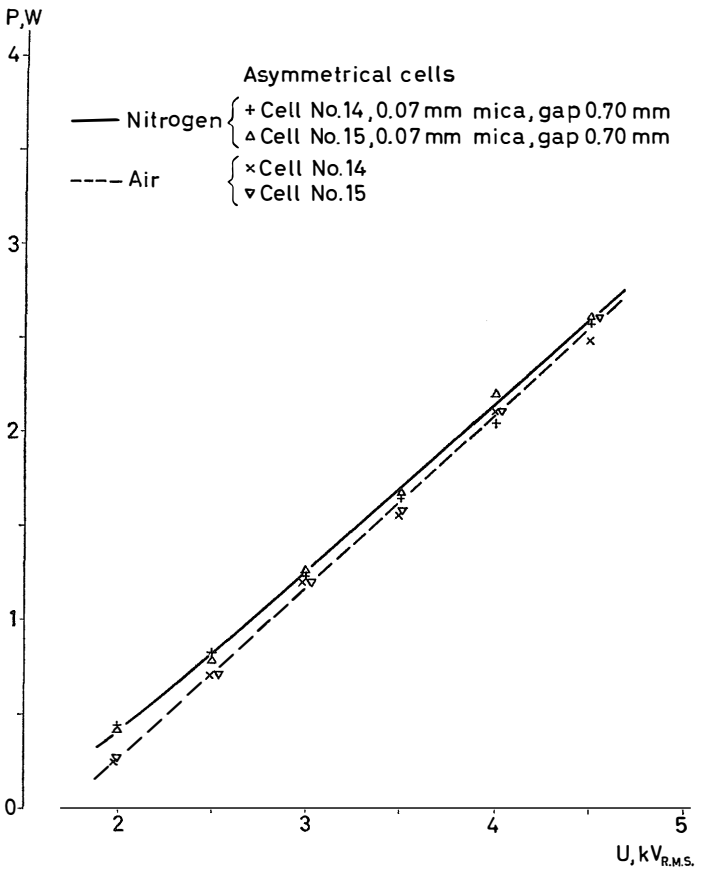

Fig. 5. Power dissipation in a cell with different atmospheres.

air in all runs with different cells, when both of the gases were applied. This finding is associated with the fact that the discharge-inception voltage of 0.7 mm gaps containing N_2 is somewhat higher than for air. Fig. 5 also illustrates the reproducibility of the measurements; the cells Nos. 14 and 15 were assembled on different days from the same electrode assemblies and spacer. The effects of variations in gap width and thickness of the dielectric can be seen in Figs. 6 and 7.

Table 1 gives the results of measurements of the dissipated power, the mean discharge current, the discharge magnitude (maximum pulse) and the corresponding pulse rate. A cell with mica was combined with external impedances in the high-voltage circuit. The effect of the associated impedances appears to be somewhat more pronounced in the readings given by the discharge detector than in the mean current readings. A second cell with a terephthalate

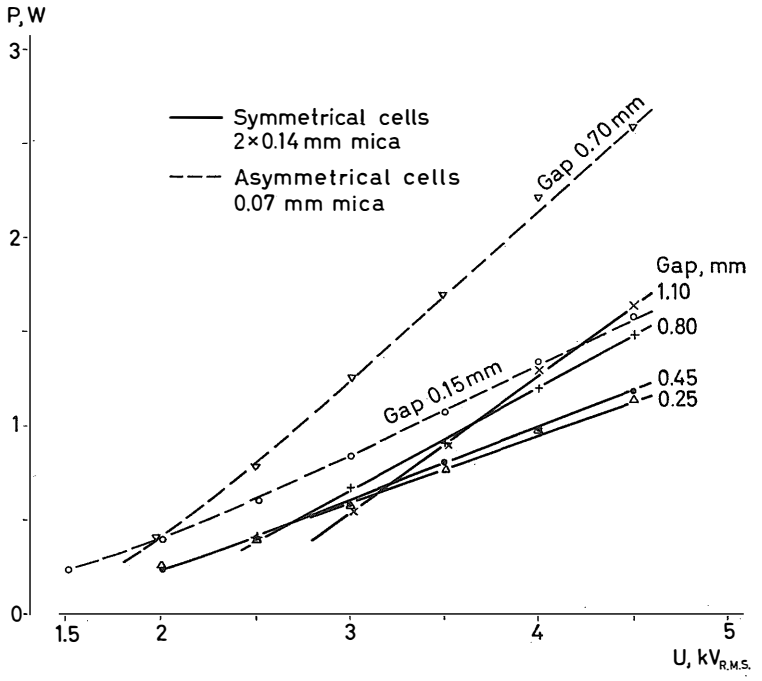

Fig. 6. Power dissipation in cells with different gap spacings.

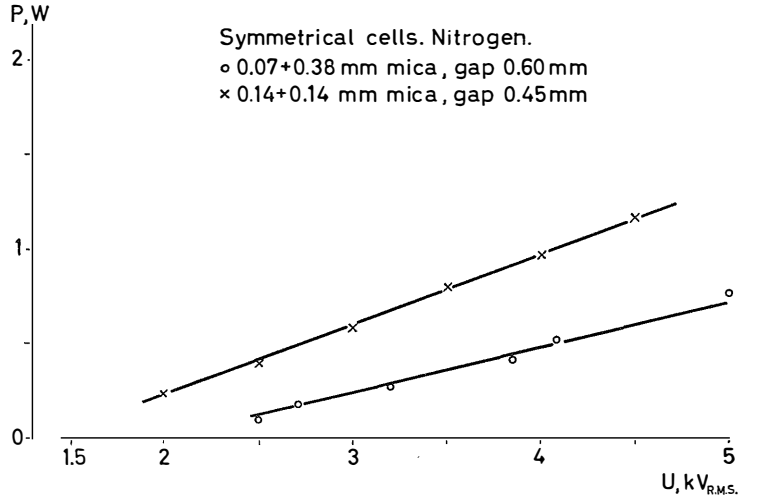

Fig. 7. Power dissipation in cells with different thicknesses of the dielectric.

Table 1. Discharge power P, mean current (positive pulses) I_{mdp}, discharge magnitude Q_{max} and pulse rate $\dot{N}$.

	3.2 kV (R.M.S.)				4.0 kV (R.M.S.)			
	I_{mdp} μA	Q_{max} nC	$\dot{N}$ Hz	P W	I_{mdp} μA	Q_{max} nC	$\dot{N}$ Hz	P W
Cell A (0.14 mm mica, gap 0.9 mm)								
Air	245	100	3300	1.09	520	100	6000	2.15
Cell A, N_2	410	200	2600	1.29	710	200	4300	2.18
Cell A, N_2, 26 nF in parallel	420	350	800	1.34	765	260	1400	1.94
Cell A, N_2, 56 nF in parallel	440	300	900	1.45	750	300	1700	2.17
Cell A, N_2, 1.3 H in series	385	200	2000[a]	1.22	695	200	4100	2.23
Cell B (0.19 PET, gap 0.45) Air								
Start	145	150	3000	—	225	30	8900	—
After 10 min.	130	30	6280	0.42	190	32	8700	0.64
After 107 min.	115	45	4600[a]	0.40				

[a] Unstable reading.

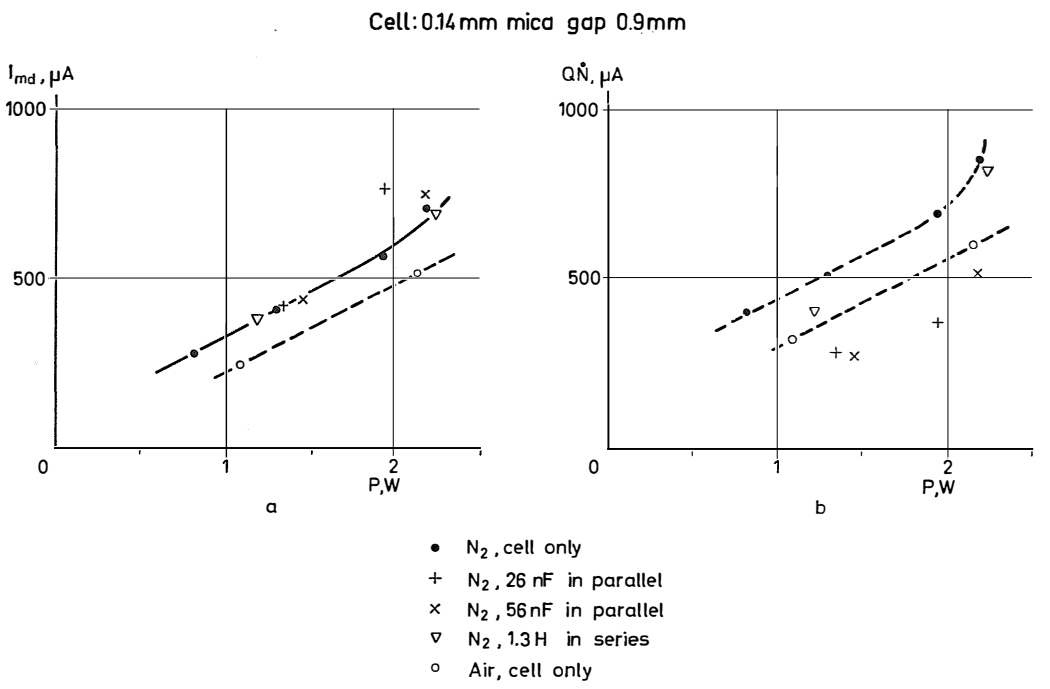

Fig. 8. Cells with external impedances: mean discharge current I_{md} and largest pulse times pulse rate, $Q\dot{N}$, as a function of the dissipated power.

foil demonstrated the existence of a time dependence of the discharge characteristics. This is probably caused by the formation of a layer of deteriorated material on the dielectric. In the present case this process appears to take 10–20 min. After this formation time, the surface attains constant properties during the subsequent progress of the attack on the material.

Fig. 8 gives the mean discharge current I_{mdp} and the product of the maximum pulse Q_{max} and the pulse rate $\dot{N}$ as functions of the dissipated power P in the mica cell mentioned in the preceding paragraph. The values concern partial discharges in nitrogen. Values are plotted for the cell without and with external impedances Z. These results indicate that $Q_{max} \times \dot{N}$ is more susceptible to changes for different values of Z than I_{mdp}. This can be understood if it is remembered that impedance variations—both in the cell and in the associated circuit—tend to influence both the amplitude and the shape of the pulse magnitude distribution and also the rate of occurrence of the discharge pulses[3]. This may influence the relation between the discharge detector readings and the statistical mean of the complete discharge pulse spectrum. In experiments with internal discharges in a gap with constant thickness, however, such changes may be expected to be of minor importance, with the possible exception of the initial stage of the exposure. Discharge detectors may, therefore, be quite satisfactory for use in such experiments. The authors wish to underline, however, the suitability, as demonstrated by the above-mentioned results, of the described method of mean pulse current measurement. This method is quite simple, relatively inexpensive in terms of equipment costs and requires a minimum of manipulation and, consequently, time.

The analysis of the experimental results both in terms of circuit parameters and the light they may throw upon the mechanisms of partial discharges between dielectric surfaces is published in a separate paper[4] (p. 103 of this issue).

Acknowledgements

The authors wish to thank Liljeholmen Kabelfabrik, Stockholm, for providing the discharge detector, and ASEA for permission to publish this paper. The work reported here forms part of a research project for which a grant has been obtained from the Swedish Technical Research Council.

Abstract

A calorimetric method for determining the power dissipation from partial discharges in a test cell is described. The influence of different experiment parameters on the power is investigated. A comparison of the measured power with electrically determined characteristics of the discharge intensity reveals the advantage of a simple mean-discharge-current measurement method for determining the discharge intensity in discharge-resistance tests on materials.

References

1. KREUGER, F. H.: Discharge detection in high voltage equipment, London 1964.
2. KELEN, A.: Partial discharges resistance testing of insulating materials. Acta Polytechnica Scandinavica El **16** (1967), pp. 3–86.
3. BUI-AI: Contribution à l'étude de la dégradation des isolants en feuilles sous l'action des décharges partielles. Thesis, Toulouse 1966.
4. KELEN, A.: A study of the mechanism of partial discharges at insulating surfaces. Acta Polytechnnica Scandinavica El **16** (1967), pp. 103–131.

A STUDY OF THE MECHANISM OF PARTIAL DISCHARGES BY INSULATING SURFACES

Andreas Kelen

Central Laboratories, ASEA, Västerås

Introduction

In a separate paper (p. 87 of this issue) the author and Aase describe a technique for the calorimetric determination of the power dissipated from partial discharges in a gap of constant width adjacent to, or sandwiched between, dielectric layers. Results illustrating the influence of different parameters on power dissipation are also presented there. This work was initiated in order to obtain a better knowledge of the relation between the usually measured electrical characteristics of partial discharges and the true energy dissipation. This was considered to be an important condition for enabling reliable discharge intensity determinations to be performed in work on the internal discharge resistance testing of materials, assuming as discussed in some detail in[21] that material degradation is nearly proportional to the dissipated energy. The purpose of the present work is to evaluate theoretically the results obtained from partial discharge calorimetry. The same notation is used as in[21], see p. 9 of this issue.

1. Results of calorimetric discharge power determinations

The power dissipation caused by partial discharges in a number of cells with gaps of constant thickness was determined by the technique described in[20]. The atmospheres used were stationary nitrogen and air. The discharge power P_k, the mean discharge current I_{md} and the discharge-inception and discharge-extinction voltages were determined. In each series of measurements I_{md} was varied through changing of the cell voltage.

Table 1 gives the characteristics of the used cells and the measuring programme. The number of individual measurements amounts to 385, 158 of these being with nitrogen. 45 results were excluded from the analysis, irrespective of whether they conformed to their group or not, for the following reasons: cell voltage too close to the inception voltage (fluctuating discharge intensity)—41, irregular I_{md}-values for normal P_k-values, i.e., suspicion of reading error—4.

If the calorimetric power values are compared with the power determined from

$$P_e = \tfrac{1}{2} I_{md} \left(1 + \frac{C_g}{C_d}\right) U_p \tag{1}$$

as derived in, for example,[8] on the assumption of a commonly used simple model, which will be discussed in some detail in 2, some general tendencies immediately appear, see Figs. 1 and 2. In the equation above, I_{md} is the mean discharge current, C_g and C_d are the capacitances of the gas gap and dielectric, respectively, and U_p is the Paschen breakdown voltage of the gap. In nitrogen the measuring points form a population, which appears to be grouped around a straight line with a slope of less than unity. The air values seem to form two distinct populations, one with a slope of about unity, and another with a lower slope. Adjacent points in the figures usually belong to different series of measurements. The average value is given for parallel results in a series. An examination of the deviations reveals that they are not systematically related to the cell parameters.

It appears, therefore, that the power as determined from I_{md}-measurements is well correlated with the actual power dissipation. The use of electrical characteristics of the power dissipated from internal discharges, e.g., in the discharge resistance testing of materials, may consequently be considered to be well justified, bearing in mind the limited accuracy of such determinations.

Table 1. Characteristics of cells and measuring programme for calorimetric discharge-power determinations.

Cell type	Atmosphere	Dielectric	k	d_g mm	d_d mm	$1+\frac{C_g}{C_d}$	U min. max. kV (R.M.S.)	I_{mdp} min. max. appr. μA	Number of results
16 A	N_2	mica	5.7	0.15	0.12	1.082	1–4	150–1300	8
	air						1–4	50–1300	7
33 A	N_2	mica	5.7	0.25	0.14	1.10	1.5–4.5	250–1250	18
	air						1.5–4.5	150–1250	18
13 A	N_2	mica	5.7	0.65	0.07	1.019	2–4	200–1500	9
	air						2–4	85–1350	9
15 A	N_2	mica	5.7	0.70	0.07	1.018	2–4.5	160–1250	6
	air						2.5–4.5	200–1200	5
14 A	N_2	mica	5.7	0.70	0.07	1.018	2–4.5	150–1250	6
	air						2–4.5	75–1200	6
32 A	air	mica	5.7	0.80	0.14	1.032	2.4–4.4	85– 900	33
25 A[a]	N_2	mica	5.7	0.90	0.14	1.027	2.8–4	280– 750	9
12 A	N_2	mica	5.7	1.03	0.12	1.021	3–4.5	350–1050	8
	air						3–4.5	100– 800	8
11 A	N_2	mica	5.7	1.18	0.12	1.018	3–4.5	330–1050	8
	air						3.5–4.5	250– 750	6
22 A	N_2	PET	3.2	0.45	0.19	1.157	2–4.5	50– 310	6
	air						2–4.5	35– 260	6
35 A	air	ep.+mica p.	4.2	0.45	0.19	1.10	2–4.5	35– 375	6
24 S	N_2	mica	5.7	0.15	2×0.14	1.328	1.5–4.5	50– 550	36
	air						1.5–4	70– 450	28
19 S	N_2	mica	5.7	0.25	2×0.14	1.197	1.5–4.5	50– 600	6
	air						1.5–4.5	50– 550	7
17 S	N_2	mica	5.7	0.45	2×0.14	1.109	1.5–4.5	85– 550	7
	air						2–4.5	70– 625	12
21 S	N_2	mica	5.7	0.60	0.48+0.07	1.132	2.5–6.25	60– 330	11
	air						2.5–4.5	20– 140	5
31 S	air	mica	5.7	0.60	2×0.14	1.082	2.2–4.4	70– 365	36
18 S	N_2	mica	5.7	0.80	2×0.14	1.061	2.25–4.5	110– 500	6
	air						2.7–4.5	100– 400	5
20 S	N_2	mica	5.7	1.10	2×0.14	1.045	3–4.5	110– 400	4
	air						3.5–4.5	120– 220	7
27 S	air	PET	3.2	0.33	2×0.19	1.427	2.5–4.5	45– 190	12
34 S	N_2	ep.+mica	4.2	0.50	2×0.19	1.18	2–4.5	40– 210	10
	air	p.					2–4.5	10– 170	12

[a] Measurements with externally connected impedances. Discharge intensity also determined with discharge detector and pulse-rate counter.

A = asymmetrical cells.

S = symmetrical cells.

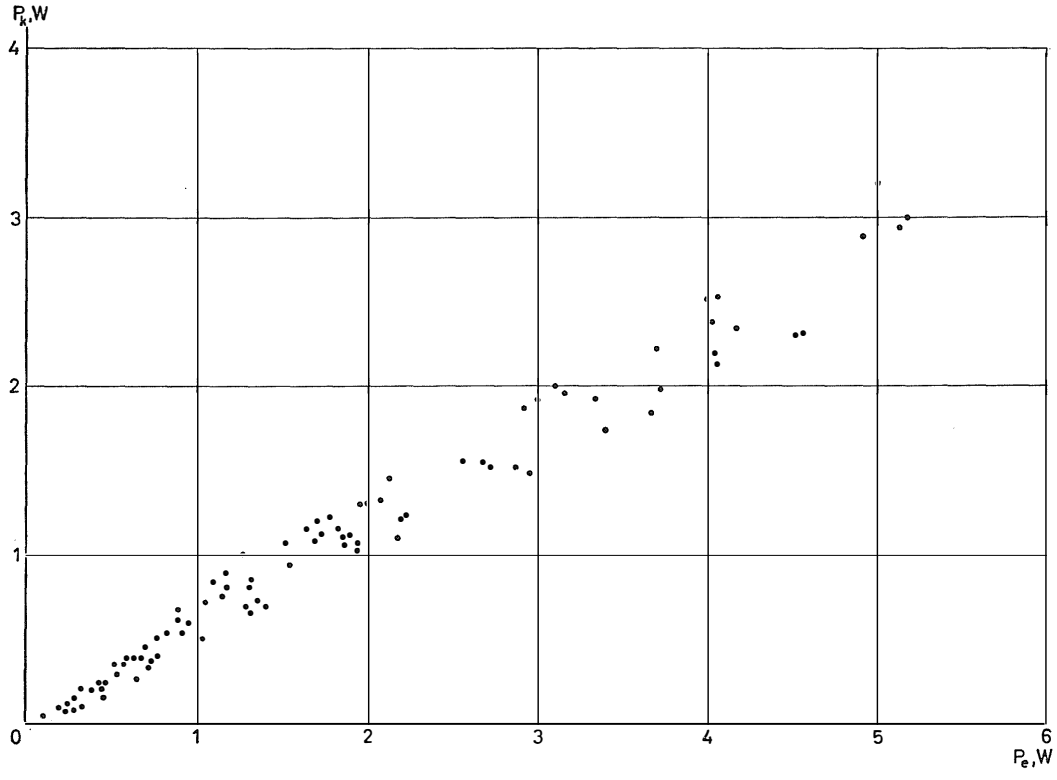

Fig. 1. Calorimetric discharge power P_k as a function of the discharge power P_e determined from electrical data (mean discharge current, Paschen breakdown voltage, cell parameters). Nitrogen.

The existence of two apparently distinct discharge regimes in Fig. 2, which is investigated in 3.2 and 4.2 suggests, however, that the test conditions should be chosen to ensure constant discharge conditions so that the spread in testing results will be reduced.

The experimental results are examined in more detail after these general findings. The confidence that can be placed in power determinations based on the externally measured discharge magnitude and inception and extinction voltages is then discussed. Finally, some aspects of partial discharge mechanisms are considered in the light of the experimental evidence.

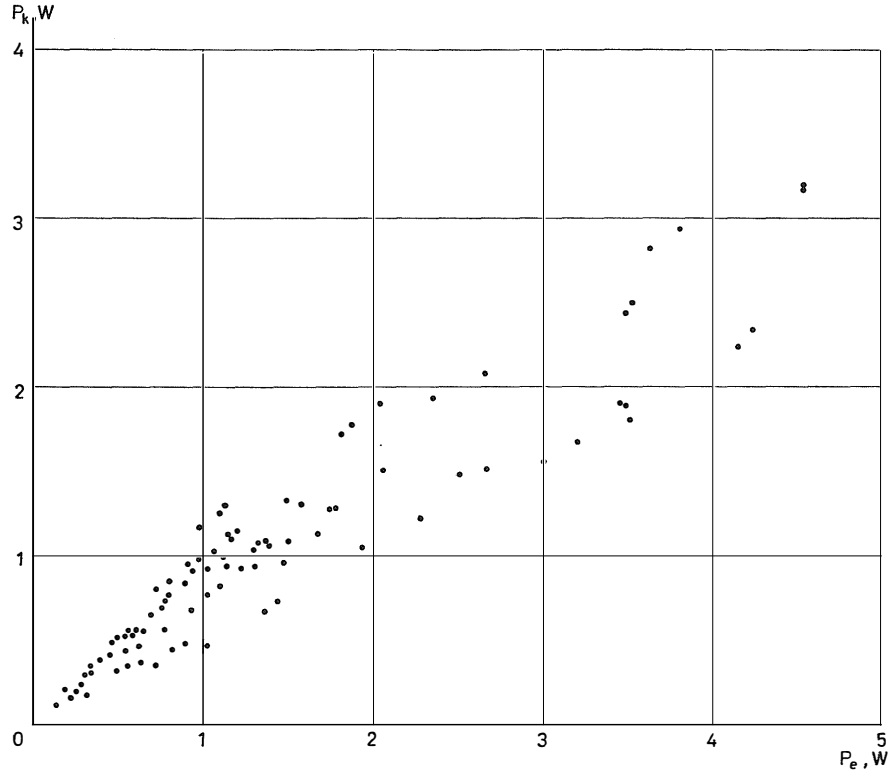

Fig. 2. Calorimetric discharge power P_k as a function of the discharge power P_e determined from electrical data. Air.

2. Derivation of a power equation

For a further evaluation of the experimental results, the power equation (1) quoted above will now be improved through the introduction of the discharge remanent voltage U_{dr}, which was assumed to be negligible in the derivation in[8].

The usual simple model of Fig. 3, which was introduced in 1932 by Gemant and v. Philipoff[14], is retained. Here, c_g denotes the capacitance of the actual discharge site, e.g., in a gap of constant width, c_d the capacitance of the solid dielectric affected by the discharge and C_p the capacitance of the rest of the object, which is capacitively coupled to the discharge site. When the rising voltage across the system reaches a level U_0, the discharge-ignition voltage U_{di} of c_g is attained and a discharge pulse locally bridges the gap. During

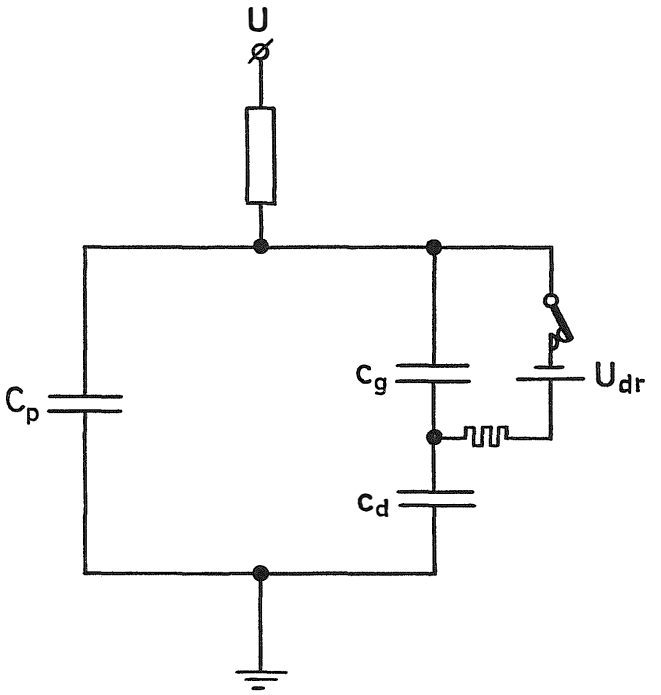

Fig. 3. Analogue model for deriving the power dissipation from partial discharges.

the very short lifetime of the discharge (of the order of 10 ns), the circuit of Fig. 3 is assumed as usual to be isolated from the voltage source owing to inductances in the voltage source and the leads. The reduction of the charge initially stored in c_g leads to a rearrangement of the charges in the circuit with a resulting decrease of U_0 to a value U_0'. After this a charge ΔQ_p is supplied to the circuit from the source with a time constant, which is normally greater than the lifetime of the discharge, but small compared with the rate of change of the applied voltage.

Changes in the system during the life of the discharge pulse may be assumed to contribute to the energy dissipation in the discharge. As far as changes in the dielectric polarisation of the solid dielectric are concerned, the high-frequency part of the permittivity is of relevance. In the case of a frequency-dependent permittivity (the low-frequency permittivity usually being superior to the high-frequency value), subsequent dielectric heating of the solid dielectric will take place.

The usual way of analysing the model which is also followed here is to compare the potential energy of the capacitance network before and after the charge redistribution caused by the discharge, and to interpret the difference as being the amount of energy dissipated as a consequence of the discharge. This can be done in an elementary way by assuming, as is indicated in Fig. 3, that a short circuit with a constant discharge remanent voltage U_{dr} is established immediately after the breakdown of c_g. This forces a charge $\Delta Q_d = c_d[(U_0 - U_{di}) - (U_0' - U_{dr})]$ to traverse the short circuit, which gives a contribution to the energy dissipation.

The derivation given in the appendix yields an expression for the energy dissipated by one discharge:

$$W = \Delta Q_p \left(1 + \frac{c_g}{c_d}\right)(U_{di} + U_{dr}) \tag{2}$$

It should be mentioned that the foundations of the above derivation are not rigorous in the sense of the actual physical mechanisms. However, the good correspondence of this simple theory with measured results obtained under experimental conditions, as given in, for example,[21], on the one hand, and the limitations of the analogy, which will be discussed in 4, on the other hand suggest that a further elaboration of the energy equation based on the present model, e.g., through the solving of differential equations for the current and voltage distributions as a function of time, is not justified.

The charge flow ΔQ_p into the circuit is an empirically given quantity. The total discharge energy dissipated by N discharges is proportional to $\Sigma^N \Delta Q_p$. The energy derived from pulse-magnitude measurements and pulse counts is correct to the extent that the measuring methods enable a proper averaging of the statistical variations of the pulse amplitude to be made in the measuring

process itself or in subsequent calculations. The pulse statistics are known to be influenced by experimental parameters.

The time average of the statistically distributed ΔQ_p's is the mean discharge current I_{md}:

$$I_{md}=\frac{\sum^{t}\Delta Q_p}{t}$$

where t is time.

With the substitution of I_{md} for ΔQ_p, Eq. (2) is transformed into an expression giving the power dissipation by discharges, which we shall call P_d. Thus,

$$P_d=\tfrac{1}{2}I_{md}(U_{di}+U_{dr})\left(1+\frac{c_g}{c_d}\right) \tag{3}$$

The voltage term shows, perhaps rather surprisingly at first sight, that the discharge power increases with the discharge remanent voltage. This is caused by a term $(U_{di}^2-U_{dr}^2)$, the factor $(U_{di}-U_{dr})$ of which enters into ΔQ_p. If conditions were arranged to give equal I_{md}'s in two circuits, one with $U_{dr}=0$ and the other with $U_{dr}=aU_{di}$, dissipation would be greater in the second circuit by a factor $(1+a)$. In terms of our model, U_{dr} can vary between the limits 0 and U_{di}. Physically speaking the upper limit of U_{dr} is certainly lower. Thus,

$$U_{di}\leq U_{di}+U_{dr}<2U_{di}$$

We shall return to the discussion of U_{di} and U_{dr} in 4.

The term $1+c_g/c_d$ reflects the contribution to the dissipation of the current, which changes the state of polarisation of c_d. The discussion of its significance has been initiated in this laboratory by Dick. Our findings are published in[8]. Subsequently this question has been investigated by Bui-Ai[7]. Other workers have independently arrived at this term[6, 13, 18, 27] without making any interpretation.

The local capacitances c_g and c_d, which are associated with the individual discharge pulse, cannot be directly determined. They are affected by several experimental parameters and are subject to statistical variations even under constant conditions. It may be assumed that $c_g/c_d=C_g/C_d$, i.e., the ratio of the gas and solid dielectric capacitances of the whole arrangement between the electrodes.

It would be incorrect to assume that c_g and c_d can be separately determined as $\epsilon_0 A/d_g$, $k\epsilon_0 A/d_d$ from measured values of the area A affected by a single discharge as observed by, for example, Mason[24], Thomas[30], Bertein[3] and Grosskreuz[15]. Instead, c_g and c_d are capacitances between a small area

A and a parallel infinite plane at distances $d_g + d_d/k$, d_d/k, respectively. As is suggested in Fig. 4, this problem is equivalent to the determining of the capacitance with edge effects between parallel plates with areas A at twice the actual distance. Because the ratio between this capacitance and the homogeneous field capacitance $\epsilon A/d$ is a constant, 2.163 (see, for example,[10] v. III p. 80), it is not necessary to derive the actual capacitances in order to obtain a correct value for c_g/c_d. This argument does not apply, however, to the time-varying field distribution during the life of the discharge.

The values of C_g and C_d used in the present work usually cause their ratio to be considerably smaller than unity. The error made in determining the entire term $(1 + C_g/C_d)$ is thus usually not important. C_g/C_d can also be written as d_d/kd_g, where d denotes thickness, and k the relative permittivity of the solid dielectric.

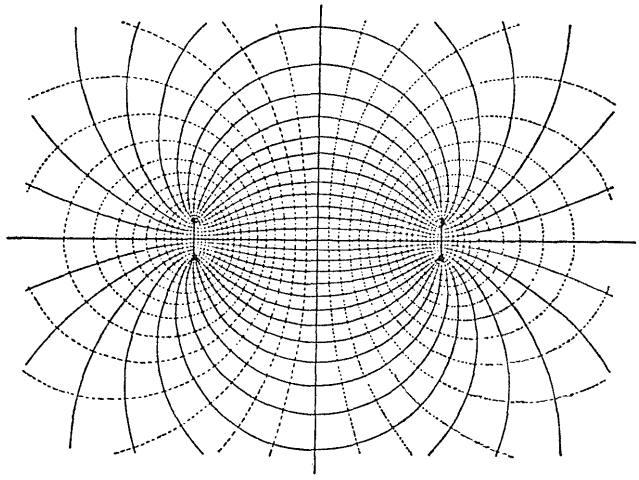

Fig. 4. Field pattern from oppositely charged parallel plane conductors with limited area. Lines of force and equipotentials.

3. Analysis of the experimental results

The calorimetric measurements yield associated values of P_k, I_{md}, U_i and U_e in cells with known d_g, d_d and k. The following approach was chosen for evaluating the experimental data: values of $(U_{di}+U_{dr})$ were calculated for each run from

$$(U_{di}+U_{dr})=\frac{P_k}{I_{mdp}\left(1+\frac{d_d}{kd_g}\right)} \tag{4}$$

A normalised result was obtained with the introduction of an index B:

$$B=\frac{U_{di}+U_{dr}}{U_p} \tag{5}$$

When U_{dr} vanishes, an upper limit of U_{di} is obtained. A direct assessment of the actual values of U_{di} and U_{dr} requires additional information.

3.1. Measurements in nitrogen

In Fig. 5 the index B for one series of measurements is shown as a function of I_{mdp}. There is no significant dependence.

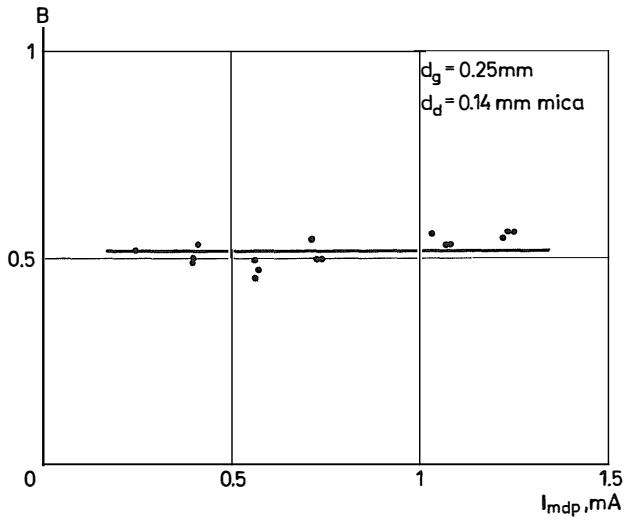

Fig. 5. The normalised voltage index B as a function of the mean discharge current (positive component) I_{mdp} in a cell with nitrogen.

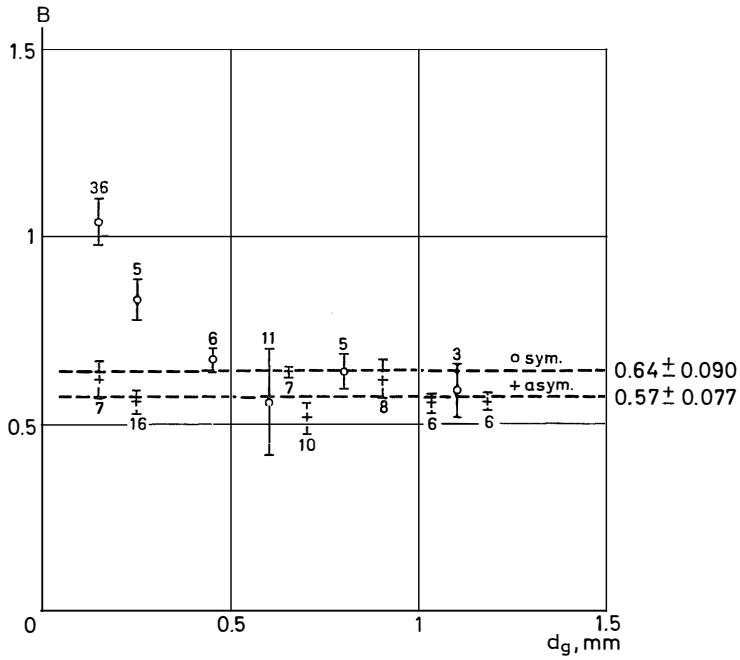

Fig. 6. The normalised voltage index B as a function of the gap width in symmetrical and asymmetrical cells with nitrogen.

The mean values and standard deviations of B are shown in Fig. 6 for different gaps d_g in asymmetrical and symmetrical cells. The mean values for all measurements with each type of cell are indicated. The B-values are normally distributed. A statistical t-test ([16], Ch. 15) shows that the deviation of the means is significant ($t=4.0$). There is a clear indication that $U_{di}+U_{dr}$ for symmetrical cells increases in narrow gaps. The 0.15 mm value representing 36 measurements is not included in the calculation of the mean value for all symmetrical cells.

3.2. **Measurements in air**

Inspection of the records for different series of measurements reveals that the B-values in some but not all series are grouped in a high and a low population. The division is governed by the discharge current. As an illustration, the B-values from an extensive series are plotted in Fig. 7 together with P_k-values. A marked transition occurs at about 600 μA. This critical current seems to vary with d_g; the thicker the gap, the greater is the critical current. It appears that the discharge regime differs in some way for low and high currents. This effect is particularly noticeable in work with asymmetrical

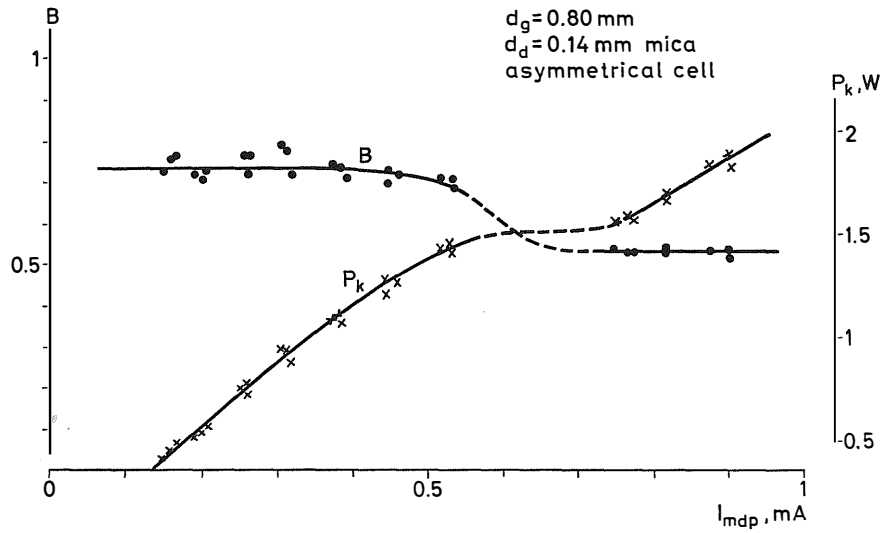

Fig. 7. The normalised voltage index B and the calorimetric discharge power P_k as functions of the mean discharge current (positive component) I_{mdp} in an asymmetrical cell with air. Gap width 0.8 mm.

cells. It has also been observed, however, with symmetrical cells. After this effect was discovered, the records for each series were inspected for the presence of this division, and the individual measuring points were allotted to a low-current group (high B-values) and a high-current group, respectively. In most cases, this could be done quite unambiguously. A few values, which might belong to either group, were intuitively allotted to one or other population. This can have only a small influence on the statistics. After this sorting and a preliminary check of the possible influence of d_g on the mean values, which was found not to be significant, mean values and standard deviations for B in the low- and high-current regimes were determined. The results of the statistical evaluation of the data are summarized in Table 2.

Table 2. B-values in air. Cells with mica.

	Asymmetrical	Symmetrical
High-current regime		
Mean value	0.56	0.68
Standard deviation	0.067	0.090
Number of observations	42	34
Low-current regime		
Mean value	0.78	0.90
Standard deviation	0.090	0.068
Number of observations	38	48

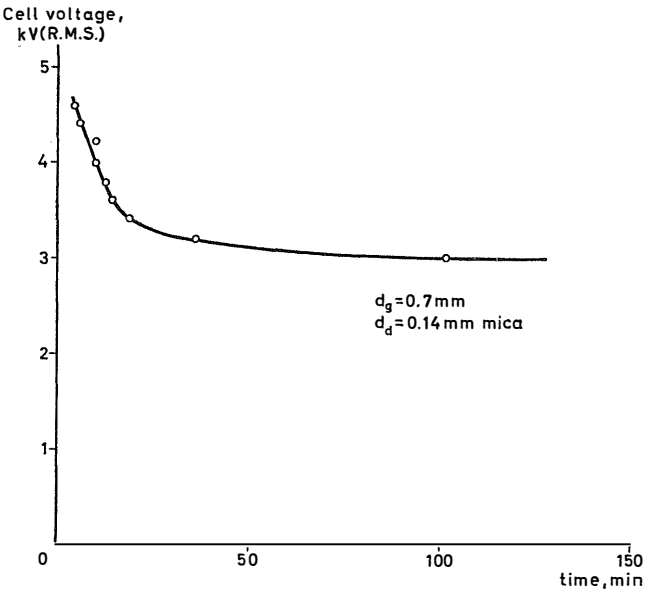

Fig. 8. The time required for the regime transition to occur as a function of the voltage applied to the cell.

A statistical t-test shows that the difference between the means for the high- and low-current regimes, respectively, is highly significant ($t>12$). The same is also true of the difference between the mean values for asymmetrical and symmetrical cells ($t>6.5$).

The results from the asymmetrical cells with gaps 0.15 and 0.25 mm and the symmetrical cell with $d_g=0.15$ mm belong entirely to the high-current population. The cells with $d_g=1.18$ and 1.03 mm (asymmetrical) and the symmetrical cells with $d_g=$ 1.10 and 0.80 mm and one of the 0.60 mm cells gave low-current readings only. In the rest of the cells the transition was observed.

This phenomenon, although not of primary importance in, for example, discharge resistance testing, deserves some attention in order to avoid unnecessary uncertainties in the interpretation of relative tests. The transition between the two regimes reveals itself in the current-voltage characteristic. The discharge current readings suggest that the phenomenon requires some time to become established after the beginning of the discharges. This time varies with the applied voltage as shown in Fig. 8. Measurements with a cell with a high-voltage electrode of about half the standard area indicate that the regime transition depends on the current rather than on the current density. The interpretation of this phenomenon is discussed in 4.

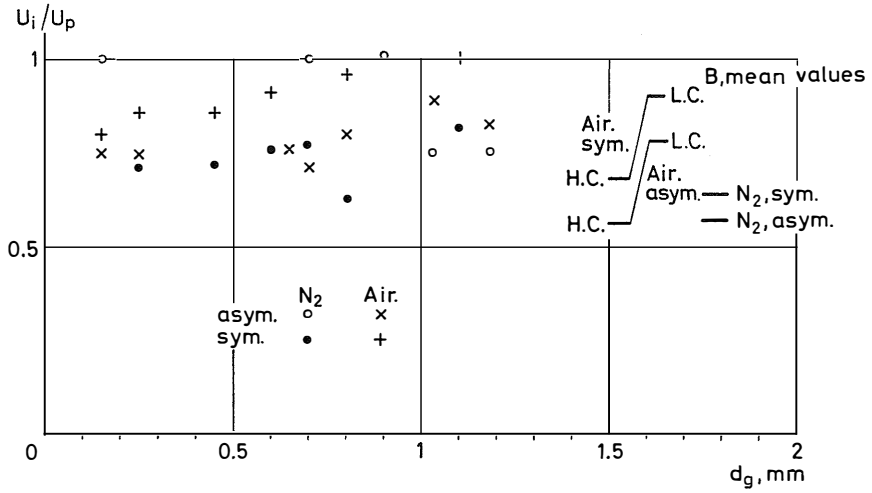

Fig. 9. Dependence of the normalised discharge-inception voltage on the gap width d_g of cells with nitrogen and air.

3.3. **The discharge-inception and discharge-extinction voltages**

These magnitudes are defined as the R.M.S. voltage between the electrodes, i.e., across the entire object, when discharges begin to appear at a gradually increasing alternating voltage (U_i) or to disappear at a decreasing voltage (U_e). Owing to local fields produced by surface charges, which are deposed on a dielectric surface by discharge pulses, U_e is always smaller than U_i. This does not imply, however, that a determination of U_i gives the true U_{di} when U_i is divided by $(1+C_g/C_d)$. Surface charges from previous discharges may provoke discharges, which gives too low a U_i-value as compared with a charge-free surface. The error depends, among other things, on the time which has elapsed after the last discharge, the surface resistivity of the dielectric, and on the sensitivity of the discharge detecting device.

The regular recording of U_i (and U_e) in our measuring routine enables a comparison of the mean value of U_i to be made for each series of measurements with U_p and $U_{di}+U_{dr}$, see Fig. 9. In Fig. 9 U_i is transformed from (R.M.S.) to (peak values). U_i is usually less than U_p but greater than $U_{di}+U_{dr}$. The standard deviation of U_i is of the order of 5 per cent.

For practical purposes U_i is usually used in calculating discharge energy or discharge power. The relation between U_i and U_{di}—assuming U_i to be the correct value—is

$$U_{di}=\frac{U_i}{1+\frac{c_g}{c_d}}$$

Thus, Eq. (3) transforms into

$$P = I_{md}\, U_i (1 + a) \tag{6}$$

where

$$a = \frac{U_{dr}}{U_{di}}$$

Experimental discharge-inception voltages are subjected to some uncertainty, as has been discussed above. U_{di}, however, is still not known with any greater accuracy and, moreover, may be affected by the experiment, e.g., owing to a varying composition of the atmosphere or varying pressure. In addition, the use of tabulated U_{di}-values, if available, requires d_g to be known with considerable accuracy. So far, therefore, Eq. (6) appears to be the most suitable approach to discharge power determinations based on the usual electrical data. In comparative tests with constant d_g, however, it is practical to retain U_{di}. The results of the present investigation are applied in a general way by using the power equation in the form

$$P \approx 0.4 U_p I_{md} \left(1 + \frac{C_g}{C_d}\right) \tag{7}$$

or

$$P \approx 0.8 U_p I_{mdp} \left(1 + \frac{C_g}{C_d}\right) \tag{7a}$$

Paschen breakdown voltages of air, nitrogen and hydrogen at atmospheric pressure as a function of the electrode spacing are given in Fig. 1.1 of[21], see p. 12 of this issue.

3.4. **Cells with organic dielectrics**

Runs with an asymmetrical cell with $d_g = 0.45$ mm with polyethylene terephthalate foil as dielectric yielded mean B-values of 0.84 in nitrogen and 0.90 in air. A symmetrical cell with $d_g = 0.33$ mm gave an average B-value of 0.72 in air. Two long-term runs were performed with this cell, the results of which are shown in Fig. 10. Runs with epoxy-impregnated mica paper in air gave an average B-value of 0.95 in an asymmetrical cell with $d_g = 0.50$ mm and $B = 0.72$ in a symmetrical cell with $d_g = 0.45$ mm. The purpose of these experiments was to ascertain whether the effects found with mica cells could also be observed in cells with organic dielectrics. The material is not sufficient to permit a detailed discussion. In work with organic dielectrics changes in U_{di}, and possibly also in U_{dr}, may arise owing to the accumulation of volatile deterioration products from the exposed surfaces.

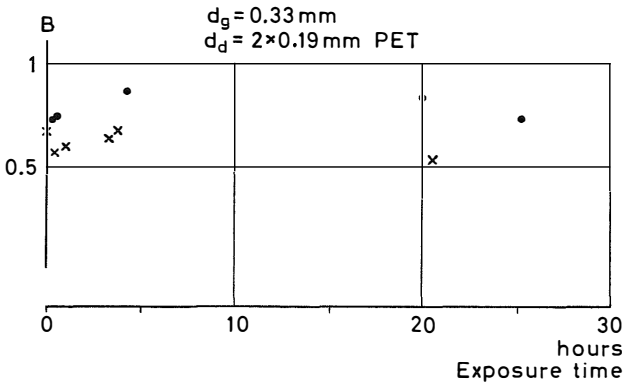

Fig. 10. Dependence of the normalised voltage index B on the exposure time in cells with polyethylene terephthalate.

4. Discussion

4.1. U_{di} and U_{dr}

The results of the measurements of $U_{di}+U_{dr}$ and the index B represent, as has been mentioned, upper limits for U_{di}, which are approached if U_{dr} is negligible. The interpretation assumes the validity of the model on which the power equation is based.

The majority of our results show that U_{di} is less than the Paschen value U_p, in agreement with results reported by Mason[24] and other workers but in contrast to the widely quoted findings of Hall and Russek[17], who state that U_{di} is equal to U_p, and of workers of the Toulouse school. Thus, Fieux[12] and Mendès[25] found that U_{di} is equal to, or slightly larger than, U_p; Bui-Ai[7] holds that the difference in electron emission properties between metals and dielectrics causes U_{di} in a gap bounded by dielectric surfaces to exceed U_p.

Experiments with A.C. breakdown in air and nitrogen have been performed in this laboratory with stainless steel electrodes with spacings of 0.1, 0.5 and 1 mm. They yielded results in good agreement with handbook values[23]. In order to obtain information about the influence of electrode properties, U_p in air was determined at a 1 mm gap spacing with high-voltage electrodes of brass, aluminium (which is always covered by oxide) and graphite (low secondary electron emission, high resistivity). The deviations between the runs were found to be 5 per cent or less. The standard deviation of each run was 1 per cent or less. The electrode material thus does not appear to influence to a marked degree U_p at atmospheric pressure of millimetre gaps with conducting electrodes.

Statements in the literature about the value of U_{dr} are sparse. Many workers prefer not to express explicit opinions and assume more or less arbitrarily that U_{dr} is negligible in their calculations, e.g.[22]. Bui-Ai advances a hypothesis that U_{dr} is proportional to U_{di}[7]. Heller[18], Riege[28], Böning[6] supported by Veverka[31] derive values of U_{dr} from calculations of the coupling effects between the discharge site and the surrounding parts of the dielectric surface through surface conductivity. Of these authors only Riege arrives at a true U_{dr} which is established during a sufficiently short time to affect the live discharge. The U_{dr}'s of Böning, Heller and Veverka, which are appropriately named "return voltages" by these authors, appear after the discharge is ex-

tinguished and have consequently no effect on the energy dissipation in the discharge. However, they influence the occurrence of subsequent discharges.

The calorimetric results discussed here cannot be interpreted unambiguously as revealing the existence of a discharge remanent voltage. Any difference from Paschen values or between different series of experiments (e.g., symmetrical and asymmetrical cells) permits an interpretation in terms of a variation in U_{di} as well as in U_{dr}. Before the question is considered any further, the peculiar phenomenon of a regime transition in the experiments with air cells will be discussed.

4.2. **The regime transition: validity of the analogue model**

An attempt could be made in the first place to explain the phenomenon as being caused by a change in the atmosphere, which affects U_{di}. Ozone and nitrous oxides, which are formed in air owing to discharge action, are strongly electronegative. Their accumulation would tend to increase U_{di}, which is proved in[5], in contrast to the observed effect. It is difficult to accept that a U_{dr} (high for low currents and low or absent for high currents) caused by a possible blocking action of the dielectric, as discussed below, can be subject to a regime transition. Moreover, it is difficult to explain in this way the occurrence of the effect in air but not in nitrogen.

The regime transition in air, however, can be interpreted if one considers the well-known fact that partial discharges against dielectric surfaces usually consist of more than one stage, i.e., an axial discharge followed by one or more generations of discharges tangential to the surface. Such a mechanism is not covered by the simple analogy model (Fig. 3) from which the power equation is derived. The experimental establishment of the limitation of this commonly applied model justifies some further discussion.

From gas discharge physics it is known that the diameter of a discharge pulse bridging a stressed gap is small, of the order of 0.1 mm. On the other hand, investigations of the area of the insulating surface affected by single discharges have revealed in many cases considerably greater sizes, with diameters up to several millimetres[3, 15, 24, 30]. The secondary events, which occur tangentially to the surface, are related to the formation of Lichtenberg patterns. Investigations of the dynamics of discharge pulses[1, 7] reveal (Fig. 11) that the primary pulse and secondary events often tend to merge, i.e., the secondary discharge finds its way through the still conducting path of the primary discharge. The relevance of these facts to the analogy model shown in Fig. 3 is a variation with time of the capacitance c_d of the part of the solid dielectric affected by the discharge, and probably also of the capacitance of the affected gas volume c_g.

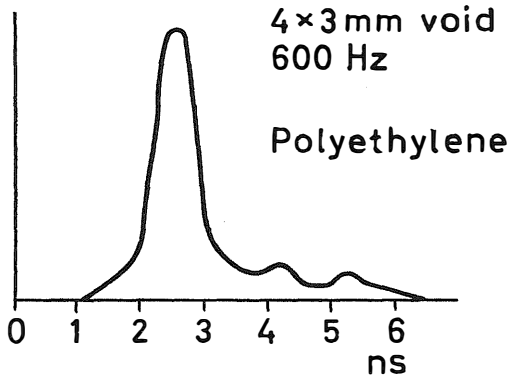

Fig. 11. Oscillogram of partial discharge pulse (according to Bailey).

A revision of the model shown in Fig. 3 in order to obtain a closer approach to reality entails considerable difficulties. The results of quantitative physical investigations of gas discharges against dielectric surfaces would be required. Even if such information were available, the resulting model would probably lack the main merit of the simple model, i.e., the possibility of obtaining the discharge power dissipation from simple electrical measurements on the object in which partial discharges occur.

The critical argument about the limited validity of the simple analogue model might be reversed to some degree, if it is observed that the error as revealed, for example, by the deviation of our B-values from unity, is not very great. Against the background of the difference between the actual discharge process and the idealisation inherent in the simple model, this appears to be rather interesting. From a practical standpoint one might contemplate improving the accuracy of energy and power determinations from electrical measurements of the object, without making changes in the idealised basic assumptions of the model, by applying an empirical correction.

Returning to the interpretation of our measurements, one cannot regard the calculated B-values as representing true values of $(U_{di}+U_{dr})$. The discussion of the voltages characterising the discharge must therefore be renewed. Two approaches appear to be reasonable:

1. The discharge-ignition voltage values found from inception-voltage determinations are accepted and used for evaluating the calorimetric results. The published results reviewed above, which are indirectly supported by our breakdown measurements with different electrode materials, point

towards the hypothesis that the Paschen breakdown figures are true or approximately true in the considered situation.

2. The calorimetric results (current, power) are examined in the light of a qualitative picture of the actual discharge process.

Case 1 does not exclude the possibility that some qualitative judgement of U_{dr} might possibly still be obtained. This can hardly be so, however, with case 2.

As to the regime transition in air, it might be suggested that it is caused by a changing pattern—on the average—of the secondary phase of the discharge. It is known from investigations by, for example, Mason, how different (number and size of side branches, etc.) the appearance of the surface discharge pattern can be, and how the appearance is affected by the composition of the atmosphere. The equilibrium concentration of ozone and nitrous oxide in stationary air is thought to play a role in this connection. The observation by Katakis and Bersis[19] that increasing ozone concentration in an ozoniser affects the appearance of the discharge pulses towards increasing intensity of the secondary events supports this view. In this connection, the decrease of the surface resistivity of the insulation[9, 4] due to discharges may also exert a certain influence.

4.3. **On discharge mechanisms**

It is tempting to speculate about the mechanisms of partial discharges.

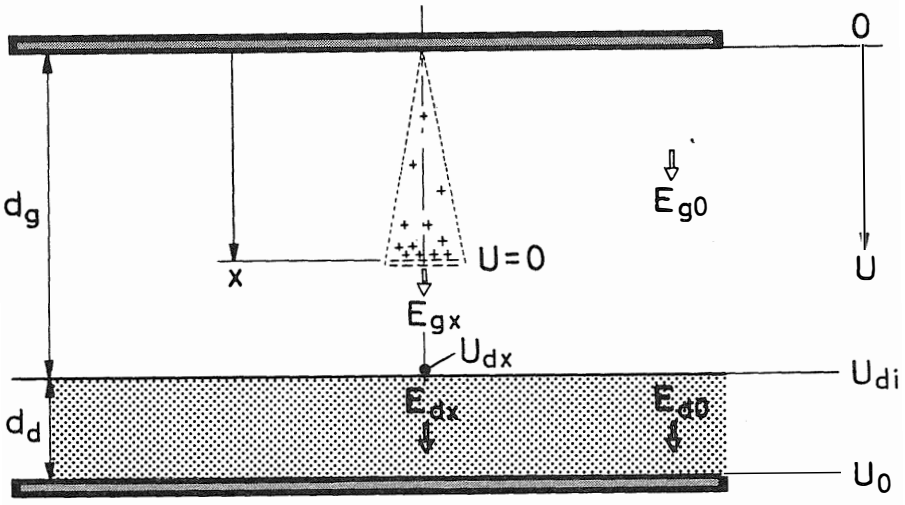

Fig. 12. Model for estimating the field intensity in front of a growing discharge in a gap bounded by a dielectric.

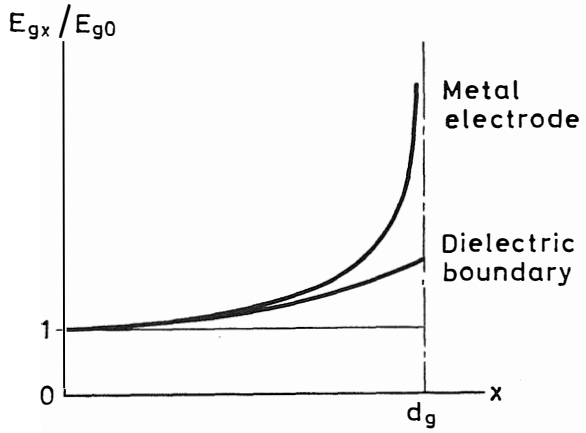

Fig. 13. Schematic diagram showing the variation of the field intensity in front of a discharge growing towards a conductor and towards insulation

There might be a difference in the conditions for the last stage of the propagation of an individual discharge pulse between metallic electrodes and against a dielectric surface. If we roughly assume, as is indicated in Fig. 12, that the head of the discharge is at cathode potential and that the field in the discharge axis is crudely represented by the one-dimensional approximation, an expression for the stress concentration in front of the discharge head is obtained:

$$\frac{E_{gx}}{E_{g0}} = \frac{d_g + \frac{d_d}{k}}{d_g + \frac{d_d}{k} - x}$$

which has its maximum value $(1+kd_g/d_d)$ for $x=d_g$. This expression applies irrespective of whether the discharge strikes from metal to dielectric, from dielectric to metal, or between dielectrics. As shown schematically in Fig. 13, E_{gx} increases only slightly with x in the final part of the discharge path, in contrast to the field at the head of a discharge between conductors, which increases as $d_g/(d_g-x)$. Discharges in gaps bounded by insulation thus seem to lack the final intensive acceleration stage owing to mirror forces, which are characteristic of discharges in narrow metal gaps.

A somewhat closer estimate of the field in front of the discharge head may be obtained, if, for example, a model consisting of two oppositely oriented coaxial dipoles representing the electron avalanche and its mirror image is assumed. The dipole moment of the avalanche is approximately $p(x)=qe^{\alpha x}/\alpha$

(q-electronic charge, α-Townsend's first coefficient). The field intensity in front of the avalanche is approximately $E(x)=p(x)(8\pi\varepsilon_o)^{-1}(d_g-x+d_d/k)^{-3}$.

When the same crude representation as above is applied, it is seen that a radial field distribution develops on the dielectric surface under the approaching discharge. The conditions for initiation of secondary, tangential discharges when, or immediately before, the primary discharge reaches the boundary may be thought to be more advantageous than for the primary discharge; its target area is bombarded by U.V. photons and—at the appropriate polarity—by electrons.

The development and ultimate size of the secondary surface discharges may be thought to depend on the properties of both the solid surface and the atmosphere. Neumärker[26] has studied the development of tangential surface discharges and found a value of 7.5 kV/cm for the voltage gradient in a growing discharge channel. Our observation of increasing B-values for narrow symmetrical gaps with nitrogen may be interpreted as being caused by a decreasing intensity of the tangential secondary discharges for narrow gap spacings.

There does not exist much evidence to permit an analysis of the type of gas discharge which constitutes partial discharges—whether of the Townsend, streamer or space-charge-enhanced single-avalanche type. In spite of the very fast rise (of the order of 2 ns) of the impulse front reported by Bailey[1] and of the extremely brief processes (0.5 ns) observed by Zavojskij[33] in discharges in narrow air gaps at VHF voltages, the multi-generation-avalanche Townsend mechanism cannot be ruled out. The relatively long initial phases of the build-up of this type of discharge would probably have escaped observation. As to the pronounced dependence of the Townsend breakdown on the properties of the electrode surfaces, existing evidence is probably too sparse to permit a judgement.

One of the quick discharge mechanisms without secondary electrode events, namely space-charge-accelerated single-avalanche breakdown[32] or streamer breakdown, i.e., the formation of a plasma channel from the inflow of electrons from secondary avalanches initiated in the gas near the head of the primary avalanche, may intuitively appear to be a more satisfactory explanation. The streamer mechanism is usually considered to be characteristic of relatively long discharges. A quantitative assessment will not be attempted here. It may be observed, however, that the radial field distribution produced by an avalanche approaching an insulating gap boundary might have some relevance to Meek's criterion for the avalanche-streamer transition (equality of the axial and radial field intensities at the avalanche head owing to field distortion by space charges).

Saxe[29] has reported interesting image-converter observations of rapid (1 to 3 ns) glow and channel propagation from cathode to anode in air.

It is usually held that avalanches can develop into streamers, when the number of electrons in the head of the discharge exceeds about 10^8. Bearing in mind that 1 pC is equivalent to about 3×10^6 elementary charges of each sign, discharges exceeding some 10^3 pC might be over-critical, even if a considerable part of the observed discharge magnitude originates from secondary tangential events by the dielectric surface, as discussed by, for example, Edelmann[11].

In the light of the results and discussion presented above, a closer study of the physics of gas discharges against dielectric surfaces would appear to be desirable.

Acknowledgements

The author thanks Mr. John Aase for most valuable assistance with the measurements, and Mr. Clas-Tore Jacobsen for stimulating discussions. He also wishes to thank ASEA for permission to publish this paper. The reported work forms part of a research project for which a grant has been obtained from the Swedish Technical Research Council.

Abstract

The results of calorimetric discharge-power determinations are interpreted in terms of the sum of the discharge-inception and the discharge remanent voltages assuming a commonly accepted analogue scheme. The adoption of this scheme, on which discharge-power determinations are usually based, is shown to be justified for practical purposes when a limited accuracy can be accepted. A closer analysis of the results reveals, however, the limitations of the scheme.

A current-dependent discharge-regime transition in air is observed and an explanation is proposed. This transition is absent in nitrogen.

A discussion of discharge mechanisms leads to the conclusion that the discharge-inception voltage of gaps with dielectric boundaries probably coincides with the Paschen values. Differences in the breakdown mechanisms in gaps with conducting and dielectric boundaries are indicated.

References

1. Bailey, C. A.: A study of internal discharges in cable insulation. IEEE Paper No. 31 PP 66–363 (1966), 9 pp.
2. Bashara, N. M.: The study of discharges in dielectric voids by photomultiplier methods. AIEE Transactions (Jan. 15, 1960) Paper No. 60–277.
3. Bertein, H.: Application de la méthode des figures de poudre à l'étude de la décharge par effluves dans les isolants. Revue Générale de l'Électricité **69** (1960): 9, pp. 461–474.
4. Boeck, W.: Ein neuer Durchschlagsmechanismus infolge Koronaentladungen an Isolierstoffen. ETZ-A **85** (1964): 22, pp. 730–731.
5. Boylett, F. D. A., Looms, J. S. T.: Effect of discharge products upon corona discharge and spark breakdown voltage. Proc. I.E.E. **110** (1963): 12, pp. 2292–2296.
6. Böning, W.: Luftgehalt und Luftspaltverteilung geschichteter Dielektrika I. Archiv für Elektrotechnik **48** (1963): 1, pp. 7–22.
7. Bui-Ai: Contribution à l'étude de la dégradation des isolants en feuilles sous l'action des décharges partielles. Thesis (Dr ès Sciences) Faculté des Sciences, Univ. of Toulouse. April 1966.
8. Dick, W., Kelen, A., Larsson, L., Sletbak, J.: On the significance of some test parameters for the discharge endurance testing of insulating materials. Elteknik **7** (1964): 8, pp. 147–150.
9. Дмитриев, А. В., Цзян Цзе-Цзянь: Изменение свойств поверхности диэлектрика под воздействием газового разряда. Ж. Т. Ф. **36** (1966):4, pp. 739–745. (Dimitriev, A. V., Chian Chieh-chiang: Property changes of dielectric surfaces exposed to gas discharges. J. Tech. Phys. USSR).
10. Durant, E.: Electrostatique. Paris 1966.
11. Edelmann, H.: Ein Beitrag zur Messung der Alterung von Polyäthylen-Folien unter dem Einfluß einer 50-Hz-Gasentladung. ETZ-A **85** (1964): 14, pp. 434–439.
12. Fieux, R.: Étude des variations de la tension de seuil et de la tension disruptive dans une cellule à décharges partielles. Thesis (Dr de spéc.) Faculté des Sciences, Univ. of Toulouse. May 1965.
13. Garton, C. G.: The energy of discharges and their interaction with solid dielectrics. Gas discharges and the Electricity Supply Industry (Intern. conf. CERL, Leatherhead, May 1962). London 1962, pp. 412–419.
14. Gemant, A., v. Philipoff, W.: Die Funkenstrecke mit Vorkondensator. Z. für technische Physik **13** (1932), pp. 425–430.
15. Grosskreuz, R.: Nachweis von Elektronenlawinen mittels elektrostatischer Ladungsbilder auf isolierenden Folien. Z. für angewandte Physik **21** (1966): 3, pp. 200–202.
16. Hald, A.: Statistical theory with engineering applications. New York 1962.
17. Hall, H. C., Russek, R. M.: Discharge inception and extinction in dielectric voids. Proc. I.E.E. Pt. II, **101** (1954), pp. 47–55.
18. Heller, B., Chládek, J.: Zur Physik der Koronavorgänge im festen Dielektrikum. Acta Techn. ČSAV **9** (1964): 1, pp. 1–16.

followed more easily, if W is separated into the three components W_p, W_g and W_d. Thus,

$$W_p=\tfrac{1}{2}C_p(U_0^2-U_0'^2)=\tfrac{1}{2}C_p(U_0-U_0')(U_0+U_0')$$

$$=\tfrac{1}{2}\frac{C_p c_d}{C_p+c_d}(U_{di}-U_{dr})\left[2U_{di}\left(1+\frac{c_g}{c_d}\right)-\frac{c_d}{C_p+c_d}(U_{di}-U_{dr})\right] \quad \text{(A 4)}$$

$$W_g=\tfrac{1}{2}c_g(U_{di}^2-U_{dr}^2)=\tfrac{1}{2}\frac{C_p c_d}{C_p+c_d}(U_{di}-U_{dr})\left[c_g\frac{C_p+c_d}{C_p c_d}(U_{di}+U_{dr})\right] \quad \text{(A 5)}$$

$$W_d=\tfrac{1}{2}c_d[(U_0-U_{di})^2-(U_0'-U_{dr})^2]$$

$$=\tfrac{1}{2}c_d[(U_0-U_{di}-U_0'+U_{dr})(U_0-U_{di}+U_0'-U_{dr})]$$

$$=\tfrac{1}{2}c_d\left[\frac{c_d}{C_p+c_d}(U_{di}-U_{dr})-(U_{di}-U_{dr})\right]$$

$$\times\left[2\left(1+\frac{c_g}{c_d}\right)U_{di}-\frac{c_d}{C_p+c_d}(U_{di}-U_{dr})-U_{di}-U_{dr}\right]$$

$$=-\tfrac{1}{2}\frac{C_p c_d}{C_p+c_d}(U_{di}-U_{dr})\left[\frac{C_p}{C_p+c_d}(U_{di}-U_{dr})+2U_{di}\frac{c_g}{c_d}\right] \quad \text{(A 6)}$$

Eqs. (A 4), (A 5) and (A 6) are brought into forms containing a common factor, which is denoted

$$\Delta Q_p'=\frac{C_p c_d}{C_p+c_d}(U_{di}-U_{dr})$$

The charge ΔQ_p necessary to restore the network from U_0' to U_0 is

$$\Delta Q_p=\frac{C_p c_d}{C_p+c_d}(U_{di}-U_{dr})\left[1+\frac{c_d c_g}{C_p(c_d+c_g)}\right] \quad \text{(A 7)}$$

Thus,

$$\Delta Q_p'=\frac{\Delta Q_p}{1+\dfrac{c_d c_g}{C_p(c_d+c_g)}} \quad \text{(A 8)}$$

The total energy change W is

$$W=\tfrac{1}{2}\Delta Q'_p\left[2U_{di}\left(1+\frac{c_g}{c_d}\right)-\frac{c_d}{C_p+c_d}(U_{di}-U_{dr})\right.$$
$$\left.+\frac{c_g(C_p+c_d)}{C_p c_d}(U_{di}+U_{dr})-\frac{C_p}{C_p+c_d}(U_{di}-U_{dr})-2U_{di}\frac{c_g}{c_d}\right]$$

$$W_{\text{4}}=\tfrac{1}{2}\Delta Q'_p\left\{U_{di}\left[2\left(1+\frac{c_g}{c_d}\right)-\frac{c_d}{C_p+c_d}+\frac{c_g(C_p+c_d)}{C_p c_d}-\frac{C_p}{C_p+c_d}-2\frac{c_g}{c_d}\right]\right.$$
$$\left.+U_{dr}\left[\frac{c_d}{C_p+c_d}+\frac{c_g(C_p+c_d)}{C_p c_d}+\frac{C_p}{C_p+c_d}\right]\right\}$$

$$W=\tfrac{1}{2}\Delta Q'_p\left\{U_{di}\left[2-\frac{C_p+c_d}{C_p+c_d}+\frac{c_g(C_p+c_d)}{C_p c_d}\right]+U_{dr}\left[\frac{C_p+c_d}{C_p+c_d}+\frac{c_g(C_p+c_d)}{C_p c_d}\right]\right\}$$

$$W=\tfrac{1}{2}\Delta Q'_p\left[1+\frac{c_g(C_p+c_d)}{C_p c_d}\right](U_{di}+U_{dr}) \qquad \text{(A 9)}$$

Insertion of Eq. (A 8) in Eq. (A 9) yields

$$W=\tfrac{1}{2}\Delta Q_p(U_{di}+U_{dr})\frac{1+\dfrac{c_g(C_p+c_d)}{C_p c_d}}{1+\dfrac{c_d c_g}{C_p(c_d+c_g)}}$$

$$W=\tfrac{1}{2}\Delta Q_p(U_{di}+U_{dr})\left(1+\frac{c_g}{c_d}\right) \qquad \text{(A 10)}$$

Eq. (A 10) follows exactly from Eqs. (A 1), (A 2), (A 3) and (A 7), whereas earlier derivations, e.g., by Dick, Sletbak and the author[8]—U_{dr} is assumed to be negligible—and by Bui-Ai[7] were carried out neglecting small terms of the type c_g/C_p, c_d/C_p, etc.

SOME OBSERVATIONS OF THE TREEING BREAKDOWN IN EPOXIDE RESINS

Andreas Kelen and Lars-Erik Larsson
Central Laboratories, ASEA, Västerås

During experimental work aimed at the development of a treeing test for insulating materials[1], the propagation of treeing channels in transparent epoxide mouldings with a point-plane electrode geometry was studied by a microscope technique. Fig. 1 shows the extension for the field direction of the longest channel as a function of time for different alternating voltages applied to the sample. The sample preparation technique is described in[1]. The growth of a tree is observed in some cases to start as soon as the voltage has been applied. In other cases the growth begins after an induction period, which can amount to several hours, possibly as a result of the erratic occurrence

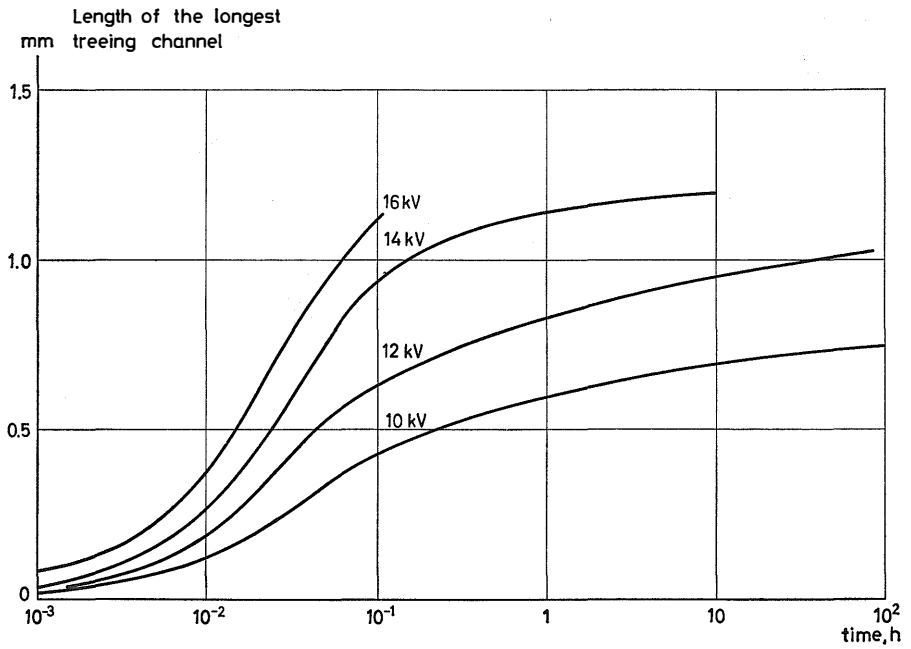

Fig. 1. Projection of the treeing channel in the field direction as a function of time at different applied voltages.

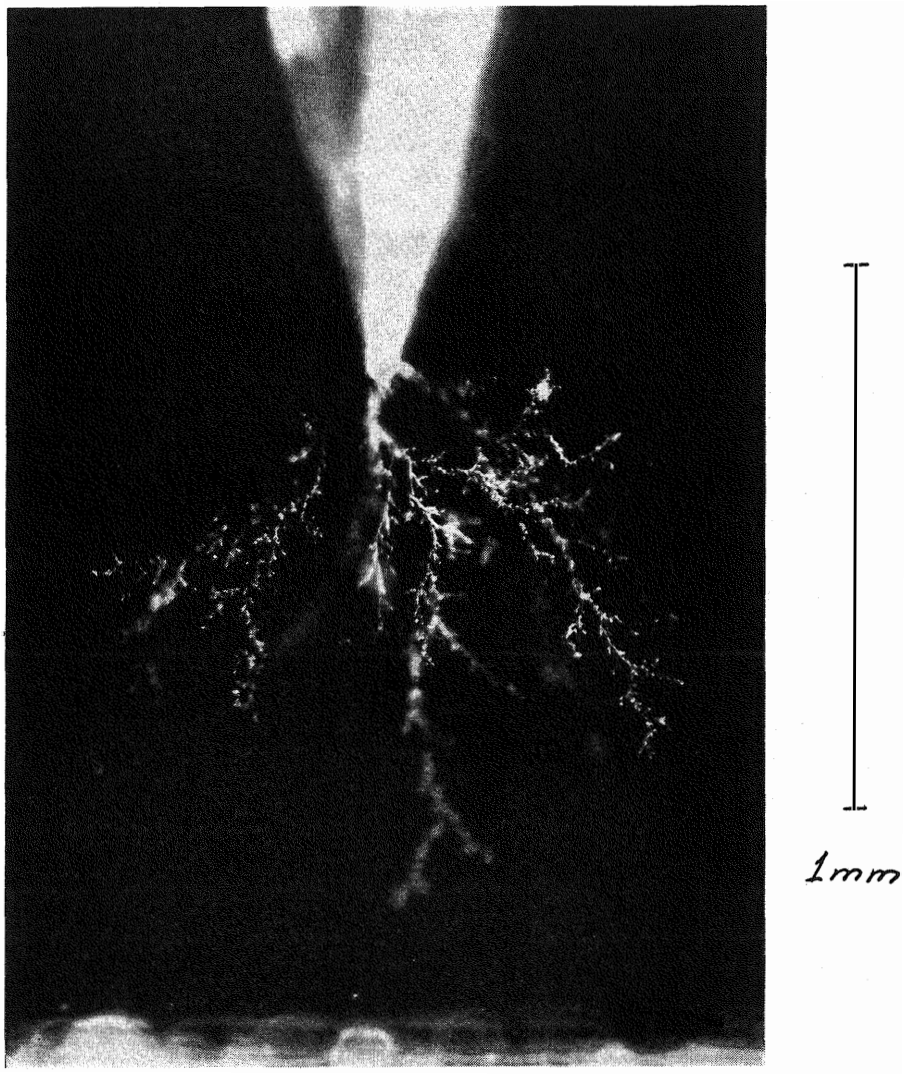

Fig. 2. Treeing pattern, first stage.

of over-voltages of sufficient amplitude. The induction period is not included in the times indicated in Fig. 1.

Branching treeing channels have been observed to propagate in other directions than the field lines would have, if the dielectric medium were assumed to be homogeneous and free from charges. Thus, retrograde side channels have been seen to propagate from a branching point on the main channel back towards the point electrode. Channels approaching the plane electrode

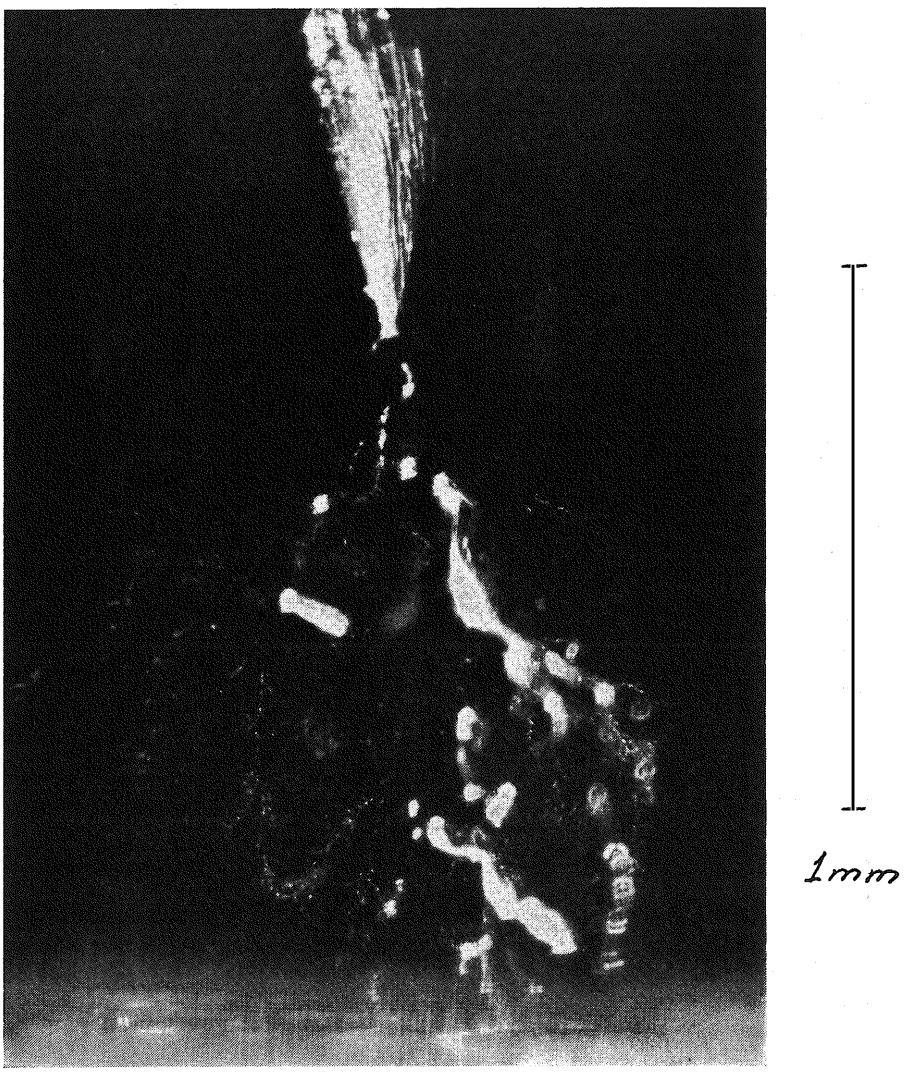

Fig. 3. Treeing pattern, first, second (at the electrode point) and third stages.

were observed in some cases to pass over its edge and return to it from the rear side. A considerable field distortion in the dielectric owing to local charge accumulation by the walls of treeing channels in thus indicated.

In many cases a considerable time elapses from the instant of the complete penetration of a treeing channel from the point to the plane electrode until breakdown. Similar findings have been reported by Olyphant[2].

We have observed the progress of the treeing degradation under the micro-

scope during voltage exposure. Our main interest was directed to the last stage of the deterioration after treeing channels have completely bridged the electrodes. Two distinct deterioration patterns could be discerned:

1. With the illumination turned off, discharges were sometimes seen to strike along the whole or part of the length of a primary treeing channel, which had been seen earlier with dark-field illumination. After such a phenomenon had occurred, the appearance of the channel in dark-field illumination had changed. It had a wider and brighter appearance (due to total reflection). While the primary channels have a hair-like appearance with a width which is not resolved (≤ 1 μm), the channel in its secondary phase has a width of 2–5 μm as estimated with an ocular micrometer. The transition of channels or parts of channels from the primary to the secondary stage appears to the eye to be instantaneous.

2. A local bubbling activity resembling gas evolution in a liquid is regularly observed in treeing channels in the primary or secondary stage. This results in a widening of the channel to 10–30 μm, the third stage. The active part of a channel has a silvery appearance, but after some time turns yellow, red or light brown. The activity may be localised or tends to propagate along the channel, in which case strings of bubbles are often seen to move. The movement may be away from, or towards, the point electrode. The "bubbles" often have a very bright silverish or red appearance. They have never been observed, however, to be self-luminous. Observation in the dark has revealed that "bubbling" is sometimes associated with flashing of neighbouring narrow channels, but this is not typical. The development of the third phase of channel growth requires considerable time, from seconds to hours. It is followed by breakdown.

Our observations may suggest a mechanism of the breakdown in a bridging treeing channel—especially the development of the third stage—similar to the mechanism of surface tracking breakdown of insulators reported by Hampton[3]. The "bubbling" sites in the channel may be interpreted as being caused by thermal effects due to current instabilities in a conducting surface layer with high resistivity on the channel walls. The local erosion observed may be caused by the thermal degradation of the polymer, possibly assisted by intensified discharge action. The propagation of "bubbling" is thought to be associated with both a pressure rise caused by polymer degradation and changes of the conduction properties of the channel wall.

It may be thought that local carbonisation at sites of current instability in a channel, if considerably lowering the surface resistivity of the wall, would tend to transfer the instabilities successively over the remaining portions of the channel and thus contribute to the ultimate breakdown.

The interpretation of our observations in terms of a high-voltage tracking mechanism may throw some light on the last phase of treeing breakdown

in polymers after primary channels have bridged the electrodes without loss of dielectric strength at the applied voltage. The mechanism should depend on material properties and geometry and on the nature of the material deterioration under the action of internal discharges and temperature. It is probably one of several competing mechanisms encountered in the ultimate stage of treeing breakdown.

Acknowledgements

The authors wish to thank ASEA for permission to publish this communication. The work forms part of a research project for which a grant has been obtained from the Swedish Technical Research Council.

Abstract

A study of the last phase of treeing breakdown after a primary channel has bridged the electrodes reveals two development stages. The last stage is discussed in the light of a known mechanism of insulator flashover.

References

1. KELEN, A.: Partial discharge testing of insulating materials. Acta Polytechnica Scandinavica El **16** (1967), pp. 3–86.
2. OLYPHANT, M. JR.: Breakdown by treeing in epoxy resins. Gas discharges and the Electricity Supply Industry (Intern. Conf. CERL, Leatherhead, May 1962), London 1962, pp. 447–460.
3. HAMPTON, B. F.: Flashover mechanism of polluted insulation. Proc. I.E.E. **111** (May 1964), pp. 985–990.

Price Sw. Kr. 20.00

GÖTEBORG 1967
ELANDERS BOKTRYCKERI AKTIEBOLAG